AFRL-RQ-WP-TR-2013-0132

AIRCRAFT STRUCTURAL RELIABILITY AND RISK ANALYSIS HANDBOOK

Volume 1: Basic Analysis Methods

Eric J. Tuegel, Robert P. Bell, Alan P. Berens, Thomas Brussat, Joseph W. Cardinal, Joseph P. Gallagher, and James Rudd

Structures Technology Branch
Aerospace Vehicles Division

JUNE 2013
Final Report

AIR FORCE RESEARCH LABORATORY
AEROSPACE SYSTEMS DIRECTORATE
WRIGHT-PATTERSON AIR FORCE BASE, OH 45433-7542
AIR FORCE MATERIEL COMMAND
UNITED STATES AIR FORCE

NOTICE AND SIGNATURE PAGE

Using Government drawings, specifications, or other data included in this document for any purpose other than Government procurement does not in any way obligate the U.S. Government. The fact that the Government formulated or supplied the drawings, specifications, or other data does not license the holder or any other person or corporation; or convey any rights or permission to manufacture, use, or sell any patented invention that may relate to them.

This report was cleared for public release by the USAF 88th Air Base Wing (88 ABW) Public Affairs Office (PAO) and is available to the general public, including foreign nationals.

Copies may be obtained from the Defense Technical Information Center (DTIC) (http://www.dtic.mil).

AFRL-RQ-WP-TR-2013-0132 HAS BEEN REVIEWED AND IS APPROVED FOR PUBLICATION IN ACCORDANCE WITH ASSIGNED DISTRIBUTION STATEMENT.

*//Signature//

ERIC J. TUEGEL, Project Engineer
Structures Technology Branch
Aerospace Vehicles Division
Aerospace Systems Directorate

//Signature//

MICHAEL J. SHEPARD, Chief
Structures Technology Branch
Aerospace Vehicles Division
Aerospace Systems Directorate

//Signature//

FRANK C. WITZEMAN, Chief
Aerospace Vehicles Division
Aerospace Systems Directorate

This report is published in the interest of scientific and technical information exchange, and its publication does not constitute the Government's approval or disapproval of its ideas or findings.

*Disseminated copies will show "//Signature//" stamped or typed above the signature blocks.

REPORT DOCUMENTATION PAGE

Form Approved
OMB No. 0704-0188

1. REPORT DATE *(DD-MM-YY)*	2. REPORT TYPE	3. DATES COVERED *(From - To)*
June 2013	Final	29 September 2009 – 01 June 2013

4. TITLE AND SUBTITLE
AIRCRAFT STRUCTURAL RELIABILITY AND RISK ANALYSIS HANDBOOK
Volume 1: Basic Analysis Methods

5a. CONTRACT NUMBER
In-house

5b. GRANT NUMBER

5c. PROGRAM ELEMENT NUMBER
62201F

6. AUTHOR(S)
Eric J. Tuegel, Robert P. Bell, Alan P. Berens, Thomas Brussat, Joseph W. Cardinal, Joseph P. Gallagher, and James Rudd

5d. PROJECT NUMBER
2401

5e. TASK NUMBER
N/A

5f. WORK UNIT NUMBER
A0FU0B

7. PERFORMING ORGANIZATION NAME(S) AND ADDRESS(ES)
Structures Technology Branch (AFRL/RQVS)
Aerospace Vehicles Division
Air Force Research Laboratory, Aerospace Systems Directorate
Wright-Patterson Air Force Base, OH 45433-7542
Air Force Materiel Command, United States Air Force

8. PERFORMING ORGANIZATION REPORT NUMBER
AFRL-RQ-WP-TR-2013-0132

9. SPONSORING/MONITORING AGENCY NAME(S) AND ADDRESS(ES)
Air Force Research Laboratory
Aerospace Systems Directorate
Wright-Patterson Air Force Base, OH 45433-7542
Air Force Materiel Command
United States Air Force

10. SPONSORING/MONITORING AGENCY ACRONYM(S)
AFRL/RQVS

11. SPONSORING/MONITORING AGENCY REPORT NUMBER(S)
AFRL-RQ-WP-TR-2013-0132

12. DISTRIBUTION/AVAILABILITY STATEMENT
Approved for public release; distribution unlimited.

13. SUPPLEMENTARY NOTES
PA Case Number: 88ABW-2013-3876; Clearance Date: 28 Aug 2013. This report contains color.

There will be additional volumes to this handbook.

14. ABSTRACT
The Aircraft Structural Reliability and Risk Handbook provides:

a) A reference on basic statistics, probability, and reliability techniques required for conducting structural risk and reliability analyses, and

b) Illustrative examples of how to apply these techniques to problems involving the nucleation and growth of fatigue cracks in metallic airframe structure.

This particular volume describes the fundamentals of probabilistic analysis and structural reliability analysis for the next flight.

15. SUBJECT TERMS
structural reliability, probability, structural integrity, failure

16. SECURITY CLASSIFICATION OF:			17. LIMITATION OF ABSTRACT:	18. NUMBER OF PAGES	19a. NAME OF RESPONSIBLE PERSON (Monitor)
a. REPORT	b. ABSTRACT	c. THIS PAGE			Eric J. Tuegel
Unclassified	Unclassified	Unclassified	SAR	116	19b. TELEPHONE NUMBER *(Include Area Code)* N/A

Table of Contents

Table of Contents (continued)

Table of Contents (concluded)

List of Figures

List of Figures (concluded)

List of Tables

1.0 INTRODUCTION

1.1 Objective of this Handbook

Risk assessment is defined in terms of the combination of the severity and likelihood of a mishap. MIL-STD-882E, *Standard Practice for System Safety* [1], addresses the two components of risk by considering four categories of severity and five levels of probability of occurrence with a grouping of the combinations into risk categories. Because MIL-STD-882E applies to all systems, the levels of mishap severity are defined in qualitative terms and the joint effects of likelihood and severity are accounted for by assigning to four Mishap Risk Categories. If the consequence of a failure is catastrophic, say loss of airplane and pilot, the risk is obviously in the most severe mishap risk category. If the consequence of a failure can be expressed in dollars, the risk can be quantified in terms of the expected loss as calculated from the product of failure probability and loss value.

USAF Airworthiness Bulletin (AWB)-013A, *Risk Identification and Acceptance for Airworthiness Determination* [2], defines airworthiness in terms of the probability of aircraft loss per flight hour. This document is directed at aircraft failures from the combination of all causes but recognizes that an aircraft comprises distinct functions. The aircraft structure is one of these ten functions. Accordingly, the requirements of the MIL-STD-1530C Aircraft Structural Integrity Program (ASIP), [3], now reflect the need to perform structural risk and reliability analyses of safety critical airframe structure. Reliability is the likelihood that a mishap will not occur, i.e., the complement of the likelihood of a mishap in MIL-STD-882E.

The *Aircraft Structural Reliability and Risk Handbook* is intended to provide guidance on performing the analyses required to assess structural reliability of airframe structure to meet the requirements of MIL-STD-1530C. Determination of risk requires that the consequences of a potential structural failure be considered along with the structural reliability. Understanding the consequence of a structural failure is fundamental to all structural engineering. And so guidance on determining the consequences of a structural failure is not addressed in this handbook.

The specific goals of this handbook are:

a) To provide a reference on basic statistics, probability, and reliability techniques required for conducting structural risk and reliability analyses, and

b) To illustrate methods for characterizing data for structural risk and reliability analyses through worked examples.

As a handbook, this document is not intended to be read from cover to cover. It is intended that the user of this handbook will refer to specific sections and examples that are similar to the particular problem that they are trying to solve.

1.2 Failure Modes Addressed

This handbook focuses specifically on the analysis methods for estimating probabilities of structural failure due to the initiation and growth of fatigue cracks in metallic structure. As an airframe ages, there are many other potential sources of damage that can lead to structural failure. These include:

a) Delamination,
b) Corrosion/material thinning,
c) Material property degradation,

d) Handling during inspections and maintenance,
e) Disbond,
f) Impact damage, and
g) Stress corrosion cracking.

At present, well-established and widely-accepted models exist only for the degradation of structural integrity due to fatigue cracking in metallic structure. Because widely acceptable models for the degradation of structural integrity via other mechanisms are not available, these mechanisms are not considered in the reliability analyses of this handbook. In the future as models for other progressive damage phenomena become available, other types of damage and failure can be added to the handbook.

1.3 Organization of this Handbook

The *Aircraft Structural Reliability and Risk Handbook* will consist of multiple volumes. This volume which is the first describes the fundamentals of probabilistic analysis and structural reliability analysis for the next event, i.e., the next flight. Subsequent volumes will address structural reliability analysis over a long series of events, i.e., thousands of flights, and how to use the results of structural reliability analyses to guide decisions on when to repair, replace, and retire aircraft.

This volume of the *Aircraft Structural Reliability and Risk Handbook* is organized as follows. Section 2.0 provides some background on structural reliability analysis. In Section 3.0, important terms are defined and common probability distributions used in structural reliability analyses are presented. Techniques for finding the best probability distribution models for a set of data are discussed in Section 4.0. Creating a model of the cumulative probability of failure over the lifetime of a part from observed failure times is described in Section 5.0. Finally, in Section 6.0, the prediction of the probability of failure for a part during the next flight from the physics of the failure mechanism is illustrated.

2.0 BACKGROUND

Since 1975, the USAF has used the damage tolerance philosophy to ensure the structural integrity of its aircraft. Damage tolerance considers the ability of structure to sustain anticipated loads in the presence of damage (fatigue, corrosion, or accidental damage) until such damage is detected (through inspections or malfunctions) and repaired. Two approaches are used to establish the damage tolerance of a structure: slow crack growth and fail safety.

Damage tolerance analyses (DTA) are deterministic. Crack sizes are determined from estimates of the largest amount of undetected damage that could be in a structure. Analyses determine how rapidly a crack of this size would grow to failure under an anticipated loading. Inspection intervals are then established so that the structure will be inspected twice before a crack of this size would grow to failure.

While this approach is judged to be conservative, there is still a small chance of a failure. The actual damage in the structure could be greater than that assumed. The loading may be more severe than was anticipated. And, individual details may have fracture toughness less than the design value. There is significant uncertainty about the future performance of the structure in this situation. A safety factor of 2 is applied to the predicted crack growth life to accommodate this uncertainty.

2.1 Probability of Failure

In 1955, Lundberg [4] recommended tackling aeronautical fatigue with statistical methods. Lundberg proposed a definition of safety in terms of the *failure rate*, which he defined as the cumulative probability of a catastrophic failure divided by the operational time. The cumulative probability of a catastrophic failure is a function of the operational time, i.e., flight hours. Lundberg suggested a permitted, or critical, failure rate of 10^{-9} per flight hour for civilian transport aircraft. This suggestion came from Lundberg's belief that there should not be more than one catastrophic failure during one or two generations, i.e., 30 to 60 years. He estimated that in a period of about 40 years (from 1953) a total of 10^{9} flight hours will be completed by commercial aviation. Thus, the critical failure rate is derived to give an expectation of 1 failure during that time. Note that physics-based models for fatigue and fatigue crack growth were in their infancy when Lundberg made this proposal. His probability of catastrophic failure was based upon test results and operational experience.

Lincoln adapted Lundgren's recommendation for military aircraft in the 1980. Since military aircraft have significantly different flight durations, but desiring to have a single metric that applies to all aircraft in the inventory, Lincoln went to a flight, rather than a flight hour, as the basic time unit for the failure rate. Lincoln called this rescaled measure the Single Flight Probability of Failure (SFPOF) [5]. Lincoln also proposed the permissible value for SFPOF as 10^{-7} failures per flight. For SFPOF greater than 10^{-7}, structural modifications or replacements should be considered to ensure continued safe operation. If the SFPOF is greater than 10^{-5} for an extended period, the failure rate is considered unacceptable. These SFPOF values are the current standard in MIL-STD-1530C. In addition, Lincoln stated that there should not be more than 1 failure expected in an aircraft fleet during the lifetime.

In addition, since more was known about the mechanics of fatigue in 1980 than in 1955, Lincoln proposed a method for calculating the SFPOF over the service life of an aircraft as a result of

fatigue crack growth and subsequent fracture [5], [6]. This method was implemented in a computer program called RISKY. RISKY was the basis for the subsequent PROF program [7] constructed by the University of Dayton Research Institute under an Air Force Research Laboratory contract. The intent of this method was to provide managers with an instantaneous assessment of the probability of a failure at a point in an aircraft's service life. Those structural elements that most affect structural integrity and drive maintenance will typically have a larger SFPOF.

2.2 Factor of Safety and Probability of Failure

In the mid-1950's, the American Society of Civil Engineers (ASCE) appointed a committee to formulate a clear definition of the factor of safety. The committee voiced a basic principle that the term "factor of safety" acquires a rational meaning possibly by its correlation with a probability of failure or survival (i.e., reliability). This principle attempts to place the concept of structural safety in the realm of physical reality where knowledge is imperfect and absolutes, such as minimum strength, do not exist. In their final report in 1966 [8], the committee concluded that it is now possible to give consideration of to all aspects of structural safety by the probabilistic approach. The report went on to develop and explain techniques for calculating structural reliability for various types of structural problems where the load carrying capacity of the structure, or strength, and the loads applied to the structure are described by probability distributions. Of particular interest to our application is the formulation and solution for problems where the load carrying capacity degrades with time in service.

2.3 Structural Reliability

The reliability of structural components and systems is different than that of technical components such as valves, pumps, generators, transistors, etc. Failures occur more rarely and the mechanisms behind the failures are different. Structural failures do not occur solely because of an aging process, but as a result of interactions between aging processes and extreme events. Thus, it is necessary to consider the influences acting from the outside (the loads) and influences acting from inside (the strength) when performing a structural reliability analysis.

Significant uncertainties exist in the probabilistic models of the loads and the strengths as a result of limited information. Estimates of failure probabilities depend on assumptions concerning the probability distributions of either time to failure or the strength and stress properties of the factors that determine failure. That is, models (functions) must be assumed for the distributions and the parameters of the models must be estimated from samples of data. Any estimate of extremely small probabilities must come from the extreme tails of the distributions. Historical records indicate that the chance of a structural fatigue failure in an airframe resulting in catastrophic consequences is very small, about 1.5 per 10^7 flight hours, as shown in Figure 1. Catastrophic consequences are considered to be loss of life, permanent total disability, irreversible significant environment impact, or monetary loss greater than or equal to $10M. Because there is never enough data to directly assess the probabilities in the tails of the distribution, the failure probabilities are obtained by extrapolating from data near the mean of the distribution. Thus, the failure probabilities must be understood as nominal probabilities, i.e., not reflecting the true, precise probability of structural failure but rather reflecting the current information about the performance of the structure. Every effort should be made to use probability distribution functions and parameter estimates that fit all available data and lead to conservative estimates of failure probability from the relevant distribution tail.

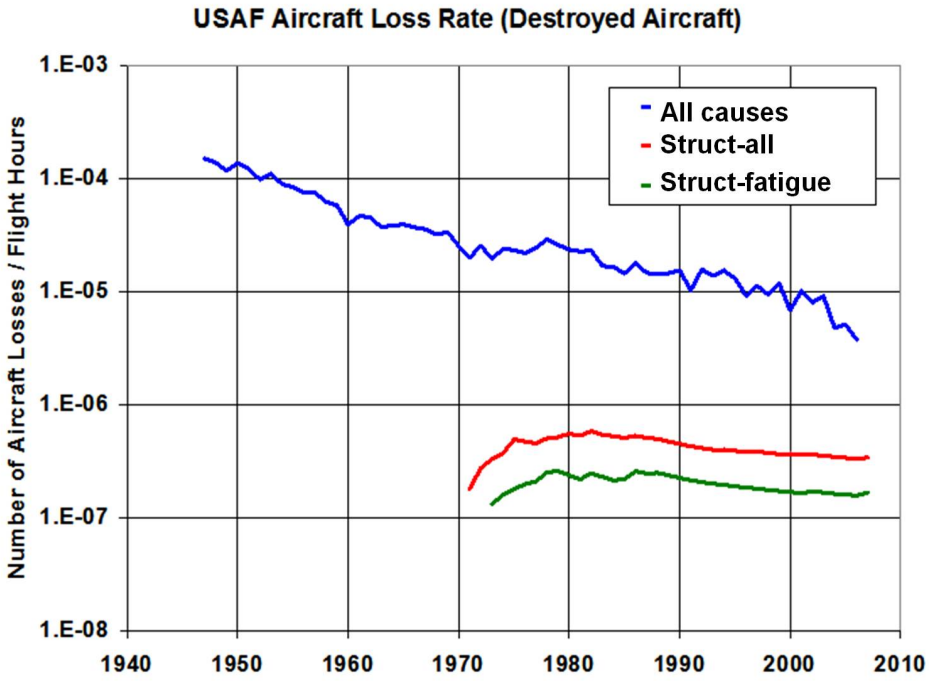

Figure 1. USAF Aircraft Loss Rate
Comparing all causes to those from structural failures and from structural fatigue failures [9]

3.0 STRUCTURAL RELIABILITY FUNDAMENTALS

This section presents a brief description of the fundamental concepts of structural reliability analysis. The reader in need of refresher on the basics of statistics and probability should consult the *NIST/SEMATECH e-Handbook of Statistical Methods*, [10] online at http://www.itl.nist.gov/div898/handbook/.

This section begins by defining important terms and concepts used in structural reliability analysis. Then, probability distributions that are commonly used in structural reliability analysis are reviewed.

3.1 Definitions

The following terms are important for structural reliability analysis.

3.1.1 Risk

Risk is the potential for losses and rewards as a result of a failure event. Risk is a characteristic of an uncertain future, and not of either the present or past. When uncertainties are resolved, or the future becomes the present, risk becomes nonexistent. Risk does not exist for historical events or events that are currently happening. Risk is evaluated in terms of both the probability of occurrence and the impact of the occurrence. The USAF uses a matrix to determine the risk in terms of a Hazard Risk Index (HRI) as shown in Figure 2.

HAZARD CATEGORIZATION		SEVERITY*			
		CATASTROPHIC (1)	CRITICAL (2)	MARGINAL (3)	NEGLIGIBLE (4)
FREQUENCY	FREQUENT (A) = or > 100/100K flt hrs	1	3	7	13
	PROBABLE (B) 10-99/100K flt hrs	2	5	9	16
	OCCASIONAL (C) 1.0-9.9/100K flt hrs	4	6	11	18
	REMOTE (D) 0.01-0.99/100K flt hrs	8	10	14	19
	IMPROBABLE (E) = or < 0.01/100K flt hrs	12	15	17	20

HIGH	CAE Risk Acceptance HRI = 1 through 5	MEDIUM	PM Risk Acceptance HRI = 10 through 17
SERIOUS	PEO Level Risk Acceptance HRI = 6 through 9	LOW	Risk Acceptance As Directed HRI = 18 through 20

*Severity is the worst credible consequence of a hazard in terms of degree of injury, property damage or effect on mission defined below:

(1) **Catastrophic:** Class A (damage > $2M / fatality / permanent total disability / loss of Aircraft)
(2) **Critical:** Class B ($500K < damage < $2M / permanent partial disability / hospitalization of 5 or more personnel)
(3) **Marginal:** Class C ($50K < damage < $500K / injury results in 1 or more lost workdays)
(4) **Negligible:** All other injury/damage less than Class C

Figure 2. USAF Airworthiness Risk Acceptance Matrix [2]

3.1.2 Reliability

Reliability is the probability that a system or component will survive, i.e., function as intended, under designated operating or environmental conditions for a specified time period. Reliability is the complement to the probability of failure,

$$\text{Reliability} = 1 - \text{Failure Probability}.$$

3.1.3 Lifetime Distribution

A lifetime distribution describes how a nonrepairable population fails over time. The lifetime distribution can be any probability density function (PDF), *f(t)*, defined over the range of time from $t = 0$ to $t =$ infinity. The corresponding cumulative distribution function (CDF), *F(t)*, gives the probability that a randomly selected unit will fail before time *t*.

3.1.4 Probability Density Function (PDF)

A PDF, $f_X(y)$, defines the probability that a continuous random variable will take a particular value. The probability that the random variable *X* will have a value within the interval from x_1 to x_2 is:

$$Pr(x_1 \leq X \leq x_2) = \int_{x_1}^{x_2} f_X(y)dy. \quad (1)$$

A PDF must be nonnegative and the total area under the PDF curve must be equal to one.

3.1.5 Cumulative Distribution Function (CDF)

A CDF, $F_X(y)$, gives the probability that a continuous random variable, *X*, will take a value less than or equal to a specified value, x_1,

$$F_X(x_1) = Pr(X \leq x_1) = \int_{-\infty}^{x_1} f_X(y)\, dy. \quad (2)$$

The value of the CDF must be greater than or equal to 0, and less than or equal to 1. The CDF is also a non-decreasing function.

3.1.6 Exceedance Distribution Function (EDF)

An EDF, $D_X(y)$, gives the probability that a continuous random variable, *X*, will take a value greater than a specified value, x_1. The sum of the CDF, $F_X(y)$, and the EDF is equal to one since the total probability is equal to one, and the CDF and EDF cover all the possibilities for the random variable *X*. Hence,

$$D_X(x_1) = Pr(X > x_1) = 1 - F_X(x_1)$$
$$= 1 - \int_{-\infty}^{x_1} f_X(y)\,dy = \int_{x_1}^{\infty} f_X(y)\,dy. \quad (3)$$

The value of the EDF must be greater than or equal to 0, and less than or equal to 1. The EDF is also a non-increasing function.

3.1.7 Hazard Rate Function (HRF)

The HRF is defined from the probability of failure of an item in the time interval t to $t+\Delta t$ with the condition that the item is functioning at time t, for small Δt. The probability that the failure time T is between t and $t+\Delta t$ with the condition that T is greater than t is given by

$$Pr(t < T \leq t + \Delta t | T > t) = \frac{f_T(t)}{1-F_T(t)}\Delta t \quad (4)$$

where $f_T(t)$ is the PDF and $F_T(t)$ is the CDF of the lifetime distribution for the item, respectively. The HRF, $h_T(t)$, is defined as

$$h_T(t) = \frac{f_T(t)}{1-F_T(t)}. \quad (5)$$

The HRF is also known as the failure rate function, the instantaneous failure rate, or force of mortality. The HRF is a measure of the proneness to failure as a function of age. The expected proportion of items of age t that fail in a short time Δt is equal to $\Delta t \cdot h_T(t)$.

The HRF is strictly not a probability. A cumulative hazard rate function, $H_T(t)$, can be defined as

$$H_T(t) = \int_0^t h_T(x)dx. \quad (6)$$

The relationship between $H_T(t)$ and the CDF of the lifetime distribution, $F_T(t)$, is

$$F_T(t) = 1 - e^{-H_T(t)}. \quad (7)$$

When t equals ∞, $F_T(\infty)$ equals 1 and $H_T(\infty)$ equals ∞. Therefore, the cumulative hazard rate function cannot be a CDF since it has values greater than 1, and $h_T(t)$ cannot be a PDF.

3.1.8 Single Flight Probability of Failure (SFPOF)

SFPOF is the probability of a failure during one flight with the condition that there has not been a failure in any of the previous flights. The SFPOF can be calculated as the product of the HRF at a specified flight, $h_T(t)$, and a time increment Δt of one flight.

3.2 Common Probability Distributions

This section introduces four of the probability distributions that are commonly used in structural reliability analysis. These include the normal, lognormal, exponential, and Weibull distributions. (The *NIST/SEMATECH e-Handbook of Statistical Methods* [10] has additional details on these and other distributions.)

Like many of the widely used statistical distributions, these are location-scale distributions. The scale parameter prescribes the spread of the distribution (wide, skewed). Examples of scale parameters are the standard deviation (σ) for normal and lognormal distributions and shape parameter (β) for Weibull. The location parameter specifies the location of a central point of the distribution. Examples of location parameters are the mean (μ) for the normal, the median (e^{μ}) for the lognormal, and the scale parameter (α) for Weibull. (Note the paradox: the Weibull scale parameter is a location parameter because about 63 percent of a population is always less than the scale parameter.)

3.2.1 Normal Distribution

The normal distribution is perhaps the best-known distribution. For a mean μ and standard deviation σ, the PDF of the normal distribution is given by

$$f(t) = \frac{1}{\sigma\sqrt{2\pi}} exp\left\{-0.5\left[\frac{t-\mu}{\sigma}\right]^2\right\}. \quad (8)$$

Figure 3 shows plots of the PDF and CDF of the normal distribution for a mean of 5 and three different values of standard deviation. A normal distribution with a mean of 0 and a standard deviation of 1 is known as the standard normal distribution. The CDF for the standard normal, usually represented by $\Phi(t)$, is tabulated in the back of most probability textbooks. Any normal distribution can be mapped into the standard normal distribution through the standard normal random variable,

$$z = \frac{t-\mu}{\sigma}. \quad (9)$$

The normal distribution has several convenient properties, including:

- Central limit theorem: The distribution of the sum of independent random variables usually tends to a normal distribution as the number of elements in the sum increases. Since scatter in real world observations can often be thought of as the sum of many random effects, the normal distribution has been found to fit many data sets over a wide range of disciplines.
- Additive property: A random variable is normally distributed if it is the sum of 2 or more independent random variables, each of which is normally distributed. Its mean is the sum of the means, and its variance (the square of standard deviation) is the sum of the variances.

Since the normal distribution extends over negative values, it is sometimes inappropriate for representing data that can only be positive. Such would be the case when the standard deviation is relatively large compared to the mean so that the normal distribution would predict a reasonably large chance of an impossible negative observation. For example, distributions of structural crack sizes typically have standard deviations that are greater than the mean, so that a normal distribution would indicate a large percentage of negative crack sizes. On the other hand, when observations that can only be positive are all far separated from zero relative to their scatter, the normal distribution can still provide a useful model. For example, a normal distribution is often fit to observations of tensile strength and fracture toughness.

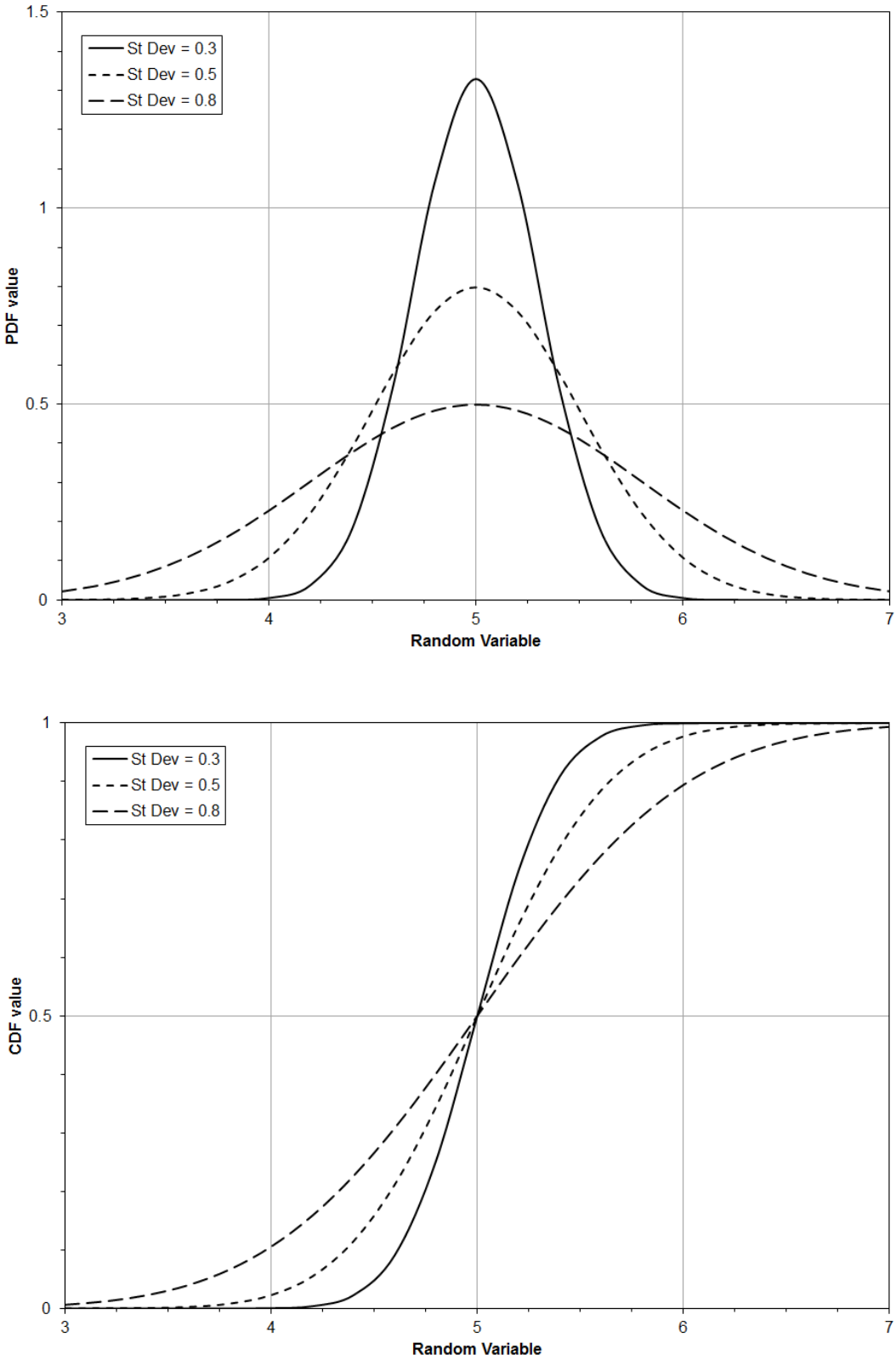

Figure 3. Normal Probability Density and Cumulative Distribution Functions

3.2.2 Lognormal Distribution

The lognormal distribution for *t* is simply a normal distribution of the natural log, *ln(t)*. The PDF of the lognormal distribution is given by

$$f(t) = \frac{1}{t\sigma\sqrt{2\pi}} exp\left\{-0.5\left[\frac{ln(t) - \mu}{\sigma}\right]^2\right\}. \quad (10)$$

In Equation (10), μ and σ are the mean and standard deviations of *ln(t)*. The median (CDF = 0.5) of the distribution of *t* is given by e^{μ}. Figure 4 shows graphs of the PDF and CDF for the Lognormal distribution for a log mean of 0 (i.e., *ln*(1.0)) and three different values of standard deviation.

The lognormal distribution has been commonly used for decades to represent the distribution of structural integrity variables such as fatigue life, strength, fracture toughness, crack growth rate, and crack sizes. It shares convenient features of the normal distribution. For example, consider this corollary to the additive property of the normal distribution: A random variable is lognormally distributed if it is the product of 2 or more independent random variables, each of which is lognormally distributed.

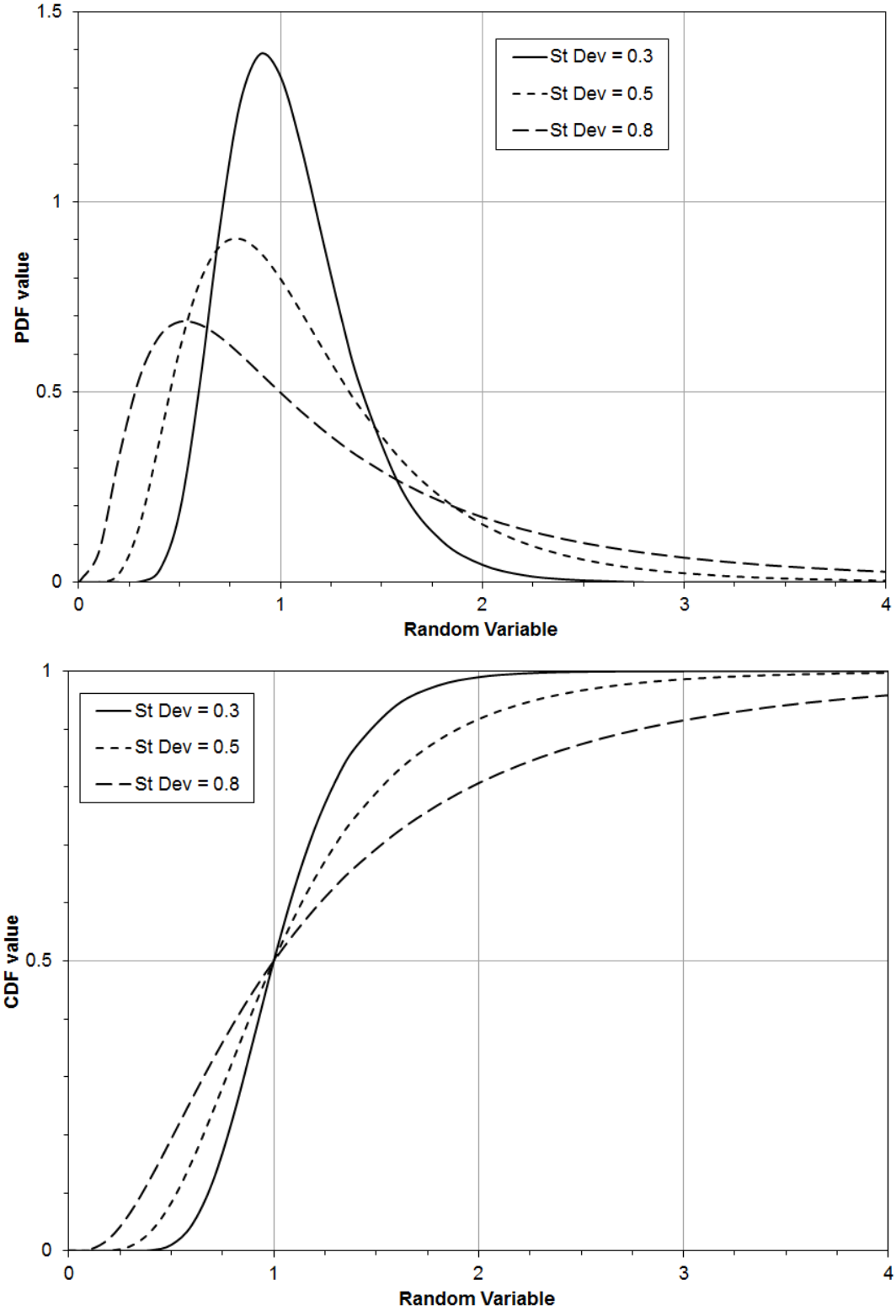

Figure 4. Lognormal Probability Functions

3.2.3 Weibull Distribution

Waloddi Weibull is credited with the introduction of the Weibull probability distribution in 1937. It was found to work well with extremely few data samples (even as few as 2 or 3). The Weibull distribution is now routinely used in reliability applications involving aircraft and propulsion system service life. Examples include:

- Fatigue life scatter in metallic alloys,
- Equivalent initial flaw size distributions,
- Crack growth rate scatter in metallic alloys.

The Weibull distribution can be a three-parameter or two-parameter distribution. The three-parameter Weibull distribution has a shape parameter α, scale parameter β, and a location parameter t_0. The Weibull distribution starts at the value of the location parameter. Thus, t_0 provides an estimate of the smallest value in the domain of the distribution. The location parameter is frequently set equal to zero for structural reliability applications; reducing to the two-parameter Weibull distribution. The PDF and CDF for the Weibull distribution are, respectively:

$$f(t) = \frac{\alpha}{\beta}\left(\frac{t-t_0}{\beta}\right)^{\alpha-1} exp\left\{-\left[\frac{t-t_0}{\beta}\right]^{\alpha}\right\}, \tag{11}$$

$$F(t) = 1 - exp\left\{-\left[\frac{t-t_0}{\beta}\right]^{\alpha}\right\}. \tag{12}$$

The mean and standard deviation of the Weibull distribution are, respectively

$$\mu = \beta\,\Gamma(1+1/\alpha) + t_0, \tag{13}$$

$$\sigma = \beta\sqrt{\Gamma\left(1+\frac{2}{\alpha}\right) - \left[\Gamma\left(1+\frac{1}{\alpha}\right)\right]^2}, \tag{14}$$

where $\Gamma(x)$ is the gamma function,

$$\Gamma(x) = \int_0^{\infty} e^{-y} y^{x-1}\, dy. \tag{15}$$

Figure 5 shows graphs of the PDF and CDF for the Weibull distribution for scale parameter (β) of 1 and three different values of shape parameter (α). (When using any program, make sure which variable is the scale parameter and which is the shape parameter.)

The two-parameter Weibull distribution is simply the case where $t_0 = 0$. When $t - t_0$ equals β, the value of the Weibull CDF is

$$F(\beta + t_0) = 1 - exp\left\{-\left(\frac{\beta}{\beta}\right)^{\alpha}\right\} = 1 - e^{-1} = 0.632. \tag{16}$$

Thus, the 2-parameter Weibull CDF at t equal to β is 0.632 regardless of the value of shape parameter α. Therefore in life calculations involving the Weibull distribution, the scale parameter β is sometimes called the characteristic life.

When the shape parameter is equal to 1, the Weibull distribution becomes equal to the exponential distribution. For a shape parameter of 2, the Weibull distribution is the Rayleigh distribution which is commonly used in dynamics. For shape parameter values between 3 and 4, the shape of the Weibull distribution is close to that of the normal distribution.

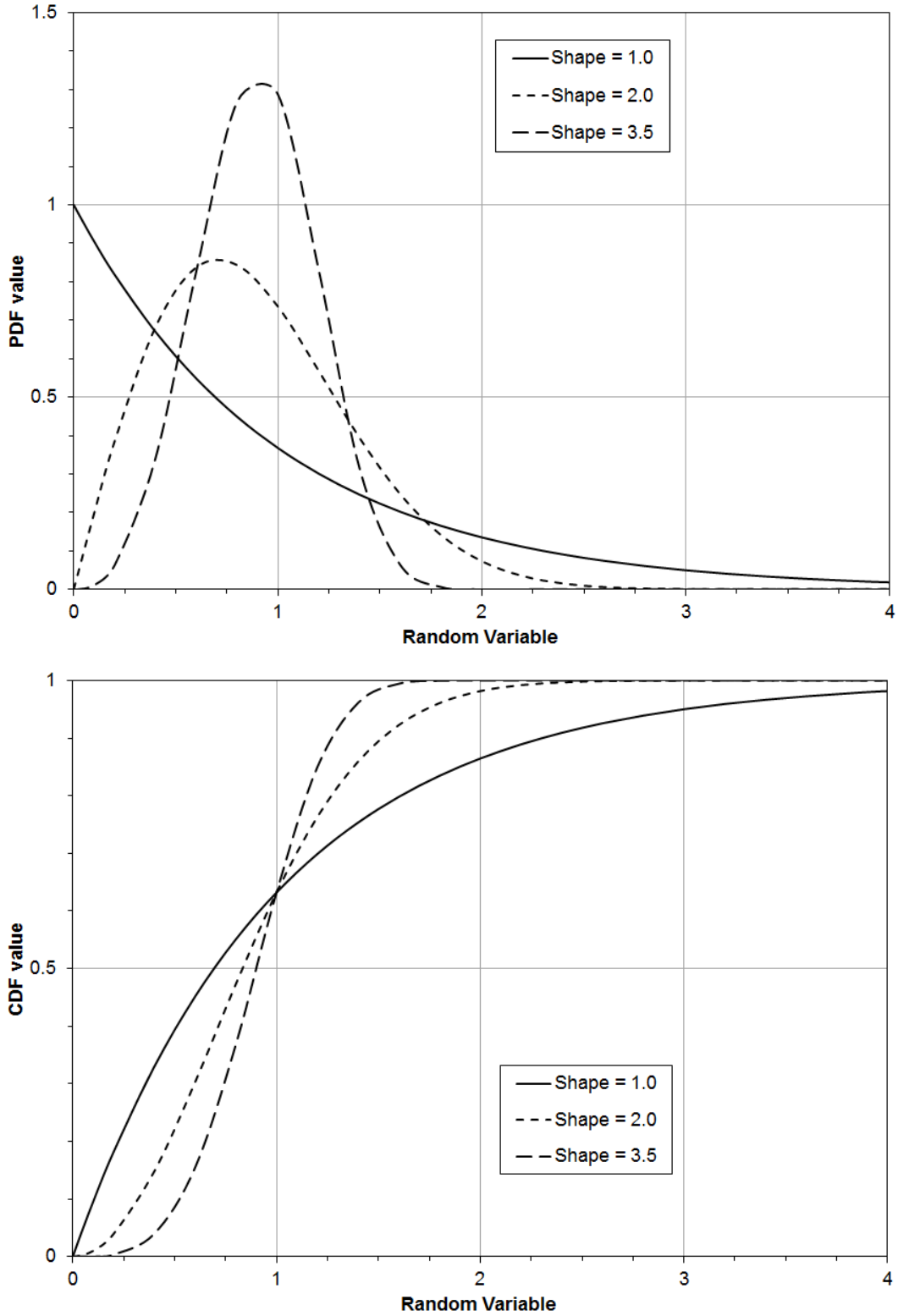

Figure 5. Weibull Probability Functions

3.2.4 Exponential Distribution

As mentioned above, the exponential distribution is the limiting case of the two- parameter Weibull Distribution with Weibull shape parameter equal to one. As a result, the exponential distribution has a single parameter, λ, sometimes called the rate parameter. The PDF and CDF of the exponential distribution are given by

$$f(t) = (1/\lambda)\, exp(-t/\lambda) \tag{17}$$

$$F(t) = 1 - exp(-t/\lambda) \tag{18}$$

Figure 6 shows graphs of the PDF and CDF for the exponential distribution for three different values of the rate parameter λ.

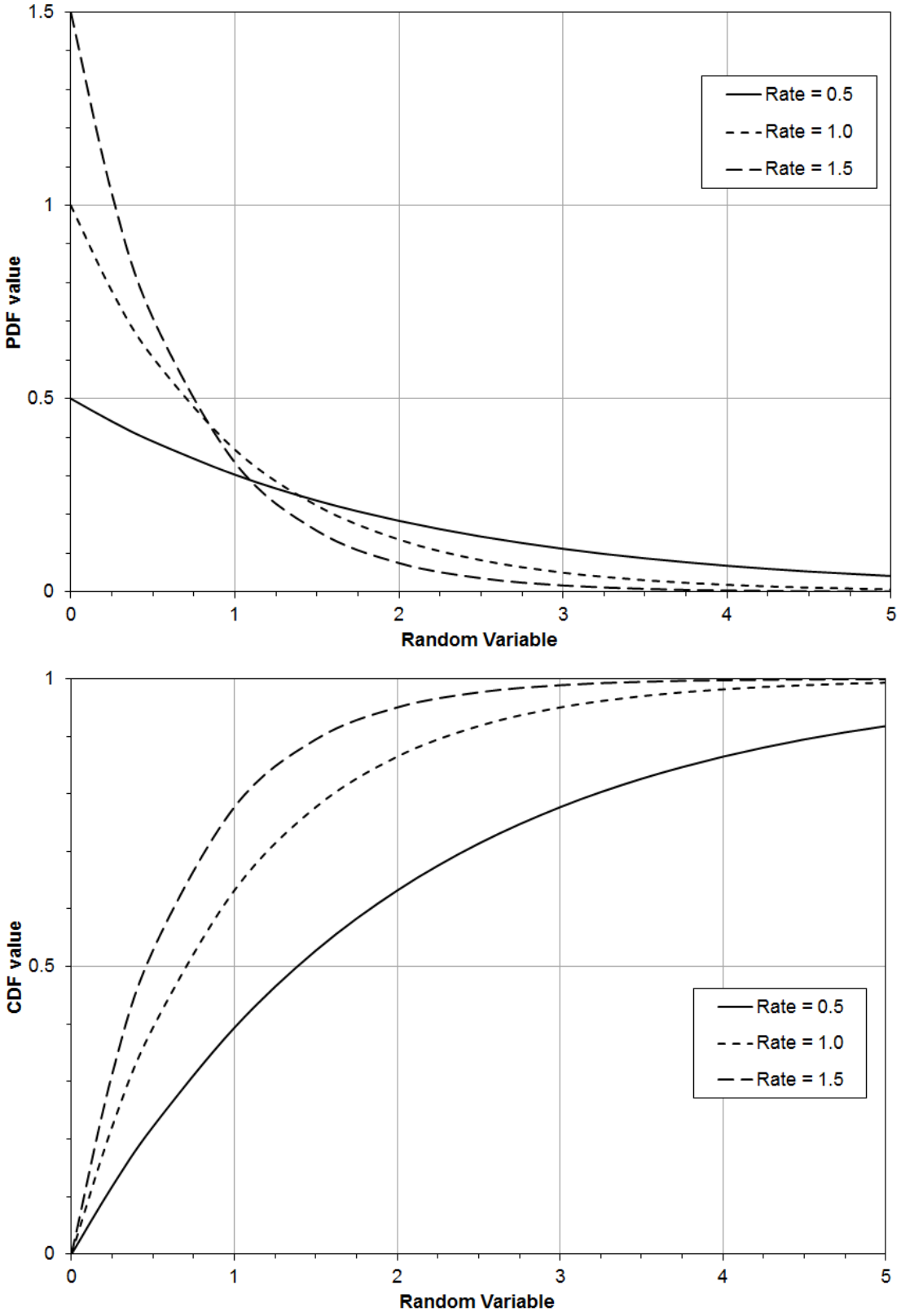

Figure 6. Exponential Probability Functions

4.0 MODELING VARIATIONS IN DATA WITH PROBABILITY DISTRIBUTIONS

An important aspect of structural reliability analysis is describing variations in observed data with a probability distribution. The focus of this section is determining the best distribution to model variability in a set of observations (test data). Sometimes, physics may guide the selection of a probability distribution. Other times, different distributions will have to be tried to see which fits the data best. Once a model probability distribution function has been selected for trial, the parameters for that distribution must be estimated. There are two approaches to accomplishing this: plotting the data on a probability graph, and analysis based on statistical theory. These approaches will be discussed in the next two sections.

4.1 Probability Plotting

Probability plotting enables the analyst to

- Visually assess the adequacy of the distribution model,
- Obtain estimates of the distribution parameters,
- Provide nonparametric estimates of the probabilities.

Data is plotted on probability graphs to estimate the distribution parameters and assess the goodness-of-fit of the distribution. Probability graphs are specifically constructed for different distribution functions, e.g., normal, lognormal, Weibull, Gumbel, etc., to produce a straight line if the data is appropriately described by that distribution.

One axis of the probability graph is either a linear or logarithmic scale corresponding to the values of the data. The other axis of the probability graph is scaled in terms of cumulative probability of the distribution for which the graph is formulated. The data are rank ordered from smallest to largest. A cumulative probability is assigned to each data point based upon its rank. The ordered pairs of data value and cumulative probability are plotted on the graph. If the plotted points lie on a straight line, or very nearly a straight line, then the slope and a point on the line can be used to find the scale and shape parameters for the distribution. Examples of probability graph formats for normal and Weibull distributions are shown in Figure 7 and Figure 8.

The probability scale in the Normal probability plot in Figure 7 is created by mapping the probability P onto the x-axis using the equation

$$x = \Phi^{-1}(P), \tag{19}$$

where $\Phi^{-1}(..)$ is the inverse of the standard normal cumulative probability function. In terms of the random variable t, the inverse probability function is

$$\Phi^{-1}(P) = \frac{t - \mu}{\sigma}, \tag{20}$$

which results in the equation

$$\sigma \cdot \Phi^{-1}(P) + \mu = t. \tag{21}$$

Thus, plotting $\Phi^{-1}(P)$ on the x-axis and the random variable t on the y-axis produces a line with slope equal to the standard deviation σ of the distribution. The value of the random variable at

which the line crosses 50 percent probability is the mean μ of the distribution. A lognormal probability graph would just change the random variable axis of the normal probability graph to a logarithmic scale. Usually the common logarithmic scale (base 10) is used since it is easier to visualize.

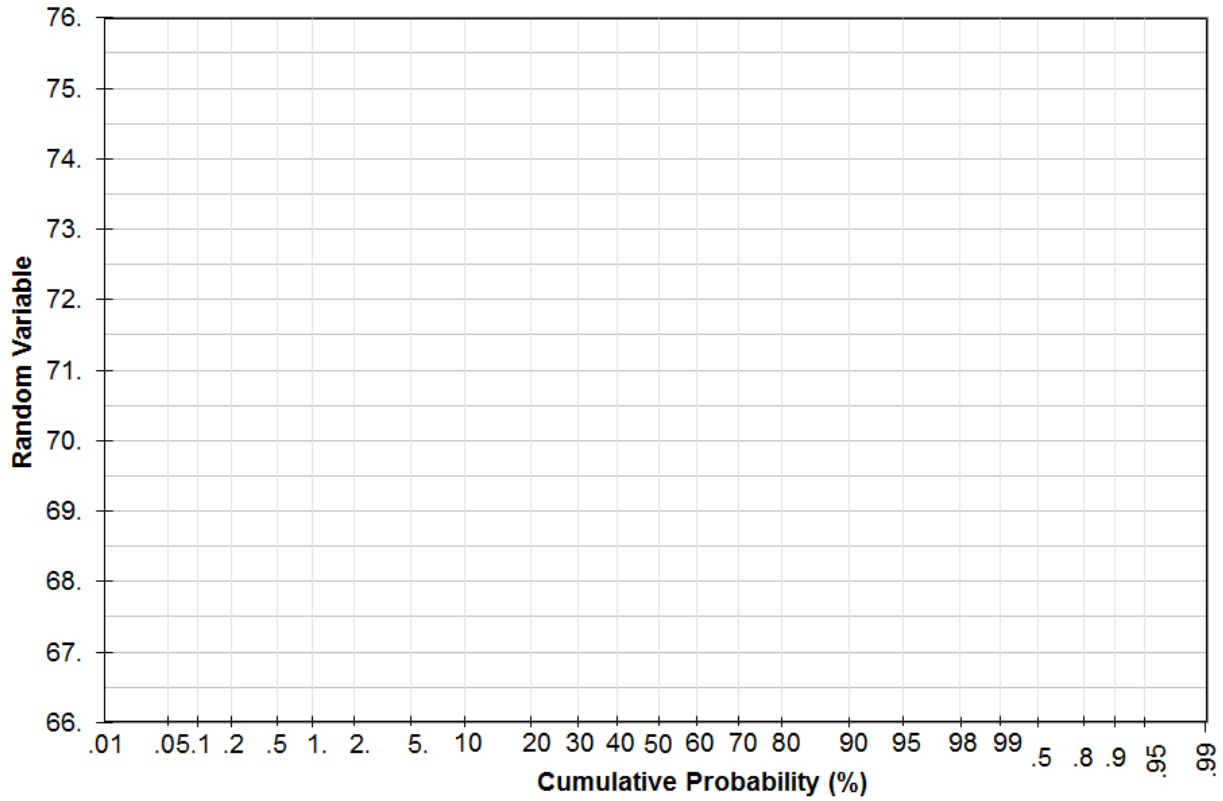

Figure 7. Normal Probability Graph Format

The probability scale for the Weibull probability graph in Figure 8 is created by mapping the probability P onto the y-axis using the function

$$y = ln\left[ln\left(\frac{1}{1-P}\right)\right], \tag{22}$$

which linearizes the Weibull distribution function as

$$ln\left\{ln\left[\frac{1}{1-P}\right]\right\} = \alpha\, ln(t) - \alpha\, ln(\beta), \tag{23}$$

or

$$y = \alpha x + b. \tag{24}$$

Thus, the logarithm of t is plotted on the horizontal axis in Figure 8. The common logarithm is used since it only differs from the natural logarithm by a constant factor.

The following example will now demonstrate how to use probability plotting to find a probability distribution for a data sample.

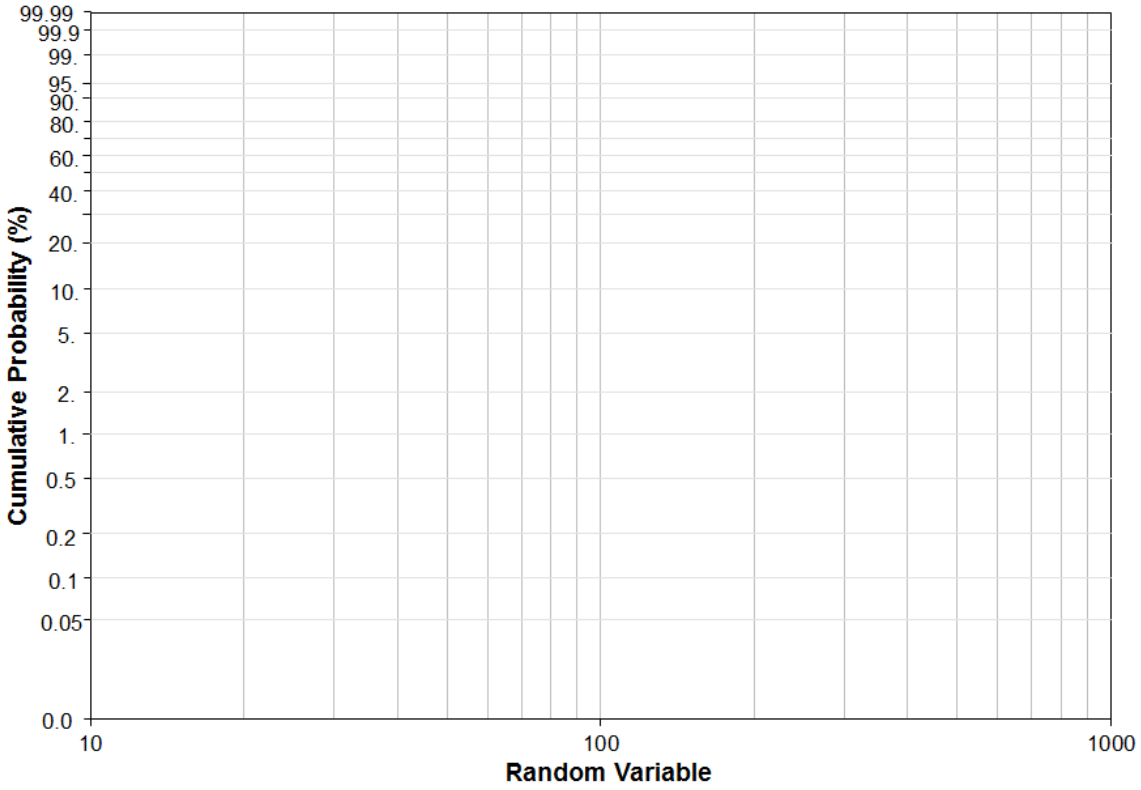

Figure 8. Weibull Probability Graph Format

4.1.1 Creating Lognormal and Weibull Probability Plots

Consider the failure times from 10 tests listed in Table 1. A lifetime distribution needs to be determined from the data. The candidate distributions are the lognormal and Weibull distributions. This will be done by plotting the data on probability plots and fitting a line to the data using a least squares estimate (LSE). The correlation coefficient will be used to determine which distribution is better at describing the variation in the failure data.

Step 1. The failure times must be ordered from smallest to largest as in Table 2. Assign an order number *i* to each failure time. The smallest failure time is 1; the largest is 10. The total number of data points is *N*.

Step 2. Estimate the cumulative probability corresponding to each failure time. There are two common ways of doing this. One is mean rank which is shown in the third column of Table 2 and calculated as

$$P = \frac{i}{N+1}. \tag{25}$$

The other method is median rank, also known as Bernard rank, which is shown in the fourth column of Table 2 and calculated as

$$P = \frac{i-0.3}{N+0.4}. \tag{26}$$

Table 1. Failure Time Results from 10 Tests

Specimen No.	Failure Time (hrs)
1	100
2	81
3	95
4	120
5	62
6	73
7	97
8	89
9	110
10	50

Table 2. Mean and Median Rank of Failure Times

Failure Time (hrs)	Order Number	Mean Rank	Median Rank
50	1	0.0909	0.0673
62	2	0.1818	0.1635
73	3	0.2727	0.2596
81	4	0.3636	0.3558
89	5	0.4545	0.4519
95	6	0.5455	0.5481
97	7	0.6364	0.6442
100	8	0.7273	0.7404
110	9	0.8182	0.8365
120	10	0.9091	0.9327

Typically, the plotting position difference between these two methods of computing rank is less than the randomness in the data [11]. Either method can be used just so that one method is consistently used when comparing data or the fit of different distributions. Median rank is preferred for the Weibull distribution, so it will be used for plotting both distributions**.**

4.1.1.1 Lognormal Probability Plot

The steps specific to constructing and analyzing a lognormal probability plot are presented in this section.

Step 3a. Plot the ordered pairs of median rank, P_i, and failure time, t_i, from Table 2 on a lognormal probability plot as in Figure 9.

Step 4a. Perform a least squares linear fit to the values $\Phi^{-1}(P_i)$ and $ln(t_i)$. The slope of the line (the standard deviation) is 0.285. The mean of the $ln(t)$ is 4.44, equivalent to a time to failure of 85.07 hours. The correlation coefficient R^2 is equal to 0.943.

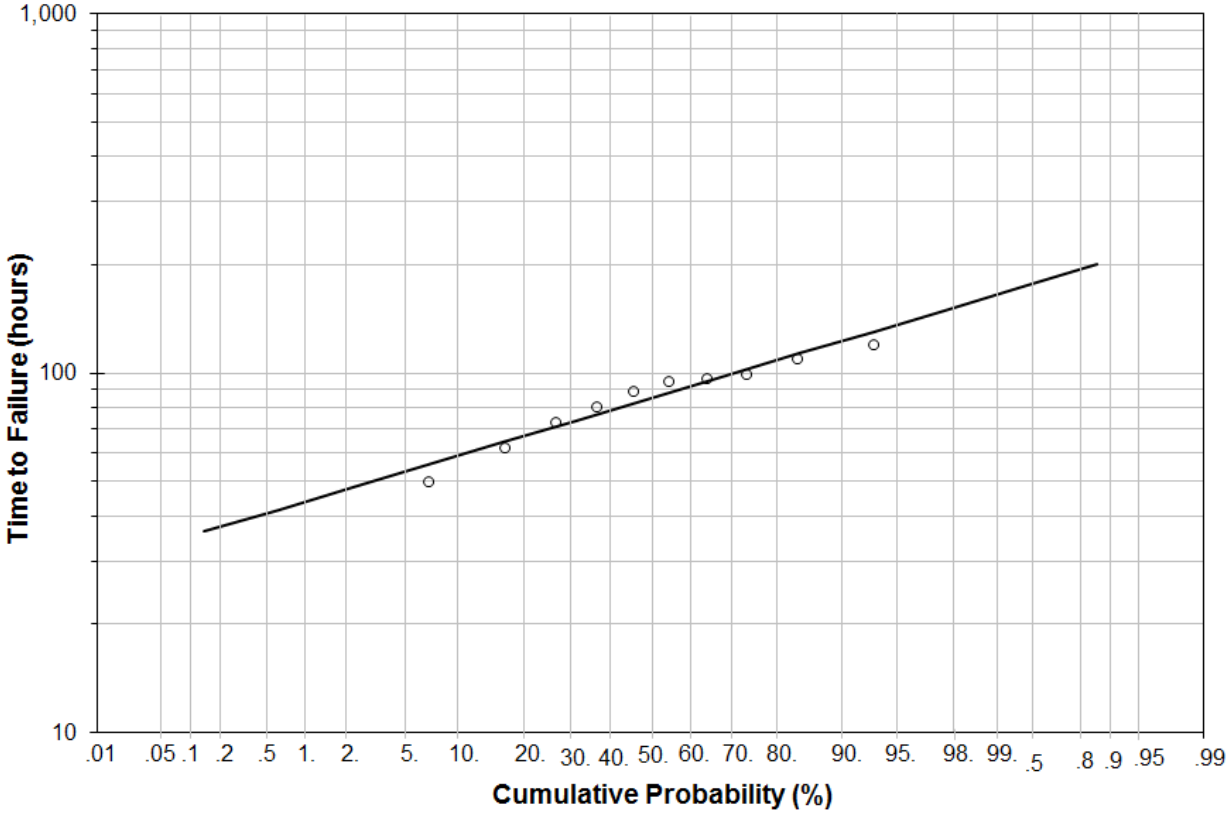

Figure 9. Lognormal Probability Plot of Failure Data

4.1.1.2 Weibull Probability Plot

The steps specific to constructing and analyzing a Weibull probability plot are presented in this section.

Step 3b. Plot the ordered pairs of median rank, P_i, and failure time, t_i, from Table 2 on a Weibull probability plot as in Figure 10.

Step 4b. Perform a least squares linear fit to the values $ln(t_i)$ and $ln(ln(1/(1-P_i)))$. The slope of the line (the shape parameter) is equal to 4.126. The failure time at a probability of 63 percent is equal to the scale parameter. For these data, the scale parameter is equal to 96.57 hours. The correlation coefficient R^2 for the fit is 0.989.

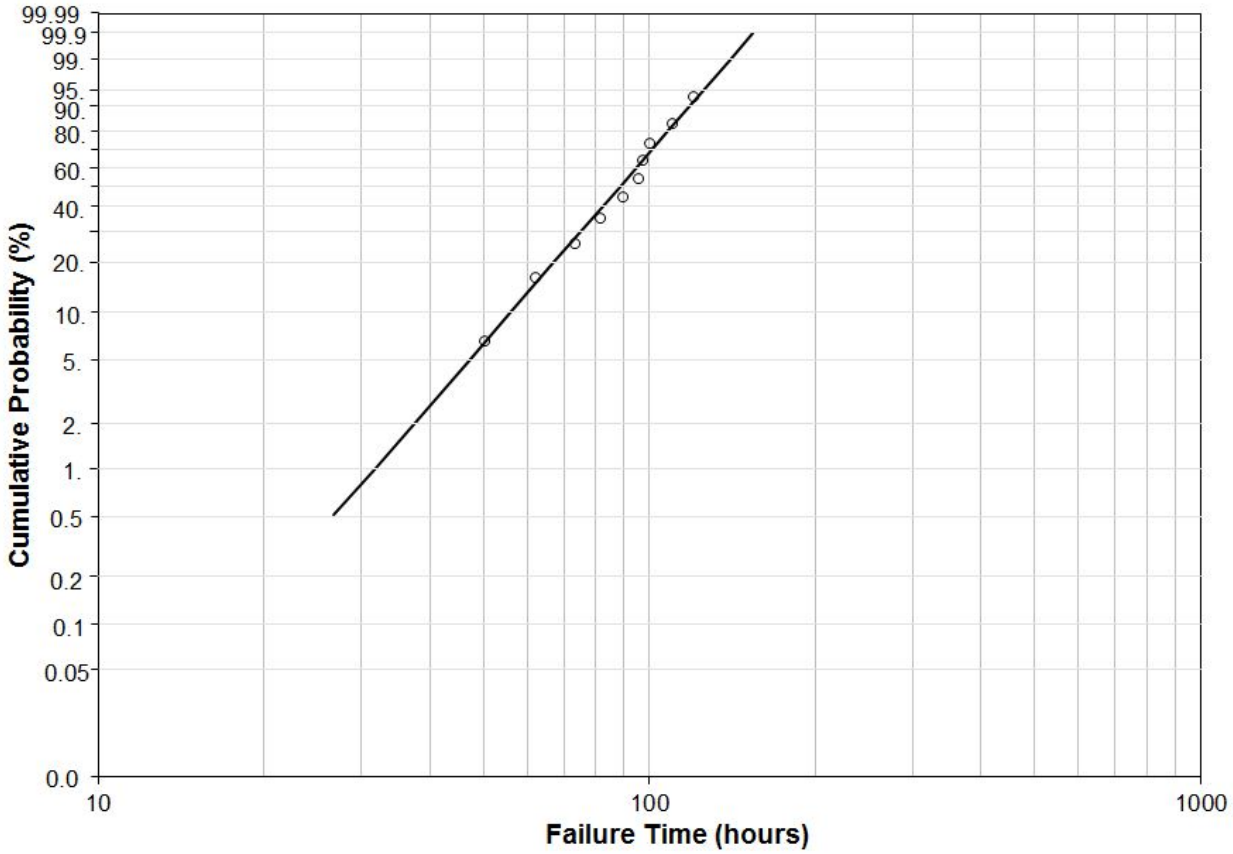

Figure 10. Weibull Probability Plot of Failure Data

4.1.2 Selecting the Best Probability Distribution Model

The probability distribution that best fits the data can be determined from the correlation coefficients R^2 for the data. Comparison of R^2 for the lognormal and Weibull probability plots shows that the failure data plots more nearly as a line on the Weibull probability plot, 0.989 versus 0.943.

4.1.3 Software-Generated Probability Plots

Probability plots can be generated in statistical software packages such as Minitab®, SuperSMITH®, etc. The plots in Figure 9 and Figure 10 were produced in Excel. Even when a probability plot is not used to fit a model distribution to a set of data, the resulting distribution should be graphed on a probability plot with the data to allow a visual assessment of how well the distribution describes the random data.

Other options exist for estimating the parameters of the distributions beside the LSE method. Maximum likelihood estimation (MLE) is the preferred option over LSE for deriving the parameters of a distribution, especially when there more than 10 data points. However, when there are fewer than 5 data points, MLE can give a biased estimate and probably should not be used [10]. When there are between 5 and 10 data points, the results of MLE should be carefully reviewed. MLE will be demonstrated in the following section.

4.2 Statistical Analysis of Data

The statistical analysis approach to determining a distribution for a data set involves four basic steps:

Step 1. Select a trial model (equation) for the distribution function. As noted, for structural reliability data, the model would likely be either a Weibull, lognormal, or normal distribution.

Step 2. Estimate the parameters of the model using standard statistical procedures – usually MLE. MLE calculates values for the parameters that are most likely to produce the observations of the data set. MLE is good for one- and two-parameter distributions. It should be used with caution for distributions with three or more parameters. MLE can be performed in Excel using the Solver utility, but statistical analysis programs, such as Minitab®, are recommended. (There are many readily available statistical analysis programs.)

Step 3. Assess the quality of the fit by calculating confidence limits and doing a statistical test for the goodness of fit.

- Confidence limits for the fit consist of an upper bound and lower bound curve. If these limits have, say, a 95 percent confidence level, then there is 95 percent confidence that any new random data point from the population would fall between the two curves. A tight confidence band is best.
- An example of a statistical goodness-of-fit test is the adjusted Anderson-Darling test, which calculates a parameter A_N^2 for comparing the fit of two or more distributions. The best fit is the one with the lowest value of A_N^2.

Step 4. Compare other models by repeating the above parameter estimation and fit tests. If the goodness-of-fit parameters differ significantly, the distribution with the better fit is generally selected. If the goodness of fit of two distributions is comparable, the distribution that gives higher probabilities in the domain of interest should be selected, or there may be physics-related reasons for selecting one over the other.

These steps will be demonstrated for a normal distribution in the following sections. The procedure for a lognormal distribution would be exactly the same, but using the logarithm of the data instead of the raw number. An example using the Weibull probability distribution is in Section 4.2.2.

4.2.1 Maximum Likelihood Estimation of Distribution Parameters

Consider the set of 34 ultimate tensile strength (UTS) results shown in Table 3. The results have been rounded to the nearest integer value of kilopounds per square inch (ksi) and ordered from smallest to largest.

Table 3. Ultimate Tensile Strength Results for 34 Tensile Specimens

Failure Stress (ksi)	Failure Stress (ksi)
67	71
68	71
68	71
69	71
69	72
69	72
69	72
70	72
70	72
70	72
70	73
70	73
70	73
71	73
71	74
71	74
71	75

These test results can be regarded as random UTS samples from a population of all material made to a particular material specification (say, 7075-T7351 Aluminum plate in a particular thickness range). This sample should include material from a variety of approved material suppliers, lots, and plates to be representative of the entire population. Assume this is the case, so that these data can be used to make statistical inferences about the UTS of this material. These values are plotted as a bar chart in Figure 11, displaying the frequency of each UTS value. The UTS values are symmetrically distributed about 71 ksi in what looks much like a normal distribution.

So, select the normal distribution as the first probability model to test against the data. Then perform a MLE of values for the mean and standard deviation of a normal distribution. This will be done using an Excel spreadsheet to illustrate the method. The spreadsheet is shown in Figure 12 and the steps are explained below.

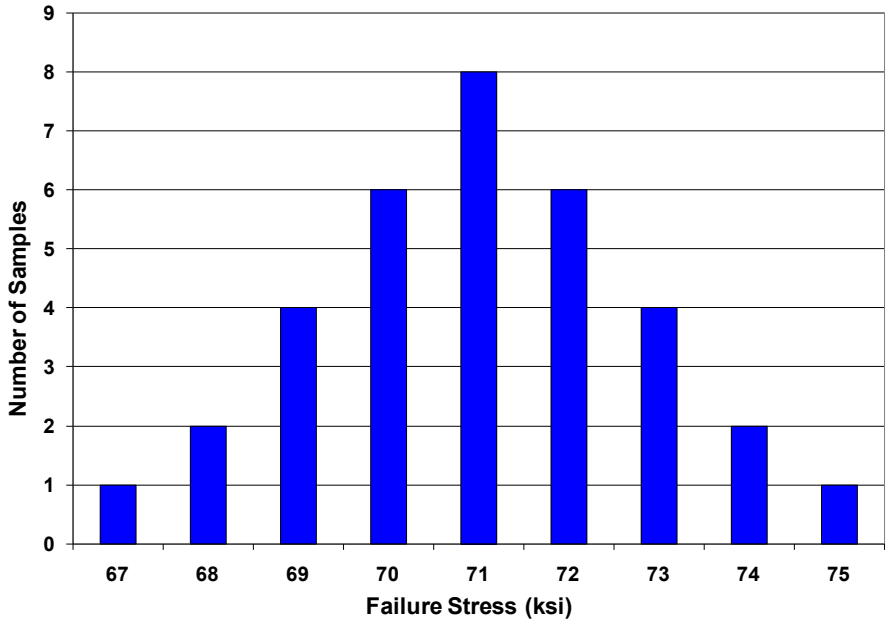

Figure 11. Frequency Plot for Tensile Strength Data

Step 1. List all of the UTS values in Col A. Although they are listed in increasing value here, it is not necessary for the MLE.

Step 2. Place initial values for the distribution mean and standard deviation in Cells B1 and B2, respectively.

Step 3. Calculate the probability of each UTS value in Cells A6 to A39 using the probability distribution chosen to model the data. In this case, the normal distribution was chosen. Cells B6 to B39 contain the normal distribution function in Excel: NORM.DIST(A6,B1,B2,FALSE) in Office 2010. Cell A6 is a specific UTS value. B1 is the mean and B2 is the standard deviation. FALSE indicates that the PDF of the Normal Distribution is to be calculated. These probability values go in the appropriate cells of Col B.

Step 4. In Col C, calculate the logarithm of the probability value in Col B. This provides numbers with magnitude greater than 1 which increases the sensitivity of the maximization algorithm that is used to find the best values for the parameters of the model distribution. In Excel, the Solver routine will be used.

Step 5. Sum all the values in cells C6 to C39 and place the value in cell C4. Maximizing this sum will also maximize the sum of all the probabilities in Col B.

Step 6. Call the Solver from the Data Tab. (The Solver is an Add-in that must be turned on by the user.) Set up the Solver to maximize Cell C4 by adjusting the values in Cells B1 and B2. Run the Solver. When the Solver has found a solution to maximize Cell C4, the values in Cells B1 and B2 are the MLE for the mean and standard deviation for a normal distribution describing this data sample.

The resulting distribution, Normal with a mean of 71.0 and standard deviation of 1.815, is compared to the data in Figure 13. The line for the distribution passes through or close to all the

data. The sample average and standard deviation can also be compared to the MLE values. The sample average is 71.0; the sample standard deviation is 1.842. The difference between the MLE and the sample standard deviations is about 2 percent and tightening the convergence criteria in the Solver for the MLE does not change its estimate of the standard deviation.

	A	B	C
1	**Mean =**	70.99999617	
2	**Std. Dev. =**	1.814957311	
3			
4		**Sum (log(P(x))) =**	-29.75362875
5	**UTS**	**P(x)**	**log(P(x))**
6	67	0.019378281	-1.71268474
7	68	0.056073712	-1.25124069
8	68	0.056073712	-1.25124069
9	69	0.119773863	-0.921637942
10	69	0.119773863	-0.921637942
11	69	0.119773863	-0.921637942
12	69	0.119773863	-0.921637942
13	70	0.188852834	-0.723876494
14	70	0.188852834	-0.723876494
15	70	0.188852834	-0.723876494
16	70	0.188852834	-0.723876494
17	70	0.188852834	-0.723876494
18	70	0.188852834	-0.723876494
19	71	0.219808079	-0.657956349
20	71	0.219808079	-0.657956349
21	71	0.219808079	-0.657956349
22	71	0.219808079	-0.657956349
23	71	0.219808079	-0.657956349
24	71	0.219808079	-0.657956349
25	71	0.219808079	-0.657956349
26	71	0.219808079	-0.657956349
27	72	0.188852394	-0.723877505
28	72	0.188852394	-0.723877505
29	72	0.188852394	-0.723877505
30	72	0.188852394	-0.723877505
31	72	0.188852394	-0.723877505
32	72	0.188852394	-0.723877505
33	73	0.119773306	-0.921639963
34	73	0.119773306	-0.921639963
35	73	0.119773306	-0.921639963
36	73	0.119773306	-0.921639963
37	74	0.056073321	-1.251243722
38	74	0.056073321	-1.251243722
39	75	0.019378101	-1.712688783

Figure 12. MLE of Normal Distribution Parameters for UTS Data

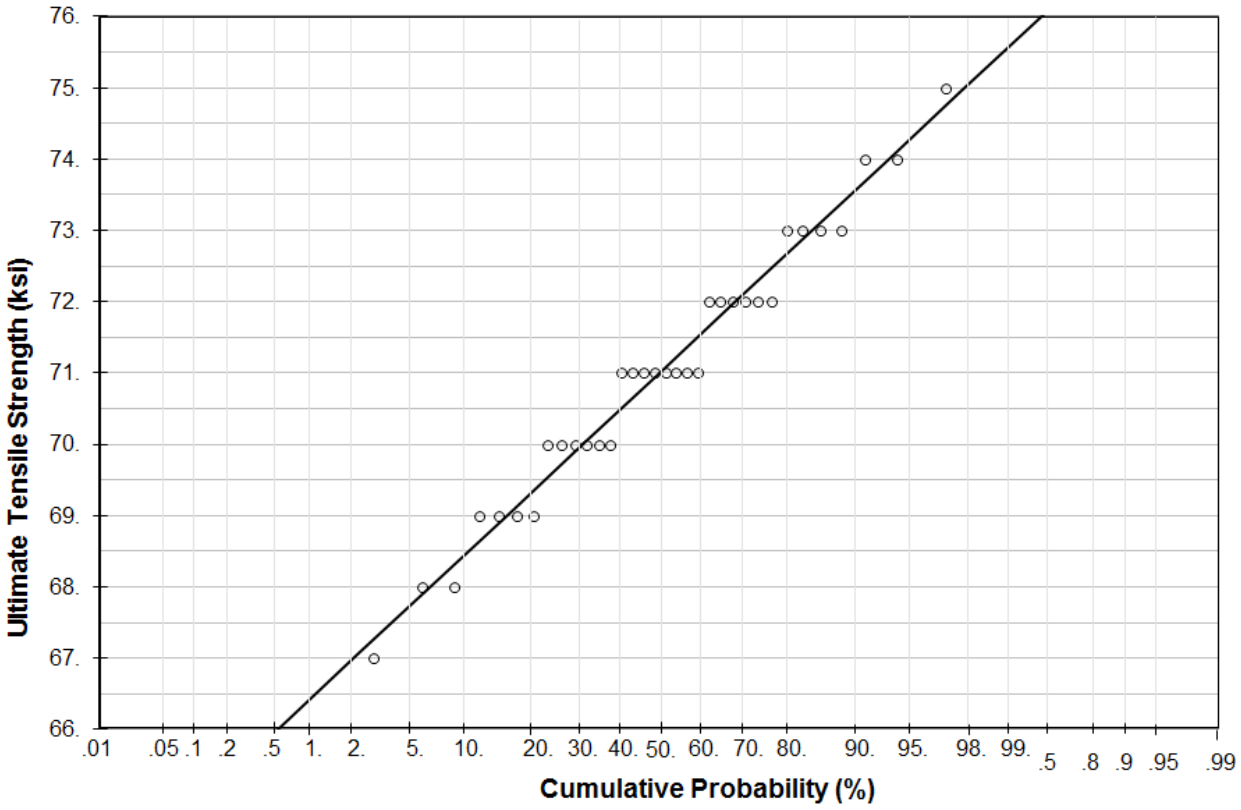

Figure 13. Graph of MLE Fit to UTS Data

4.2.2 Limitations of Least Squares and Maximum Likelihood Estimates

As mentioned in Section 4.1.3, when there are fewer than 5 data points, MLE can give a biased estimate of a distribution. MLE is the preferred option over LSE for deriving the parameters of a distribution when there are a large number of data points, usually more than 10. In this section, this point will be reinforced by considering an instance where limited data is initially available. Later, additional data becomes available. The distributions derived by LSE and MLE at both times are developed and compared.

4.2.2.1 Initial Data and Forecast

During inspections of this non-safety-of-flight titanium part over a 6 month period, cracks was discovered in 6 of 42 parts on 21 inspected aircraft. The inspection results and the flight hours when the cracks were found are presented in Table 4. The total accumulated flight hours for each part are listed in the table. A lifetime distribution was constructed using the following process in order to perform a reliability analysis to determine the magnitude of the issue. Those parts without cracks are treated as suspended, or censored, data. There are sophisticated techniques for handling suspensions [11] when the suspension times are mixed in amongst the failure times. However, sometimes it is just easier to just consider the data from failed components and ignore the suspended data. That is the approach that will be taken here. No attempt was made to adjust the flight hours to a reference crack size.

Table 4. Initial Cracking Data for Titanium Aircraft Part

A/C	Side	Flight Hours	Crack Size, in.	Side	Flight Hours	Crack Size, in.
1	LH	346.5	-	RH	346.5	-
2	LH	1424.4	-	RH	1424.4	1.05
3	LH	517.3	-	RH	517.3	-
4	LH	682.3	-	RH	682.3	-
5	LH	647.4	-	RH	647.4	-
6	LH	654.5	-	RH	654.5	-
7	LH	910.4	-	RH	910.4	-
8	LH	1249.7	2.56	RH	1249.7	-
9	LH	415.1	-	RH	415.1	-
10	LH	1116.0	4.20	RH	1158.0	1.59
11	LH	646.8	-	RH	646.8	-
12	LH	495.3	-	RH	495.3	-
13	LH	410.6	-	RH	410.6	-
14	LH	1094.6	-	RH	1094.6	-
15	LH	1125.0	-	RH	1125.0	-
16	LH	1301.0	1.00	RH	1301.0	-
17	LH	921.7	-	RH	921.7	-
18	LH	429.0	-	RH	429.0	-
19	LH	846.6	-	RH	846.6	3.20
20	LH	767.5	-	RH	767.5	-
21	LH	839.8	-	RH	839.8	-

A Weibull probability plot was constructed for the six cracked parts as shown in Figure 14. Since there were only six data points, both LSE and MLE were used to find a model Weibull distribution. The lines for these two fits are also shown in Figure 14. For the LSE fit, the shape parameter was 5.76 and the scale parameter was 1,274 FH. For the MLE fit, the shape parameter was 8.22 and the scale parameter was 1,257 FH. It appears from Figure 14 that the LSE fit provides a better fit to the data. In addition, the LSE fit provides a more conservative estimate of the POF for early failures such as at 846.6 FH.

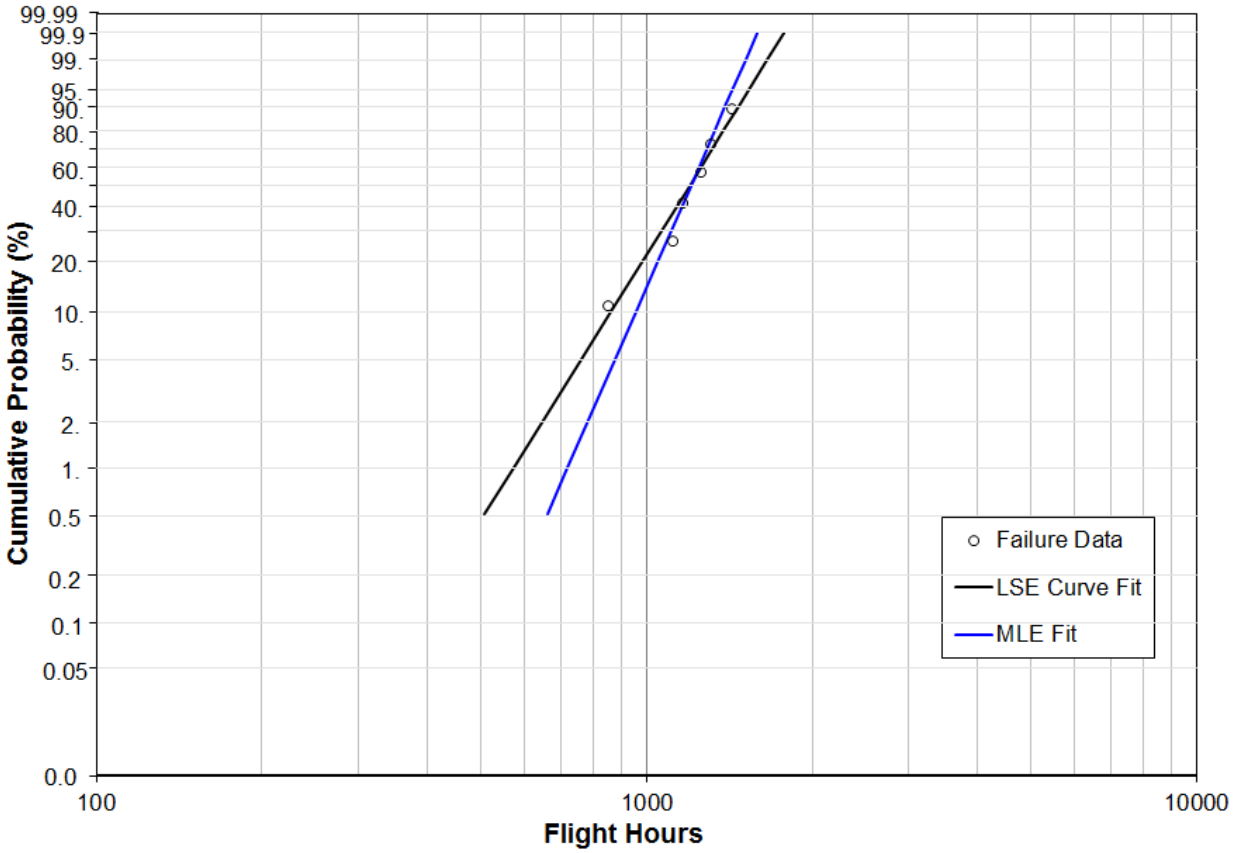

Figure 14. Weibull Probability Plot of Initial Cracking Data

4.2.2.2 Additional Data and a Revised Lifetime Distribution

Continuing inspections over the next several years resulted in cracking in all 21 affected aircraft and 41 of 42 parts. These inspection results are presented in Table 5. A revised lifetime distribution was constructed from these data for comparison to the original estimate. These data were treated as 41 cracking failures with no suspensions and without attempting to adjust the data to a common crack length in updating the lifetime distribution.

The updated LSE and MLE probability distribution fits to the data are shown on the Weibull probability plot in Figure 15. For the LSE fit, the shape parameter was 3.75 and the scale parameter was 1,453 FH. For the MSE fit, the shape parameter was 3.16 and the scale parameter was 1,468 FH. The locations of both lines have moved to the right of the initial distribution estimates. The shape parameter of the MLE fit distribution decreased by a factor of 2.5, while the shape parameter of the LSE fit distribution decreased by a factor of 1.5. The difference between the updated LSE and MLE shape parameters was less than 20 percent. Because of the large number of data points to which the Weibull distribution was fit, it is expected that the MLE provides the better fit to the data. Visually, this does not appear to be the case, but the goodness of the fit will be quantitatively determined in Section 0 on goodness-of-fit testing.

Notice in Figure 15 that the early failures (about 1,000 flight hours and less) have a steeper slope than the later failures. This usually indicates that there are different failure mechanisms acting in

these two life regimes (e.g., surface vs. subsurface crack formation, large alpha particle vs. a scratch from a drill). It could also be that those aircraft were flown more severely.

Table 5. Additional Cracking Data for Titanium Aircraft Part

A/C	Side	Date	Flight Hours	Crack Size, in.	Side	Date	Flight Hours	Crack Size, in.
1	LH	9/14/01	486.3	1.25	RH	8/12/02	874.2	1.00
2	LH	5/8/02	1619.4	4.94	RH	9/22/00	1424.4	1.05
3	LH	12/3/02	1222.9	1.30	RH	5/21/02	1222.9	1.00
4	LH	9/13/01	1033.6	1.00	RH	5/24/01	946.6	2.38
5	LH	6/9/03	1065.1	1.25	RH	1/7/05	1648.7	1.38
6	LH	-	-	-	RH	11/13/02	1018.2	0.75
7	LH	11/9/01	1429.3	3.00	RH	11/9/01	1429.3	1.90
8	LH	1/25/01	1249.7	2.56	RH	10/31/05	2311.2	1.13
9	LH	12/21/01	1000.2	2.50	RH	3/22/02	1191.2	0.84
10	LH	1/4/01	1116.0	4.20	RH	1/19/01	1158.0	1.59
11	LH	8/29/01	996.9	2.13	RH	6/13/02	1189.2	1.31
12	LH	5/10/02	1756.0	1.00	RH	10/22/01	1043.0	1.25
13	LH	4/12/02	954.8	1.87	RH	7/10/02	1139.0	1.15
14	LH	10/30/02	1520.7	1.19	RH	10/12/01	1313.6	0.63
15	LH	6/27/03	2292.0	1.13	RH	1/10/02	1772.2	1.06
16	LH	9/22/00	1301.0	1.00	RH	7/5/05	2709.8	2.09
17	LH	2/26/01	968.0	1.00	RH	3/20/01	968.0	3.50
18	LH	7/30/03	1661.4	5.63	RH	4/15/03	1477.8	0.50
19	LH	9/14/01	1127.0	0.81	RH	8/31/00	846.6	3.20
20	LH	6/10/03	1604.0	0.91	RH	10/9/01	1200.7	0.88
21	LH	10/9/01	1424.0	1.13	RH	10/9/01	1424.0	5.50

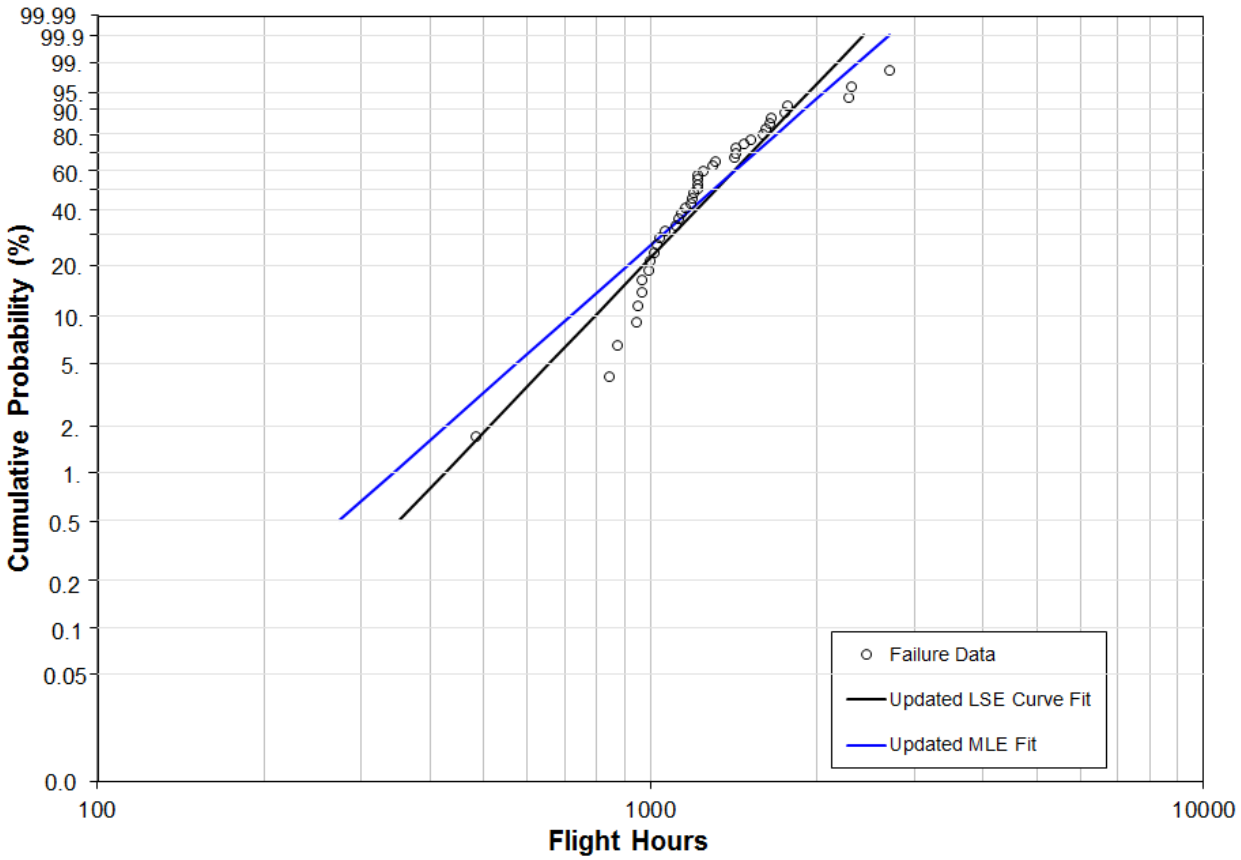

Figure 15. Updated Lifetime Distribution From Additional Cracking Data

4.2.3 Confidence Band for Normal Probability Distribution

A confidence band is used to represent the uncertainty in the estimate of a probability distribution based on limited data. Uncertainty in the probability distribution estimate decreases with an increasing amount of data resulting in a narrower confidence band. Confidence bands are approximate and are generally more accurate with more data. The real uncertainty is greater than the confidence band because assumptions were made about the data and the probability distribution used to model the data.

A confidence band is defined in terms of a confidence level *100α%* where *(1-α)* is the probability that all data in a sample of the specified size from a population will be within the confidence band. As the parameter α decreases toward zero and the confidence level increases, the width of the confidence band also increases. So, while a band with high confidence might be desired, such a confidence band may be so wide that it is of little value.

In this section, a two-sided confidence band will be determined for the normal distribution used to describe the UTS data in Figure 13. This band is for upper and lower probabilities for each value of UTS. The steps and equations used apply only to normal and log-normal distributions. The steps for determining a two-sided confidence band are as follows [11]:

Step 1. Determine the desired confidence level *100(1-α)%*. Confidence levels of 90 percent and 95 percent are common choices; 95 percent will be used in this example.

Step 2. Calculate $k_{\alpha/2}$ equal to $\Phi^{-1}(\alpha/2)$, where $\Phi^{-1}(p)$ is the inverse of the standard normal distribution (mean of 0, standard deviation of 1). The inverse of the standard normal distribution is the function that maps a probability p back to the value of the random variable x that is associated with the probability p in the standard normal function. The value $\alpha/2$ is used for a two-sided confidence bands since symmetry requires that half of the probability of being outside the confidence band be above the confidence band and half below. For this example,

$$k_{\alpha/2} = \Phi^{-1}\left(\frac{0.05}{2}\right) = -1.96. \tag{27}$$

Step 3. Choose a UTS value to calculate the values of the upper and lower confidence bands at. Then determine the standard normal variate for the value,

$$Z = \frac{x - \mu}{\sigma}, \tag{28}$$

where x is the UTS value, μ is the mean, and σ is the standard deviation. Start at one end of the curve with x equal to 66 ksi. From Section 4.2.1, the MLE mean is equal to 71 ksi, and the MLE standard deviation is 1.815. Thus,

$$Z = \frac{66 - 71}{1.815} = -2.755. \tag{29}$$

Note that Z is also the distance between the selected UTS value and the mean in units of standard deviations.

Step 4. Compute the standard normal variates associated with the left and right band probabilities for the selected UTS value using the following equations:

$$z_l \cong Z + k_{\alpha/2}\sqrt{\frac{1}{N} + \frac{Z^2}{2(N-1)}}, \tag{30}$$

$$z_r \cong Z - k_{\alpha/2}\sqrt{\frac{1}{N} + \frac{Z^2}{2(N-1)}}, \tag{31}$$

where N is the number of data points in the sample. In this example, N equals 34. For a UTS of 66 ksi,

$$z_l \cong -2.755 + (-1.96)\sqrt{\frac{1}{34} + \frac{(-2.755)^2}{2(34-1)}} = -3.50, \tag{32}$$

$$z_r \cong -2.755 - (-1.96)\sqrt{\frac{1}{34} + \frac{(-2.755)^2}{2(34-1)}} = -2.01. \tag{33}$$

Step 5. Find the probability values associated with the left and right confidence bands at the selected UTS from the standard normal distribution function. For this example, the probability P_l of the left confidence band at UTS of 66 ksi is

$$P_l = \Phi(-3.50) = 0.0002. \tag{34}$$

The probability P_r of the right confidence band at 66 ksi is

$$P_r = \Phi(-2.01) = 0.0222. \tag{35}$$

Step 6. Repeat Steps 3 through 5 to fill in the values in Table 6. The resulting confidence band is plotted as the dashed curves in Figure 16. The values in columns 1 and 3 are the *y*- and *x*-coordinates for the left dashed curve, respectively. The values in columns 1 and 5 are the *y*- and *x*-coordinates for the right dashed curve, respectively.

Table 6. Left and Right Confidence Band Probabilities

UTS	z_l	P_l	z_r	P_r
66	-3.4996	0.0002	-2.0101	0.0222
67	-2.8329	0.0023	-1.5748	0.0576
68	-2.1745	0.0148	-1.1314	0.1289
69	-1.5305	0.0629	-0.6734	0.2504
70	-0.9124	0.1808	-0.1895	0.4248
71	-0.3361	0.3684	0.3361	0.6316
72	0.1895	0.5752	0.9124	0.8192
73	0.6734	0.7496	1.5305	0.9371
74	1.1314	0.8711	2.1745	0.9852
75	1.5748	0.9424	2.8329	0.9977
76	2.0101	0.9778	3.4996	0.9998

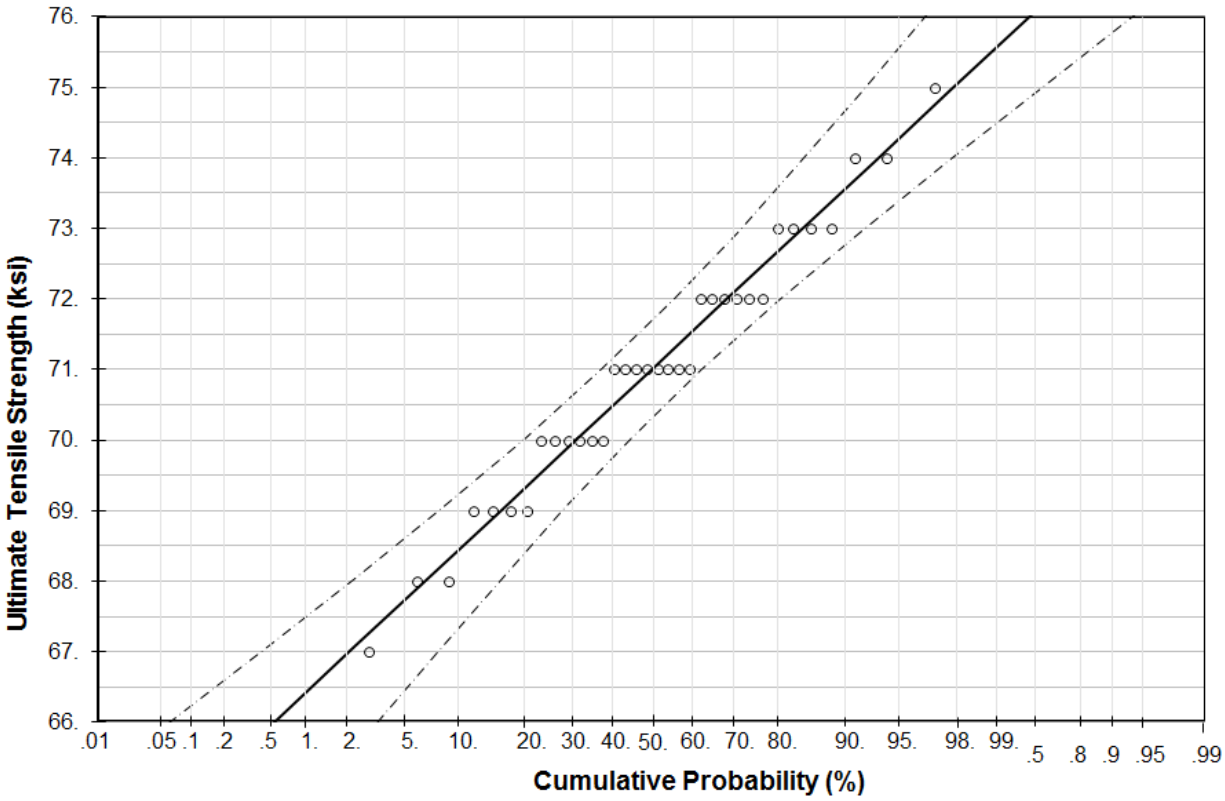

Figure 16. Plot of Confidence Band for UTS Data

4.2.4 Goodness-of-Fit Test

Goodness-of-fit tests are a quantitative measure of whether the selected probability distribution fits the data. A goodness-of-fit test produces a single number that is compared against a criterion to determine if the probability distribution adequately describes the variation in the data. When two or more distributions satisfy the criterion, the numbers for each distribution provide a means to determine which distribution provides the best fit.

There are many goodness-of-fit tests: correlation coefficient, likelihood ratio, chi-squared, Kolmogorov-Smirnov (KS), Anderson-Darling (AD), Cramer-von Mises (CvM), etc. Each test has its own strengths and weaknesses. For those distributions that can be plotted as a on a probability plot, the correlation coefficient, R^2, provides a measure of the goodness of fit, i.e., how linear the data is. When MLE is used to find the distribution parameters for more than one probability distribution, the distribution with the largest probability (cell C4 in Figure 12) is the distribution that best fits the data.

The KS, AD, and CvM tests are all very similar. They are based on the empirically determined distribution function. They are only valid for continuous distributions that are completely specified, though all three have been modified to handle situations where the distribution parameters are estimated from the data sample. The difference between these three tests is their test statistics. Thus, the critical values for establishing that the fit of a distribution is acceptable are different. But all three tests should yield the same conclusion though they each may be more discriminating for a particular distribution type. The AD and CvM tests have an advantage over

the KS test in that they can be modified to handle censored samples where testing may have been stopped without a failure. Because of this advantage, the AD test will be demonstrated here.

4.2.4.1 Anderson-Darling Goodness-of-Fit Test

The forty-one fatigue cracking data in Table 5 and the two Weibull probability distributions constructed using LSE and MLE in Section 4.2.2.2 will be used to demonstrate the AD test. The calculation of the AD test parameter is shown in Table 7 and explained step-by-step in the text that follows.

Step 1. List all the FH to cracking, t_i, from smallest to largest in the first column. Place the rank i for each cracking time in the second column. The total number of data points N is 41.

Step 2. Calculate the quantity $(2i - 1)/N$ for each cracking time in the third column.

Step 3. Calculate the expected probability $F(t_i)$ for each cracking time using the CDF for which the goodness-of-fit is being tested. The values are placed in the fourth column. In this example, the distribution being tested is a Weibull distribution with shape parameter of 3.16 and scale parameter of 1,468 FH.

Step 4. In the fifth column, calculate the natural logarithm of each of the expected probabilities, $ln[F(t_i)]$, from the fourth column.

Step 5. Calculate the natural logarithm of 1 minus the expected probability for the cracking time with rank N+1-i, $ln[1\text{-}F(t_{N+1-i})]$, in the sixth column. For example, for t_i equal to 486.3 FH, rank i equals 1, calculate the natural logarithm of 1 minus the expected probability for the cracking time with rank 41, or t_i equal to 2,709.8 FH.

Step 6. For each row in the table, calculate the quantity

$$A_i = \left(\frac{2i-1}{N}\right)\{ln[F(UTS_i)] + ln[1 - F(UTS_{N+1-i})]\} \tag{36}$$

in the seventh column, that is the value in column 3 times the sum of the values in columns 5 and 6.

Step 7. Calculate the Anderson-Darling goodness-of-fit statistic as the sum of column 7 minus the number of data points N,

$$A_N^2 = -\sum_{i=1}^{N} A_i - N. \tag{37}$$

Step 8. Compare the Anderson-Darling goodness-of-fit statistic, A_N^2, to the allowable critical percentile value, $A_{cr}^2(\alpha)$, for a specified significance level α from Table 8. If A_N^2 is less than $A_{cr}^2(\alpha)$, the test distribution is accepted at that level of significance. A significance level of 0.05 is frequently chosen. For this example, the goodness-of-fit statistic is 1.7224 which is less than the allowable critical value at all significance levels except α equal to 0.15. The Weibull distribution with shape parameter of 3.16 and scale parameter of 1,468 FH provides a good representation of the times when fatigue crack were found.

Table 7. Anderson-Darling Goodness-of-Fit Test for MLE Weibull Distribution

		Shape =	3.16			
N =	41	Scale =	1468		$A^2_N = -\Sigma A_i - N =$	1.7224
FH @ Cracking, t_i	Rank, i	$(2i-1)/N$	$F(t_i)$	$\ln[F(t_i)]$	$\ln[1- F(t_{N+1-i})]$	A_i = Col 3 * [Col 5 + Col 6]
486.3	1	0.0244	0.0300	-3.5065	-6.9379	-0.2547
846.6	2	0.0732	0.1611	-1.8259	-4.1964	-0.4407
874.2	3	0.1220	0.1766	-1.7336	-4.0872	-0.7099
946.6	4	0.1707	0.2212	-1.5089	-1.8132	-0.5672
954.8	5	0.2195	0.2265	-1.4850	-1.7613	-0.7126
968	6	0.2683	0.2353	-1.4470	-1.4786	-0.7849
968	7	0.3171	0.2353	-1.4470	-1.4432	-0.9164
996.9	8	0.3659	0.2550	-1.3665	-1.3637	-0.9988
1000.2	9	0.4146	0.2573	-1.3575	-1.3231	-1.1115
1018.2	10	0.4634	0.2700	-1.3094	-1.1179	-1.1248
1033.6	11	0.5122	0.2811	-1.2692	-1.0212	-1.1731
1043	12	0.5610	0.2879	-1.2451	-0.9190	-1.2140
1065.1	13	0.6098	0.3043	-1.1898	-0.9190	-1.2859
1116	14	0.6585	0.3433	-1.0692	-0.9083	-1.3023
1127	15	0.7073	0.3519	-1.0444	-0.7039	-1.2366
1139	16	0.7561	0.3614	-1.0177	-0.6828	-1.2857
1158	17	0.8049	0.3766	-0.9766	-0.6012	-1.2699
1189.2	18	0.8537	0.4019	-0.9116	-0.5636	-1.2593
1191.2	19	0.9024	0.4035	-0.9075	-0.5630	-1.3271
1200.7	20	0.9512	0.4113	-0.8884	-0.5614	-1.3791
1222.9	21	1.0000	0.4296	-0.8449	-0.5614	-1.4063
1222.9	22	1.0488	0.4296	-0.8449	-0.5299	-1.4418
1224	23	1.0976	0.4305	-0.8428	-0.5167	-1.4921
1224.4	24	1.1463	0.4309	-0.8420	-0.5140	-1.5544
1249.7	25	1.1951	0.4519	-0.7944	-0.4726	-1.5141
1301	26	1.2439	0.4948	-0.7037	-0.4485	-1.4332
1313.6	27	1.2927	0.5053	-0.6825	-0.4337	-1.4430
1424	28	1.3415	0.5968	-0.5162	-0.4205	-1.2565
1429.3	29	1.3902	0.6011	-0.5090	-0.3628	-1.2120
1429.3	30	1.4390	0.6011	-0.5090	-0.3396	-1.2211
1477.8	31	1.4878	0.6399	-0.4465	-0.3300	-1.1553
1520.7	32	1.5366	0.6730	-0.3960	-0.3147	-1.0920
1604	33	1.5854	0.7337	-0.3097	-0.2975	-0.9625
1619.4	34	1.6341	0.7443	-0.2953	-0.2944	-0.9637
1648.7	35	1.6829	0.7638	-0.2694	-0.2682	-0.9048
1661.4	36	1.7317	0.7720	-0.2587	-0.2682	-0.9125
1756	37	1.7805	0.8282	-0.1885	-0.2568	-0.7930
1772.2	38	1.8293	0.8369	-0.1781	-0.2499	-0.7830
2292	39	1.8780	0.9832	-0.0169	-0.1944	-0.3968
2311.2	40	1.9268	0.9849	-0.0152	-0.1756	-0.3676
2709.8	41	1.9756	0.9990	-0.0010	-0.0305	-0.0621

Table 8. Allowable Critical Percentile Values for Anderson-Darling Test Statistic

Significance, α	0.15	0.10	0.05	0.025	0.01
$A^2_{cr}(\alpha)$	1.610	1.933	2.492	3.070	3.857

4.2.4.2 Comparing Two Model Distributions with the Anderson-Darling Goodness-of-Fit Test

Recall from Section 4.2.2.2 that the LSE fit to the cracking data in Table 5 gave a shape parameter of 3.75 and a scale parameter of 1,453 FH, instead of the MLE values of 3.16 and 1,468 FH. The AD goodness-of-fit test can be used to determine which of these two distributions provide the better model for the cracking data. The model distribution with the lowest value of A^2_N provides the better fit. From Table 7, the value of A^2_N for the Weibull distribution with MLE parameters is 1.7224. A^2_N is calculated below in Table 9 for the Weibull distribution with LSE-derived parameters. In this case, A^2_N is equal to 1.6922. Thus, the LSE fit Weibull distribution provides a slightly better fit to the crack data in Table 5 than does the MLE. This is despite the fact that with more data MLE is supposed to provide the better fit.

4.2.5 Statistical Analysis in Statistical Software

There are many statistical software packages available that can perform the statistical analysis of data and provide plots of the results. Among these are Minitab®, SuperSMITH®, and Crystal Ball. In addition, templates can be created in Excel to perform these analyses.

Table 9. Anderson-Darling Goodness-of-Fit Test for LSE Weibull Distribution

		Shape =	3.75			
N =	41	Scale =	1453		$A^2_N = -\Sigma A_i - N =$	1.6922
FH @ Cracking, t_i	Rank, i	$(2i-1)/N$	$F(t_i)$	$\ln[F(t_i)]$	$\ln[1- F(t_{N+1-i})]$	A_i = Col 3 * [Col 5 + Col 6]
486.3	1	0.0244	0.0164	-4.1128	-10.3519	-0.3528
846.6	2	0.0732	0.1236	-2.0908	-5.7003	-0.5701
874.2	3	0.1220	0.1382	-1.9788	-5.5247	-0.9151
946.6	4	0.1707	0.1817	-1.7055	-2.1058	-0.6507
954.8	5	0.2195	0.1871	-1.6763	-2.0346	-0.8146
968	6	0.2683	0.1959	-1.6301	-1.6530	-0.8808
968	7	0.3171	0.1959	-1.6301	-1.6061	-1.0261
996.9	8	0.3659	0.2161	-1.5320	-1.5017	-1.1099
1000.2	9	0.4146	0.2185	-1.5211	-1.4488	-1.2314
1018.2	10	0.4634	0.2317	-1.4624	-1.1862	-1.2274
1033.6	11	0.5122	0.2433	-1.4134	-1.0655	-1.2697
1043	12	0.5610	0.2506	-1.3840	-0.9402	-1.3038
1065.1	13	0.6098	0.2681	-1.3166	-0.9402	-1.3761
1116	14	0.6585	0.3105	-1.1697	-0.9272	-1.3809
1127	15	0.7073	0.3200	-1.1394	-0.6851	-1.2905
1139	16	0.7561	0.3306	-1.1070	-0.6608	-1.3366
1158	17	0.8049	0.3475	-1.0569	-0.5682	-1.3080
1189.2	18	0.8537	0.3761	-0.9779	-0.5263	-1.2841
1191.2	19	0.9024	0.3779	-0.9730	-0.5256	-1.3524
1200.7	20	0.9512	0.3868	-0.9498	-0.5239	-1.4018
1222.9	21	1.0000	0.4078	-0.8970	-0.5239	-1.4209
1222.9	22	1.0488	0.4078	-0.8970	-0.4891	-1.4537
1224	23	1.0976	0.4088	-0.8945	-0.4747	-1.5028
1224.4	24	1.1463	0.4092	-0.8935	-0.4717	-1.5651
1249.7	25	1.1951	0.4335	-0.8359	-0.4270	-1.5093
1301	26	1.2439	0.4835	-0.7266	-0.4013	-1.4030
1313.6	27	1.2927	0.4959	-0.7013	-0.3857	-1.4051
1424	28	1.3415	0.6043	-0.5036	-0.3717	-1.1743
1429.3	29	1.3902	0.6094	-0.4952	-0.3120	-1.1223
1429.3	30	1.4390	0.6094	-0.4952	-0.2884	-1.1277
1477.8	31	1.4878	0.6555	-0.4224	-0.2788	-1.0433
1520.7	32	1.5366	0.6946	-0.3644	-0.2636	-0.9649
1604	33	1.5854	0.7652	-0.2677	-0.2465	-0.8152
1619.4	34	1.6341	0.7772	-0.2520	-0.2435	-0.8097
1648.7	35	1.6829	0.7993	-0.2240	-0.2180	-0.7439
1661.4	36	1.7317	0.8085	-0.2125	-0.2180	-0.7456
1756	37	1.7805	0.8693	-0.1401	-0.2071	-0.6182
1772.2	38	1.8293	0.8783	-0.1298	-0.2005	-0.6042
2292	39	1.8780	0.9960	-0.0040	-0.1488	-0.2869
2311.2	40	1.9268	0.9967	-0.0034	-0.1319	-0.2606
2709.8	41	1.9756	1.0000	0.0000	-0.0165	-0.0327

5.0 LIFETIME DISTRIBUTIONS FROM ACTUAL FAILURE DATA

5.1 Overview

This section discusses how to construct the lifetime distribution for a population of engineering structures using failure data. This approach does not consider the underlying physics of the failure. It is based entirely on the time to failure and an assumption that all items in the population are similar.

The probability distribution constructed in the probability plotting example of Section 4.1 is a lifetime distribution constructed from failure data. The available data were times to failure during a test. The goal was to construct the lifetime distribution from estimates of the probability of failure as a function of the test time.

The failure data can be from tests or actual service. Time can be expressed in terms of number of flight hours, number of flights, number of landings, etc. The Weibull distribution is frequently chosen to model the lifetime distribution from failure data. The lognormal and exponential distributions are also sometime used. The normal distribution is rarely used because it allows the possibility of having a failure before the part goes into service.

This section also includes demonstrations of how the lifetime distribution can be used to make decisions regarding maintenance, modification and retirement of aircraft.

5.2 Estimating the Lifetime Distribution

5.2.1 Estimating Distribution Parameters

Situations in which a single failure point, such as in a full-scale durability test, is all that is available to construct a lifetime distribution are common. When a single failure occurs, it is reasonable to interpret the observed test life as the mean of the probability distribution. Unless there are reasons to suspect an early failure, a random sample is most likely to fail within +1 and -1 standard deviation of the mean life since a majority of the population should fail within one standard deviation of the mean.

This assumption is conservative if the test article has two or more independent equivalent details – symmetric right- and left-hand sides for example. In that case, a more rigorous estimate of the population percentile represented by the first failure can be obtained from Bernard's median rank equation (Section 4.1.1). Accordingly, the estimated population percentile of the first of two equivalent details to fail is the median rank value

$$MR = \frac{(1-0.3)}{(2+0.4)} \times 100\% = 29.2\%. \tag{38}$$

Thus, the first test failure in this situation is an estimator for the 29.2 percentile population value.

The above not withstanding, a single test failure will be assumed to be an estimator of the population mean. The Weibull scale parameter (β) can be calculated from the test-estimated mean (μ) and the shape parameter using Equation (13), which is repeated here:

$$\mu = \beta\, \Gamma(1+1/\alpha) + t_0, \tag{13}$$

In Microsoft Excel, the value of the gamma function can be found using the following expression:

$$\Gamma(1+1/\alpha) = exp(\text{GAMMALN}(1+1/\alpha)) \quad (39)$$

Table 10 provides the values of $\Gamma(1+1/\alpha)$ for several different values of the shape parameter α.

Table 10. $\Gamma(1+1/\alpha)$ Values for Select Values of α

Shape Parameter, α	$1 + 1/\alpha$	$\Gamma(1+1/\alpha)$
2	1.5	0.88623
2.5	1.4	0.88726
3	1.33333	0.89298
3.5	1.28571	0.89975
4	1.25	0.90640
4.5	1.22222	0.91257

When there is only one test result or observation, the shape parameter α must be assumed. Freudenthal [12] has proposed the following characteristic Weibull shape parameters for aerospace metallic materials:

- High strength steels (F_{tu} > 200 ksi): α = 2.0 to 2.5,
- Titanium alloys: α = 2.5 to 3.0,
- Low strength steels (F_{tu} < 200 ksi): α = 3.0 to 3.5,
- Aluminum alloys: α = 3.5 to 4.5.

The recommendations are based upon alloys and fabrication techniques from the 1960's and 1970's, or earlier. It is possible that developments in alloy processing have changed the scatter in some material properties. It is also possible that fabrication practices dominate the scatter in structure, not some material characteristic. These observations, along with the fact that statistical conclusions drawn from a single data point are always suspect, should be kept in mind when using the Freudenthal shape parameter values. They are good estimates when there is not enough information to determine a shape parameter, but they are not absolute limits.

In Section 3.2.3, it was noted that a shape parameter of 2 produced a Rayleigh distribution and a shape parameter in the range of 3 to 4 produced a symmetric distribution very similar in shape to a normal distribution. The suggested shape parameters for all these materials are in this range. Thus, the characteristic shape parameter for aluminum alloys and low strength steel produce a symmetric (close to a normal) distribution. While the characteristic shape parameter for titanium and high strength steel alloys produce Rayleigh–like distributions that are skewed in the direction of more frequent earlier failures.

5.2.2 Weibull Distribution: Estimated from a Single Failure

The Forward Main Landing Gear (MLG) trunnion collar (Figure 17) failed during the full-scale landing gear durability test after 2,310 simulated landings. The root cause was fatigue, originating at the threads. The crack depth at failure was only 0.04 inches. The life deficiency was confirmed by an element test of the trunnion.

The trunnion collar threads are loaded in tension and have a root radius of 0.005 inches to 0.009 inches. Due to the tolerance on root radius, the stress concentration factor (K_T) ranges from 10 to 13. This wide variation in peak stress causes increased fatigue scatter.

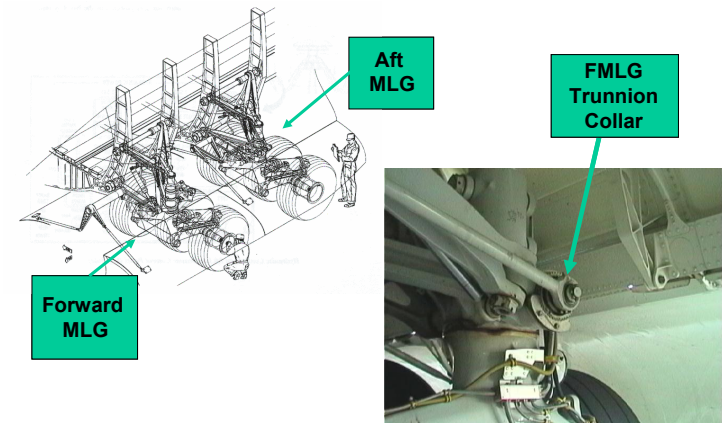

Figure 17. Forward Main Landing Gear Trunnion

At the time of test failure, 31 aircraft were already in service. The purpose was to determine current risk and how it would increase as the 31 aircraft continued to operate. A Weibull distribution was assumed. With only a single failure point, the parameters of the distribution were estimated as follows.

Since only the test failure time was known, two assumptions had to be made in the analysis:

- The trunnion collar was made from 300M steel with F_{tu} = 280 ksi. A Weibull shape parameter of $\alpha = 2.0$ was assumed, the lower bound of the "typical range" for the material which represents more scatter than 2.5, the upper bound of the typical range.
- The durability test failure time was assumed to be the mean (50 percent) of the distribution. Equation (13) was used to find the scale parameter, or characteristic life:

$$\beta = \frac{\mu}{\Gamma\left(1+\frac{1}{2}\right)} = \frac{2310}{0.88623} = 2{,}605 \text{ landings.} \qquad (40)$$

Using $\alpha = 2.0$ and β = 2,605 landings, the probability of a trunnion collar failure was calculated for a single Forward MLG on each of the 31 aircraft at the current number of landings as shown in Table 11. Accounting for two forward trunnions on each aircraft (right-side and left-side), the summation for the fleet gave an expected number of ($2 \times 1.3 =$) 2.6 failed trunnion collar in the fleet for the number of landings at that point in time. Recall from Section 2.1 that Lincoln felt that more than 1 failure in a fleet during the service life was not acceptable. Lincoln recommended that the number of failures in the fleet be kept below 0.5 to ensure this. Clearly, the present design does not meet this criterion.

Table 11. Fleet Status and Expected Trunnion Failures Calculation

Aircraft	Landings	*F(t)*
1	630	0.05681
2	683	0.06643
3	379	0.02094
4	700	0.06966
5	690	0.06775
6	600	0.05167
7	733	0.07612
8	600	0.05167
9	700	0.06966
10	552	0.04391
11	600	0.05167
12	166	0.00405
13	648	0.06000
14	500	0.03617
15	500	0.03617
16	794	0.08872
17	506	0.03703
18	855	0.10213
19	511	0.03775
20	484	0.03393
21	563	0.04564
22	542	0.04237
23	362	0.01913
24	640	0.05857
25	278	0.01132
26	670	0.06401
27	200	0.00588
28	200	0.00588
29	100	0.00147
30	100	0.00147
31	51	0.00038
$\Sigma F(t)$ =		1.31836

The other criterion is based upon the SFPOF. From Sections 3.1.7 and 3.1.8, the SFPOF is equal to the HRF, Equation (5), times a Δt of one flight. For a Weibull distribution (Section 3.2.3), the HRF is equal to

$$h_T(t) = \left(\frac{\alpha}{\beta}\right) \times \left(\frac{t}{\beta}\right)^{(\alpha-1)}. \tag{41}$$

In this example, with $\alpha = 2$ and $\beta = 2{,}605$ landings, the SFPOF becomes, in terms of number of aircraft landings, t:

$$\text{SFPOF} = \Delta t \cdot h_T(t) = 2.95 \times 10^{-7} \times t. \quad (42)$$

After one landing, the estimated SFPOF is greater than the value considered safe for long term military operation of 10^{-7} per flight. And after 340 landings, the estimated SFPOF will exceed the value of 10^{-5} per flight, which is considered unacceptable.

Based on this analysis, a proof-test retrofit program was conducted to remove cracked trunnion collars and to extend the life of uncracked parts. Four trunnion collars failed during proof testing. If they had remained in service and failed, each service failure would have resulted in a Class A mishap at over $1M each in damage. The Weibull distribution estimated from a single test failure provided information that enabled decisions that protected the safety of the fleet.

5.2.3 Weibull Distribution: Estimating from Multiple Component Fatigue Tests with a Single Run-Out

If several tests are conducted and each provides a measure of time to failure, the data can be plotted to obtain the best-fit Weibull parameters as discussed in Section 4.1. But the problem becomes more complex when not all the times to failure are known. This is the problem of "censored data." There are two types of censored data:

- Right-censored data: Tests that end before the desired failure point is obtained, either because the operator stops the test or because failure occurs but not by the relevant failure mode. Also called "suspensions" or "run-outs."
- Left-censored data: Tests in which the failure occurs at some unknown point between time A and time B; for example between scheduled inspections.

Censored data are an important consideration. When some data are identified as censored, that usually increases the scale parameter. The censored data must be taken into account in order to estimate the Weibull parameters that represent the population.

Run-outs are tests that are stopped prior to failure. A run-out is an example of "censored data" because the exact fatigue life is unknown, but the life is known to exceed the value reached without failure. One method of estimating a distribution when the data include run-outs is the rank-regression method.

Consider Table 12 which contains results from seven replicate tests, each stopped either at failure or at 5 design lifetimes. The second column of the table shows that six specimens failed prior to five design lifetimes and the seventh specimen is a run-out, reaching 5 lifetimes without failure. In this example the run-out is the seventh point in the rank order. Following the method in Section 4.1, the six failure times are ranked from smallest to largest in the second column of Table 12. The third column is the Bernard rank value, Equation (26), of F(t) for each point with the total number of data points N equal to seven. The fourth and fifth columns are $x = ln(t)$ and $y = ln\{ln[1/(1-F(t))]\}$, the coordinate values of the Weibull plot.

The Weibull distribution was fit to the values in the fourth and fifth columns for the six failure points in Table 12 using LSE. The Weibull probability plot of these data and the distribution fit to the data is shown in Figure 18. The LSE equation of the straight line through the six failure points is

$$y = 2.8046x - 4.0195. \quad (43)$$

Extrapolating this straight line upward to $y_7 = 0.9054$, an estimate of t_7, the estimated life of the run-out, is 5.69 lifetimes. The estimated life is shown as a hollow red square; the original run-out is shown as a solid red square. The estimated Weibull parameters for this problem are $\alpha = 2.8046$, and $\beta = exp(4.0195/2.8046) = 4.192$ design lifetimes.

Table 12. Censored Data: 7 Tests with 1 Run-Out

Rank	Design Lifetimes, *t*	Bernard Rank, *F(t)*	*x = ln(t)*	*y = ln{ln[1/(1-F(t))]}*	Linear Est. of *t*
1	1.9	0.09459	0.64185	-2.308880	1.84030
2	2.5	0.22973	0.91629	-1.343182	2.59675
3	3.1	0.36486	1.13140	-0.789840	3.16312
4	3.7	0.50000	1.30833	-0.366513	3.67848
5	4.3	0.63514	1.45862	0.008195	4.20429
6	4.8	0.77027	1.56862	0.385842	4.81030
7	5+	0.90541	1.60944	0.857880	5.69204

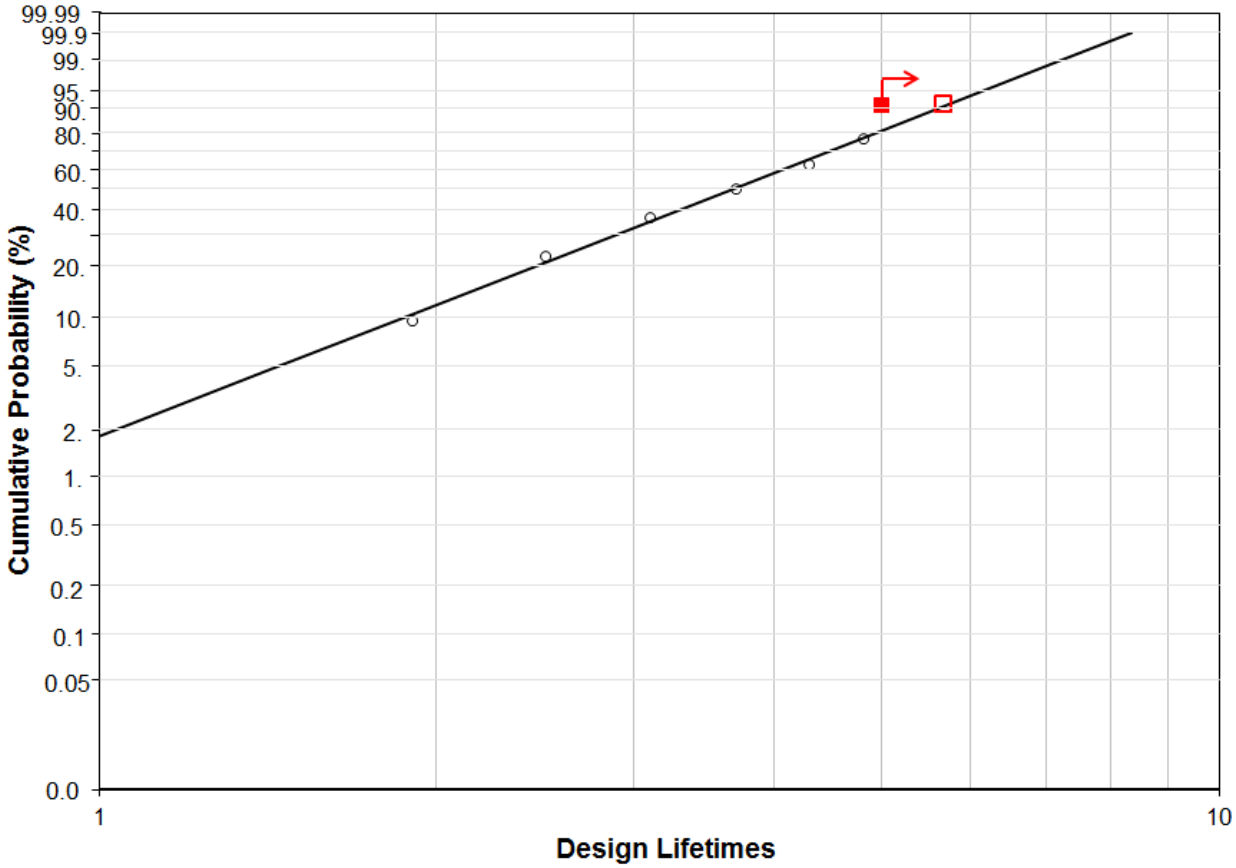

Figure 18. Weibull plot of Data from Single Run-out Example

This is another example of a situation where the MLE method does not produce a better answer than the LSE.

The MLE estimated Weibull parameters are $\alpha = 3.901$ and $\beta = 4.011$ design lifetimes.

Figure 19 shows a graphical comparison of the MLE (green line) and the least squares (black line) results. Clearly, the LSE provides a better fit to the sample data. For data sets with a large number of data, MLE gives a better result. However when there are less than five data points, and sometimes less than ten, the MLE can be biased [10]. In this example, the number of data points is six which is right in the middle of range where MLE should be used with caution.

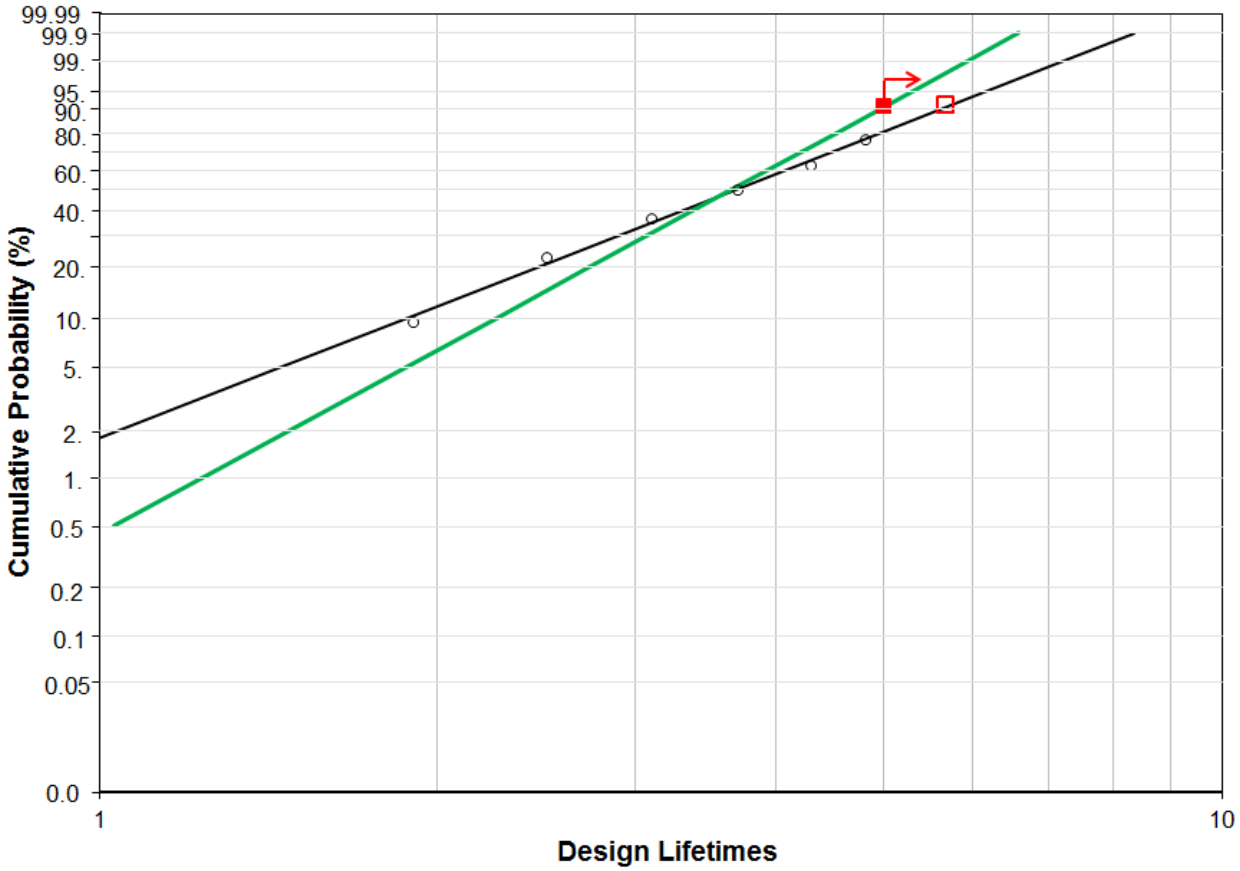

Figure 19. MLE and LSE Weibull Distributions for Single Run-Out Example

5.2.3.1 Confidence Band for Weibull Distribution

In this section, a two-sided confidence band will be determined for the Weibull distribution used to describe the fatigue life data in Table 12 and Figure 18. This band is for upper and lower probabilities for each fatigue life. The equations used apply only to Weibull distributions. Recall from Section 0 that confidence bands are only approximate and are generally more accurate with more data. The steps for determining a two-sided confidence band are as follows [11]:

Step 1. Determine the desired confidence level *100(1-α)%*. Confidence levels of 90 percent and 95 percent are common choices; 95 percent will be used in this example.

Step 2. Calculate $k_{\alpha/2}$ equal to $\Phi^{-1}(\alpha/2)$, where $\Phi^{-1}(p)$ is the inverse of the standard normal distribution (mean of 0, standard deviation of 1). The inverse of the standard normal distribution is the function that maps a probability p back to the value of the random variable x that is associated with the probability p in the standard normal function. The value $\alpha/2$ is used for a two-sided confidence bands since symmetry requires that half of the probability of being outside the confidence band be above the confidence band and half below. For this example,

$$k_{\alpha/2} = \Phi^{-1}\left(\frac{0.05}{2}\right) = -1.96. \tag{44}$$

Step 3. Choose a fatigue life t to calculate the values of the upper and lower confidence bands at. Then determine the quantity

$$U = \alpha[ln(t) - ln(\beta)], \tag{45}$$

where α is the shape parameter, and β is the scale parameter. From Equation (23),

$$U = ln\left\{ln\left[\frac{1}{1-P(t)}\right]\right\} \tag{46}$$

Start at one end of the curve with t equal to 1 design lifetime. Then,

$$U = 2.8046[ln(1) - ln(4.192)] = -4.0195. \tag{47}$$

Step 4. Compute the parameters associated with the lower and upper band probabilities for the selected fatigue life using the following equations:

$$u_l \cong U + k_{\alpha/2}\sqrt{\frac{1.168 - 0.1913U + 1.1U^2}{N}}, \tag{48}$$

$$u_u \cong U - k_{\alpha/2}\sqrt{\frac{1.168 - 0.1913U + 1.1U^2}{N}}, \tag{49}$$

where N is the number of data points in the sample. In this example, N equals 6. For a fatigue life of 1 design lifetime,

$$u_l \cong -7.5717, \text{and } u_u \cong= -0.4672.$$

Step 5. Find the probability values associated with the lower and upper confidence bands at the selected fatigue life from Weibull CDF,

$$P_i = 1 - exp[-exp(u_i)]. \tag{50}$$

For this example, the probability P_l of the lower confidence band at a fatigue life of one design lifetime is

$$P_l = 1 - exp[-exp(-7.517)] = 0.0005. \tag{51}$$

The probability P_r of the upper confidence band at one design lifetime is

$$P_u = 1 - exp[-exp(-0.4672)] = 0.4657. \quad (52)$$

Step 6. Repeat Steps 3 through 5 to fill in the values in Table 13. The resulting confidence band is plotted as the dashed curves in Figure 20. The values in columns 1 and 3 are the *x*- and *y*-coordinates for the left dashed curve, respectively. The values in columns 1 and 5 are the *x*- and *y*-coordinates for the right dashed curve, respectively. The 95 percent confidence band for this example is large because only 6 data points were available to construct the distribution.

Table 13. Data Points for 95 Percent Confidence Band for Weibull Distribution

Life, Design Lifetimes	u_l	P_l	u_u	P_u
1	-7.5717	0.0005	-0.4672	0.4657
1.5	-5.5189	0.0040	-0.2457	0.5426
2	-4.0844	0.0167	-0.0666	0.6076
2.5	-3.0006	0.0485	0.1013	0.6693
3	-2.1560	0.1093	0.2794	0.7335
3.5	-1.5010	0.1998	0.4890	0.8042
4	-1.0125	0.3046	0.7495	0.8795
4.5	-0.6679	0.4012	1.0656	0.9451
5	-0.4327	0.4773	1.4213	0.9841
5.5	-0.2694	0.5341	1.7927	0.9975
6	-0.1506	0.5769	2.1619	0.9998
6.5	-0.0594	0.6103	2.5197	1.0000
7	0.0139	0.6372	2.8621	1.0000
7.5	0.0750	0.6597	3.1879	1.0000
8	0.1274	0.6789	3.4975	1.0000
8.5	0.1734	0.6956	3.7917	1.0000
9	0.2143	0.7103	4.0713	1.0000
9.5	0.2513	0.7235	4.3376	1.0000
10	0.2851	0.7355	4.5915	1.0000

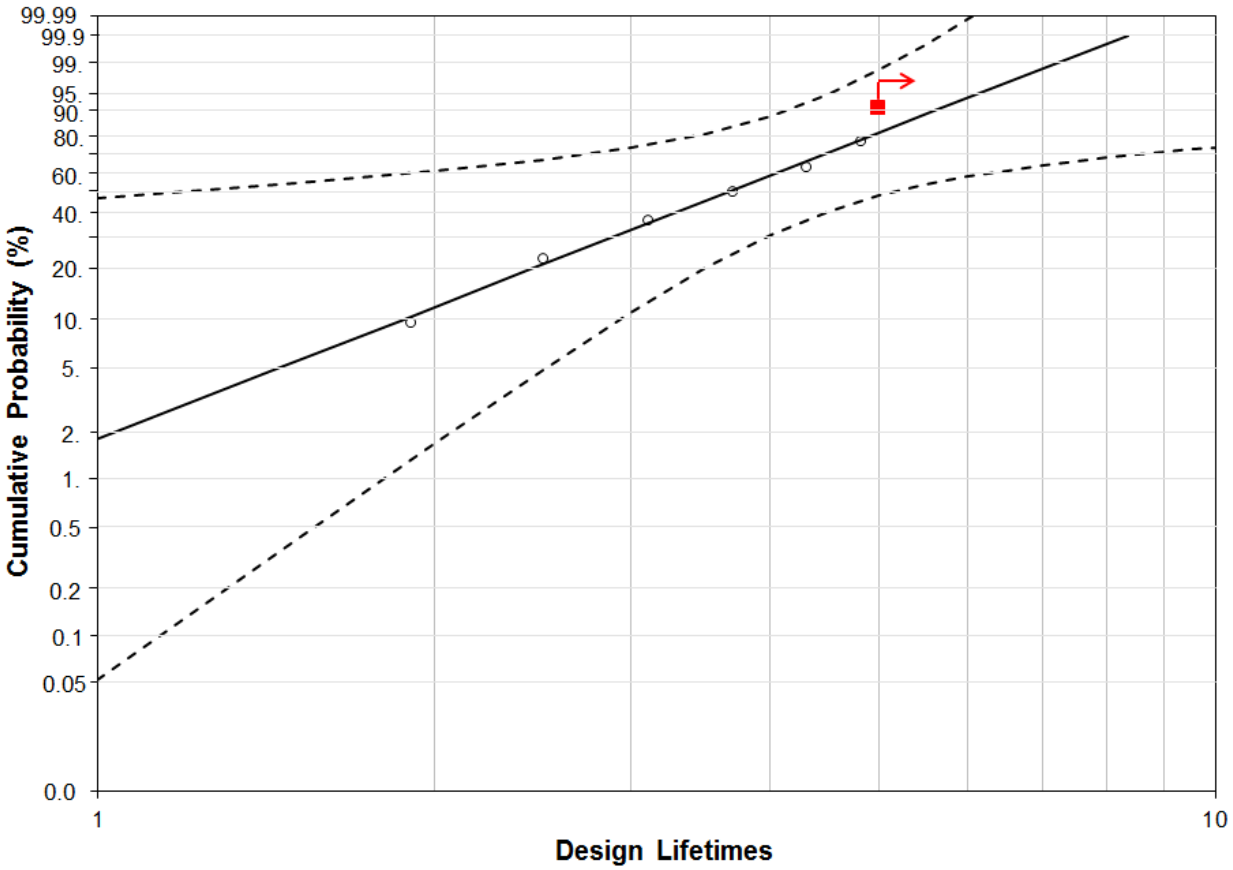

Figure 20. Weibull Probability Plot Showing 95 Percent Confidence Band

5.3 Using the Lifetime Distribution to Forecast Fleet Failures

The main purpose for constructing a lifetime distribution is to be able to forecast the expected number of failures in a given time period. Because of the uncertainties and the scarcity of data, these forecasts may not be highly accurate. But they provide a feel for the magnitude of the risks being taken if remedial action is not taken. However, if the forecasted expected number of failures seems to be way out of line with reality, then it is possible that something is being overlooked in the analysis. As Laplace, the father of probability theory, said, "probability theory is nothing but common sense reduced to calculation." This quote applies equally well to structural reliability theory. So, if a result does not agree with your common sense, you need to investigate why it does not agree.

In the following sections several examples of forecasting the expected number of failures will be worked.

5.3.1 Basic Forecast of the Expected Number of Failures in a Fleet

A forecast of the expected number of failures in a fleet of 20 aircraft at a particular location is needed as a function of flight hours in order to support the scheduling of inspections and repairs. For this example, assume that data have established that the lifetime distribution is well represented by a Weibull distribution and that estimates of the relevant parameters for the Weibull distribution are a shape parameter α of 4.0 and a scale parameter β of 1,000 FH. Table 14 shows the current FH status of the fleet.

Table 14. Fleet Status and Cumulative Number of Failures Expected

Aircraft #, i	Current FH, t_i	$F(t_i)$	FH @ 1 Month from Now	$F(t_i)$
1	400	0.0253	420	0.0306
2	380	0.0206	400	0.0253
3	360	0.0167	380	0.0206
4	340	0.0133	360	0.0167
5	320	0.0104	340	0.0133
6	300	0.0081	320	0.0104
7	280	0.0061	300	0.0081
8	260	0.0046	280	0.0061
9	240	0.0033	260	0.0046
10	220	0.0023	240	0.0033
11	200	0.0016	220	0.0023
12	180	0.0010	200	0.0016
13	160	0.0007	180	0.0010
14	140	0.0004	160	0.0007
15	120	0.0002	140	0.0004
16	100	0.0001	120	0.0002
17	80	0.0000	100	0.0001
18	60	0.0000	80	0.0000
19	40	0.0000	60	0.0000
20	20	0.0000	40	0.0000
	$\Sigma F(t_i)$ =	0.1147		0.1454

With the lifetime distribution, it is easy to calculate the cumulative number of failures expected in the fleet prior to some time. The expected number of failures N_f for n aircraft each having been flown a unique number of flight hours t_i is given by

$$N_f = \sum_{i=1}^{n} F(t_i), \tag{53}$$

where $F(t)$ is the lifetime distribution. In this example, $F(t)$ is a Weibull distribution with a shape parameter of 4.0 and a scale parameter of 1,000 flight hours.

The cumulative numbers of failures expected now (current status) and by the end of the next month are calculated in third and fifth columns of Table 14 as follows. While it is nonsense to talk about the expected number of failures for the past or present (the failures either occurred or not), the value of the lifetime distribution can be found at the current time for purposes of determining the expected number of failures during the next month.

Step 1. Determine current Weibull $F(t)$ for each aircraft using $\alpha = 4.0$ and $\beta = 1{,}000$ service FH (Column 3 of Table 14).

Step 2. Sum *F(t)* for each aircraft to estimate cumulative number of failures expected at the current time.

Step 3. Add the number of flight hours expected to be flown in the next month to the Current Flight Hours in column 2 to get the age of each aircraft at the end of the next month. This is the value in column 4 of Table 14. In this example, 20 FH were added to the current flight hours for each aircraft.

Step 4. Determine Weibull *F(t)* for each aircraft (Column 5 of Table 14) and sum to estimate cumulative number of failures expected one month from now (0.145).

Step 5. Repeat step 3 for the other 11 months (not shown in Table 14).

The cumulative number of failures expected for the next 12 months are plotted in Figure 21. The number of failures expected during each month is the difference between the cumulative number of failures expected in a month and the preceding month. The number of failures expected monthly is plotted as the red curve in Figure 21. Though the analysis indicates that one failure in the fleet can be expected to occur during the next 12 months, the chance of the failure occurring in any particular month is quite low.

Note: If the lifetime distribution is developed from test data rather than service data, then a standard test spectrum was likely used in all the tests. The flight hours determined from the lifetime distribution are based upon this standard test spectrum. When applying this test-derived time to aircraft in service, the actual flight hours at which failure would be expected needs to consider the severity of the service load history relative to the test spectrum. If the service history is more severe than the test spectrum in terms of its potential for increasing the size of a crack that might be in the structure, then the actual flight hours to failure will be less than test-derived time to failure as determined by using the concept of equivalent flight hours [13]. If the service history is less severe than the test spectrum, then the actual flight hours to failure will be more than the test-derived time.

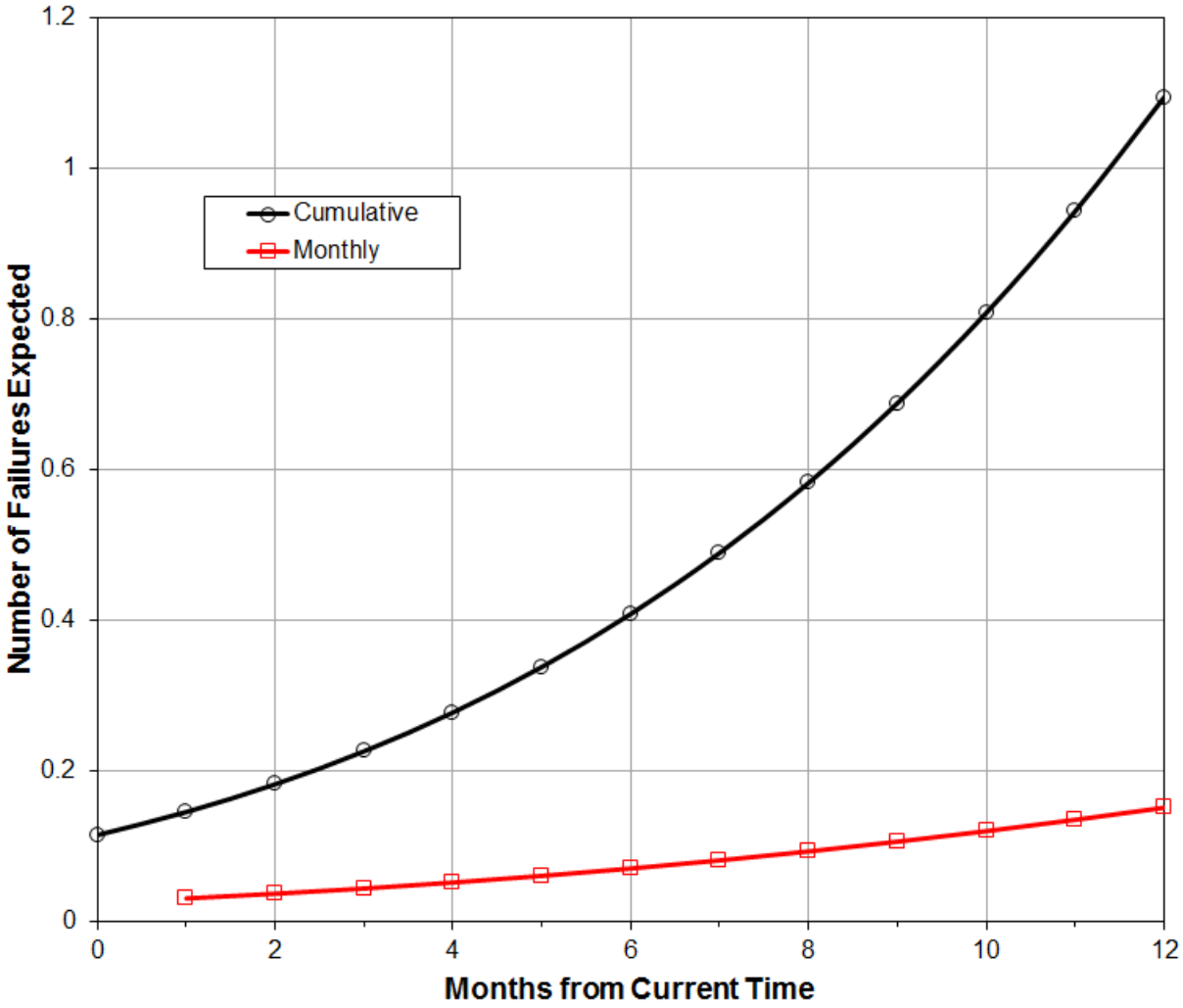

Figure 21. Number of Fleet Failures Expected by Month

5.3.2 Forecasting When to Rework Structural Detail

The airframe for a fighter aircraft experienced significant cracking at the base of a fuselage lug where the wing attaches during the full-scale durability test. The material was Ti-6Al-4V, Beta Annealed. Based on the crack initiation life in the test, the estimated mean flight hours μ when a major repair is required was 9,663 FH.

Before the short-life detail could be re-designed, 52 aircraft had been built with the original design, both left and right sides. The plan for these aircraft was to rework the lugs early enough to only perform a minor blend. To minimize the impact on operations, the question was, "How urgent is the scheduling of that rework?" This trade-off called for an estimate of the expected number of major repairs that would be required as a function of the flight hour limit for the rework.

The calculations required a Weibull shape parameter appropriate for titanium. Plotted results in Figure 22 are for the range of shape parameters for Titanium, $\alpha = 2.5$, 2.75, and 3.0. The Weibull scale parameter β for each assumed α is calculated from Equation (13), which is repeated here, and values of the Γ-function from Table 10:

$$\mu = \beta\,\Gamma(1+1/\alpha) + t_0. \quad (13)$$

The scale parameter associated with each shape parameter value is calculated in Table 15.

Table 15. Scale Parameter Calculated from Distribution Mean

Mean, μ	t_0	Shape Parameter, α	$\Gamma(1+1/\alpha)$	Scale Parameter, β
9,663	0	2.50	0.88726	10891
9,663	0	2.75	0.88986	10859
9,663	0	3.00	0.89298	10821

The cumulative number of repairs expected before time t is given by $F(t)$ times 104, the number of affected details on the 52 affected aircraft. For example, for α of 3.0 and β of 10,821 FH at 1,850 FH, the value of the Weibull distribution is 0.005 and the cumulative number of repairs expected is 0.52. The cumulative number of repairs expected as a function of flight hours is plotted for all three shape parameters in Figure 22. To minimize the chance of a major repair, the rework should be completed prior to the cumulative number of repairs expected in the 52 aircraft becoming 0.5. The analysis indicates that the rework should begin before each aircraft reaches 1,300 FH, but certainly no later than 1,800 FH. If the rework were scheduled according to the traditional practice of the test life divided by four, the time limit for the rework to begin could be extended to 2,400 FH but there is a good probability that at least one major repair would be required.

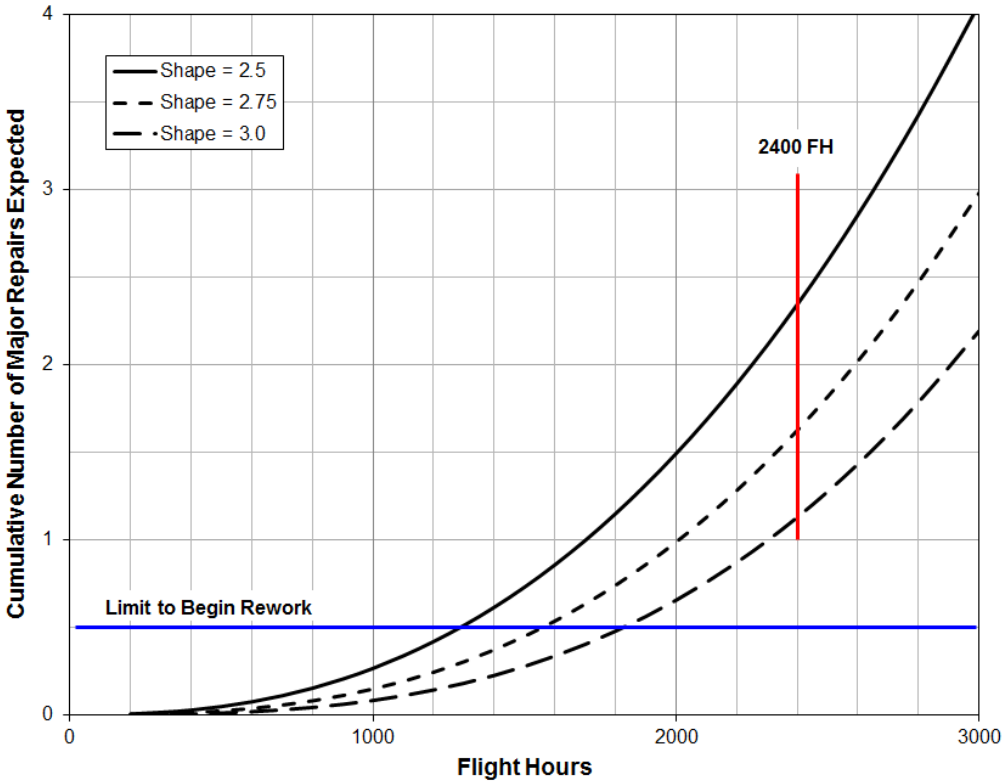

Figure 22. Time Limit to Begin Wing Lug Rework

6.0 LIFETIME DISTRIBUTIONS FROM THE PHYSICS OF FAILURE

6.1 Overview

In many instances, it is possible to estimate the lifetime distribution for a structure or a component from the physics of the problem before any reliability tests have been performed or failures occur in service. This is accomplished by estimating how likely the loads applied to the structure are to exceed the resistance of the structure to failure, i.e., the strength. Thus, probability distributions to describe the variability and uncertainty in the applied loads L and the structural strength S are required.

If the uncertain strength S of a structure is described by the PDF $f_S(s)$, then a structural component subjected to a known load l has a probability of failure P_f of

$$P_f = Pr(S \leq l) = F_S(l) \tag{54}$$

where $F_S(s)$ is the CDF of the strength. In general, the applied loads are also variable and uncertain. The probability of the applied load L occurring is then described by a PDF $f_L(l)$. If the loads are independent of the strength, then the probability of failure is determined by

$$P_f = Pr(S \leq L) = Pr(S - L \leq 0) = Pr\left(\frac{S}{L} \leq 1\right) =$$

$$\iint_D f_S(x) f_L(y) dy dx, \tag{55}$$

where D is the domain of integration indicated in Figure 23. Integration results in either of the following two equations:

$$\int_0^\infty f_S(x) \int_x^\infty f_L(y) dy dx = \int_0^\infty f_S(x)[1 - F_L(x)]dx = \int_0^\infty f_S(x) D_L(x) dx, \tag{56}$$

where $F_L(x)$ is the CDF for $f_L(x)$ and $D_L(x)$ is the EDF; or

$$\int_0^\infty f_L(y) \int_0^y f_S(x) dx dy = \int_0^\infty f_L(y) F_S(y) dy. \tag{57}$$

This is the fundamental equation in structural reliability theory [8]. Applications of the fundamental equation are presented in this section. The situation of one random variable, strength, was briefly discussed above and is further developed in the next section. Then, the more complex situation of two random variables is discussed. Finally, the section concludes with the situation of three random variables.

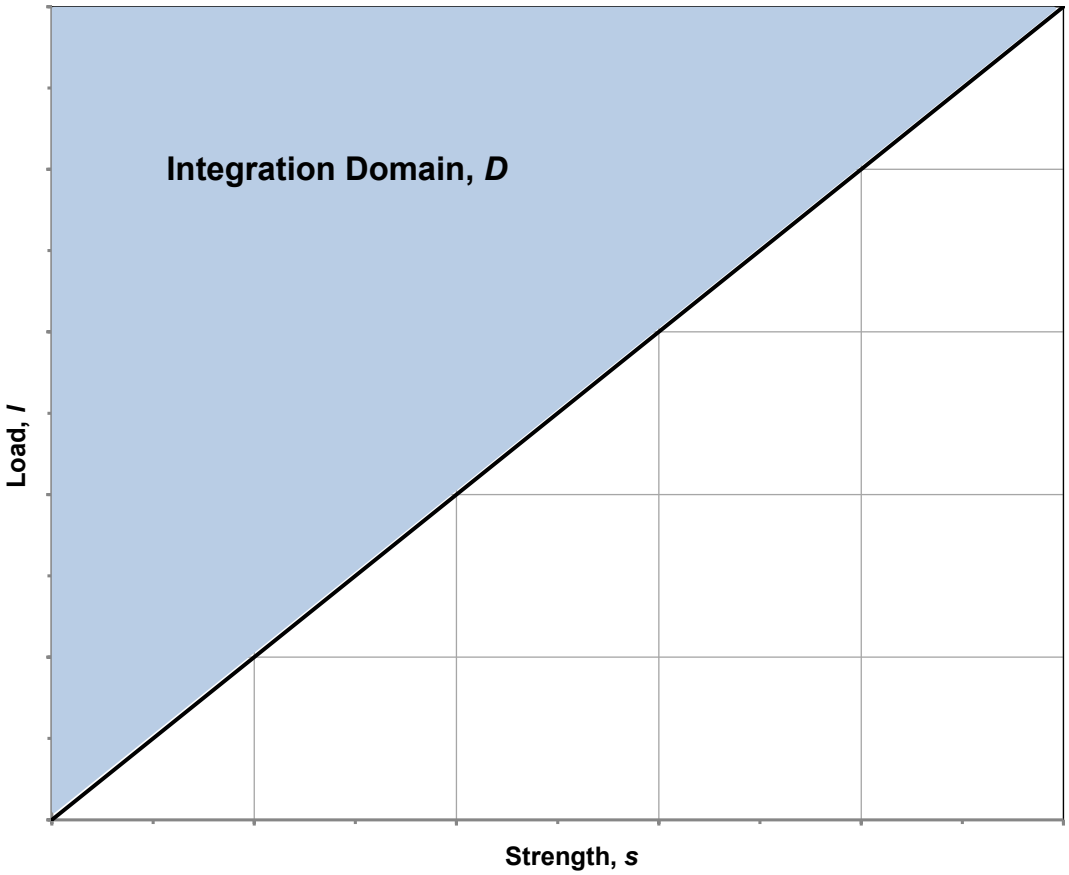

Figure 23. Integration Domain for Reliability Integral

The resistance to failure, or strength, degrades with continued operation as a result of fatigue crack growth, for instance. This adds more uncertainty, as well as complexity, to the mathematical description. This situation of strength degradation is not dealt with in this volume. It will be discussed in a later volume of this handbook. Since the POF beyond the next flight is not considered here, the SFPOF, or failure rate, as a function of time cannot be calculated in the examples that follow.

6.2 Probability of Failure: One Random Variable

The situation of having only one random variable in a structural reliability problem is unlikely to occur. This problem is presented as a building block to the more realistic situations of two, three, or four random variables.

A simplistic example of a single random variable problem would be testing a number of coupons in a test machine by applying the same maximum stress to each coupon. If the strength of a specific coupon is greater than the maximum stress, the coupon will not fail. If the strength is less than the maximum stress, it will fail. But until the test is performed, it is uncertain as to whether the strength of an individual coupon is greater than, equal to, or less than the applied stress. The strength of any one coupon is thus described by a probability distribution.

Suppose the coupons being tested come from different lots of a material for which the UTS is known to be normally distributed with a mean of 71.0 ksi and a standard deviation of 1.815. (This is the distribution from Section 4.2.1.) A normal distribution is not usually recommended

for random variables that do not have values less than or equal zero. But in this instance, the probability of a UTS less than zero is

$$Pr(UTS \leq 0) = \Phi\left(\frac{0-71}{1.815}\right) = \Phi(-39.12) = 0, \quad (58)$$

where $\Phi(z)$ is the standard normal distribution. Suppose that each coupon is placed in a testing machine and loaded in tension to a stress of 65 ksi. The probability that any one coupon will fail under this stress is the probability that the strength is less than or equal to 65 ksi,

$$\text{POF} = Pr(UTS \leq 65\ ksi) = \Phi\left(\frac{65-71}{1.815}\right) = \Phi(-3.31) = 0.00047. \quad (59)$$

6.3 Probability of Failure: Two Random Variables

A structural reliability problem involving two or more random variables is more typical. This would be the case where there is uncertainty about the maximum load that a structural will experience in some period of time and also uncertainty about the strength of the structure. Usually, the maximum load and the strength of a structure are independent so that Equation (56) can be used. However, the product of a PDF and an EDF is not usually a function that can be readily integrated. Numerical integration is required.

6.3.1 Two Random Variables Example: Strength and Maximum Load

This example is derived from a presentation by Cornog and Lincoln at the 1988 Aircraft Structural Integrity Program Conference [14]. Because of increased weight and changes in the load spectra experienced by the F-16, a static test of an F-16C wing produced in the Block 30 configuration was conducted to determine the static margin of safety. The design Wing Bending Moment (WBM) for this configuration had increased 22 percent from the original F-16A design.

The left wing failed near the root due to compressive buckling at 128 percent of Design Limit Load (DLL), Figure 24. Restrictions were placed on the F-16C/D fleet that maintained a 1.5 factor of safety but a decision had to be made as to whether or not to modify the wing to the restore the original ultimate load capability. The probability of an unmodified wing buckling in service was calculated in order to help make the decision of whether or not to modify the wing. Thus, the POF in this example is the probability of the upper wing skin buckling.

It was decided that an acceptable level of risk for the wing would be the risk routinely accepted by the public when driving an automobile during an average commute, or the POF during a flight should be less than 10^{-7}, and that the expected number of failures in the fleet should be less than one airframe. The POF during a flight calculated in this example is the failure distribution evaluated over an increment of time equal to one flight. It is not the product of the hazard rate and an increment of time. Thus, it is not the SFPOF as defined in this handbook.

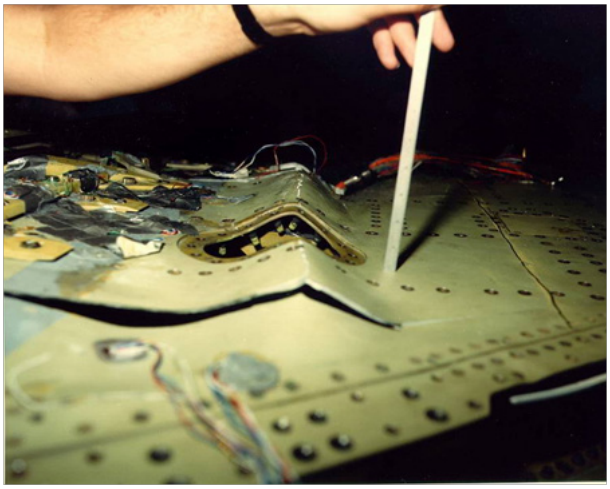

Figure 24. F-16 Block 30 Wing Failure at 128 Percent DLL

The steps for calculating the POF during a flight are:

Step 1. Use Equation (56),

$$P_f = Pr(S \leq L) = Pr(S - L \leq 0) = \int_0^\infty f_S(x) D_L(x) dx. \qquad (56)$$

Step 2. Estimate the PDF for the strength of a wing, $f_S(x)$,

Step 3. Estimate the EDF for the maximum load experienced during a flight, $D_L(x)$,

Step 4. Substitute these distributions into Equation (56), and perform the numerical integration.

The estimation of the distributions and numerical integration of their product are discussed in the following sections.

6.3.1.1 Estimation of the Distribution for the Strength of a Wing

It was decided to model the distribution of strength with a two parameter Weibull distribution. The Weibull is good choice for a distribution when there is little data because as noted in Section 3.2.3, it can describe symmetric distributions like a normal distribution or skewed distributions like the lognormal.

The test failure was caused by buckling and was influenced by wing skin and spar thicknesses, the material properties of the skin and spar, and boundary conditions. Accordingly, wing skin and spar thicknesses were measured on a number of aircraft. Properties of the wing skin and spar materials and variation of the properties were reviewed. These data were used to infer mean and scatter values for the Weibull strength distribution. As explained in [14], Cornog and Lincoln concluded that a Weibull shape parameter of 24 was appropriate. This value is similar to the Weibull shape parameter of 19 estimated for the ultimate strength of aircraft structure by Freudenthal and Wang [15]. The thickness and material properties of the failed wing were all found to be nominal with respect to samples of other wings. This fact justified the assumption that the failure of the test wing at 128 percent DLL was a reasonable estimate of the mean strength. A value of 130.9 percent DLL for the scale parameter was found using Equation (13),

$$\beta = 128\%\ \text{DLL}/\ \Gamma(1+1/24) = 128\%\ \text{DLL}/0.9776 = 130.9\%\ \text{DLL}, \qquad (60)$$

where $\Gamma(\ldots)$ is the gamma function.

The coefficient of variation (ratio of mean to standard deviation) provides a check on the reasonableness of the values for the shape and scale parameters. This combination of parameters gives a coefficient of variation of 5.2 percent. Typically, the coefficient of variation for strength should be less than 10 percent.

The PDF for the Weibull distribution with values of 24 and 130.9 percent DLL for the shape and scale parameters is shown in Figure 25.

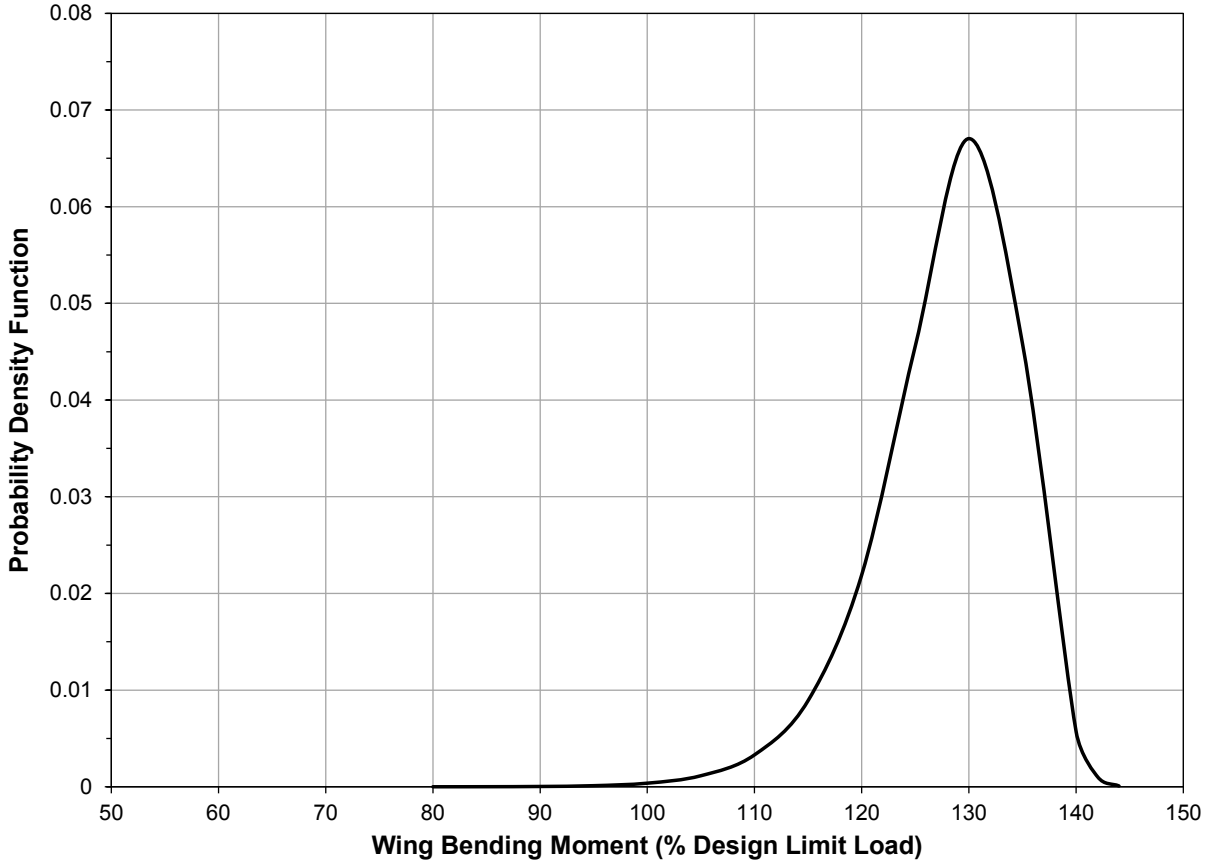

Figure 25. Weibull PDF for Wing Strength

6.3.1.2 Estimation of the Exceedance Distribution for the Maximum Stress per Flight

About 7,500 hours of recorded flight data from the F-16A/B aircraft were available and were considered to be representative of the loads to be encountered by the F-16C/D. Since the Air Combat Maneuver mission had a dominant effect on the frequency of the larger loads, this mission was chosen to represent the loads in the probability of failure calculation [14]. The number of load exceedances per 1,000 hours for this mission is given in Table 16. A graph of the exceedance curve is presented in Figure 26. The magnitude of the loads was normalized by the wing root bending moment at Design Limit Load.

Table 16. Load Exceedances for Dominant Mission

Wing Bending Moment (% DLL)	Exceedances per 1000 Flight Hours	Exceedances per Flight (880 flights/1000 FH)	Probability of Exceeding WBM during a Flight
60	1468	1.67	1
65	1118	1.27	1
70	629	0.71	0.71
75	265	0.30	0.30
80	70	0.08	0.08
85	15	0.02	0.02
90	3	0.003	0.003
91	2	0.002	0.002

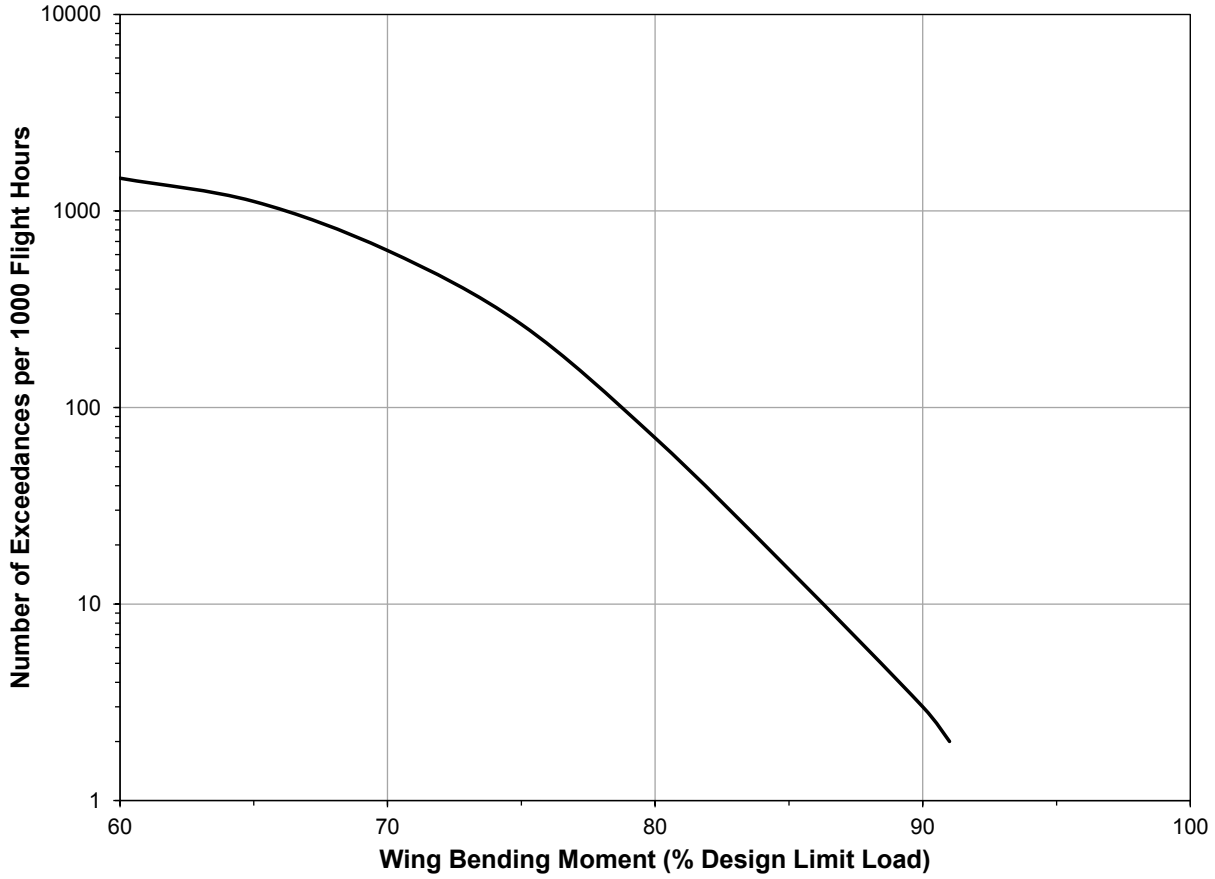

Figure 26. Wing Bending Moment Exceedances per 1000 Hours

The load exceedances per 1,000 hours must be converted to the EDF for a flight. In this particular application, the probability of exceeding percent DLL was derived from the number of exceedances per 1,000 hours as follows:

Step 1. Convert the exceedances per 1,000 hours to the number of exceedances per flight by dividing the counts by the average number of flights in 1,000 hours. There were 880 flights in 1,000 flight hours. This is the third column in Table 16.

Step 2. If the number of exceedances per flight for a load is greater than or equal to 1, then the probability of exceeding that load is one. If the number of exceedances per flight for a load is less than 1, then the probability of exceeding that load is the exceedances per flight. This is the fourth column in Table 16.

Step 3. Extrapolate the probability of exceedances to at least the limit condition (100 percent DLL), if the curve does not extend to that level already. While the load should never exceed limit load, there are rare over-g events that can be considered in the reliability analysis. So the EDF can be extrapolated beyond 100 percent DLL, but there is no need to go beyond 150 percent DLL.

When steps 1 and 2 were performed, the resulting Exceedance Distribution Function (EDF) per flight shown in Figure 27 was obtained. Cornog and Lincoln extrapolated to higher bending moments using a Weibull distribution fit to the exceedance distribution below 90 percent DLL.

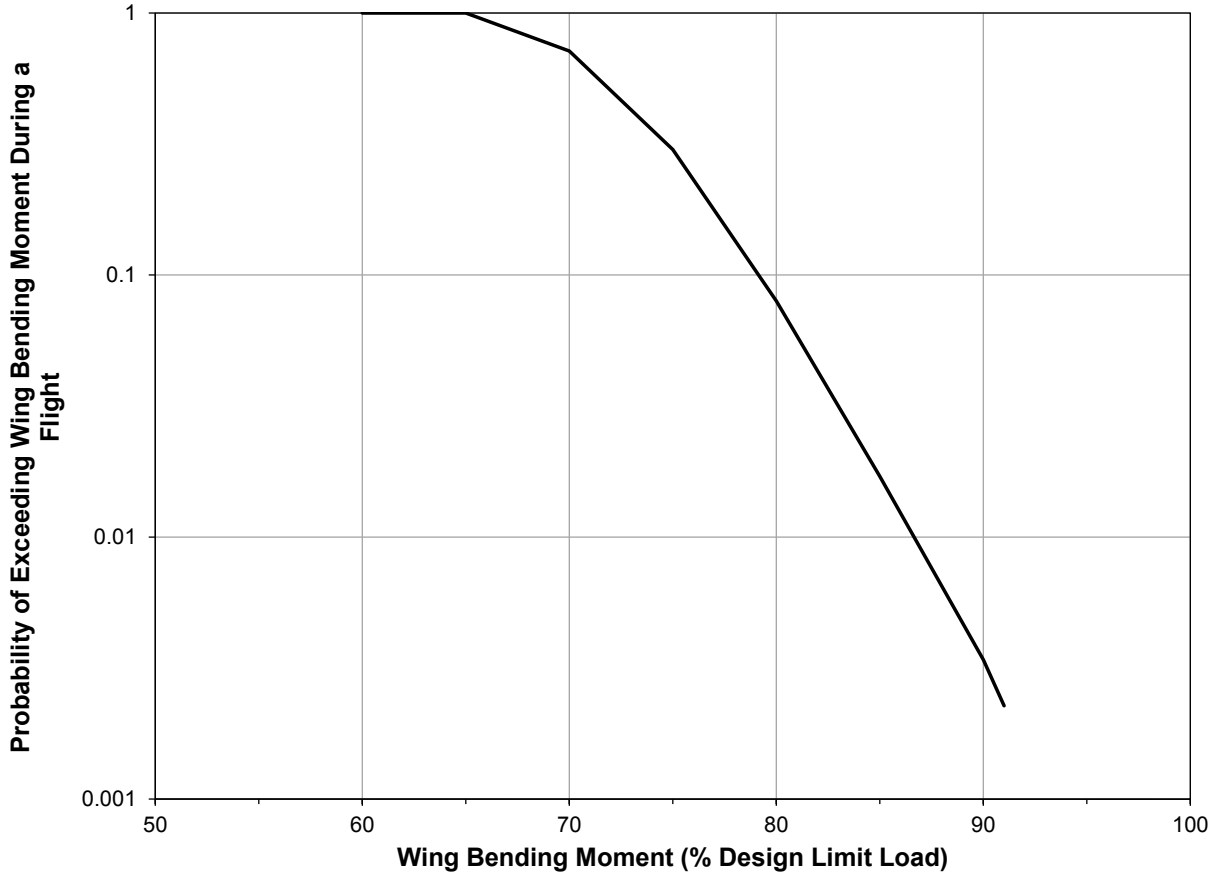

Figure 27. Probability of Exceeding WBM in a Flight

The Weibull distribution was extrapolated as follows. The values 70 percent to 91 percent DLL along with the associated probability of occurrence were graphed on a Weibull probability plot as shown in Figure 28. The probability of occurrence is one minus the probability of

exceedance. The probability of occurrence for 60 percent and 65 percent DLL is zero which cannot be plotted on a Weibull plot. A LSE line was fit to just the four highest load points: 80 percent, 85 percent, 90 percent, and 91 percent DLL. These four points had a correlation of 99.7 percent .Whereas, when all the points were considered the correlation was 97.5 percent .The shape parameter for the Weibull distribution (the slope of the line) is 6.74. The scale parameter is 69.5 percent DLL.

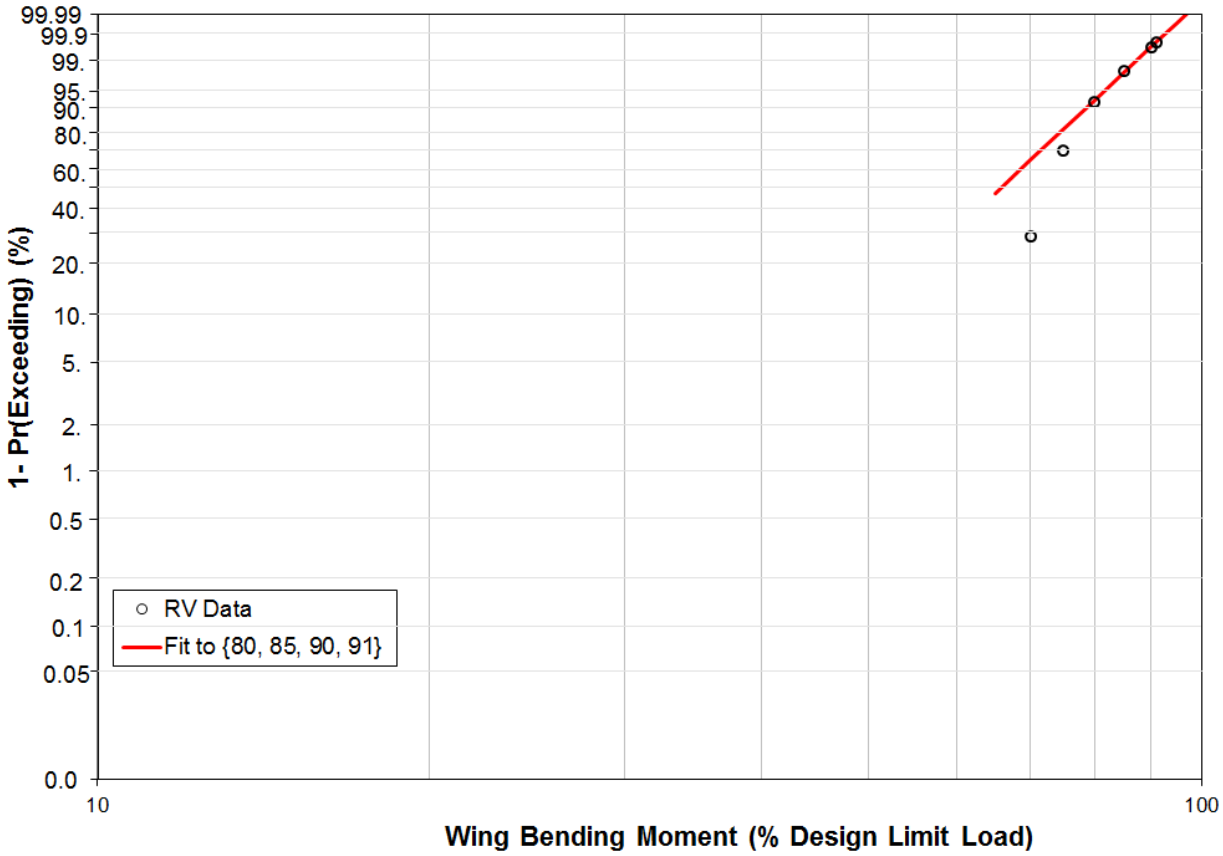

Figure 28. Weibull Extrapolation of WBM EDF

The final EDF for Wing Bending Moment in a flight was extrapolated to 150 percent DLL using the probabilities in Table 16 up to 75 percent DLL and the Weibull distribution above 80 percent DLL. The EDF at 5 percent DLL increments are given in Table 17 and graphed in Figure 29. The Wing Bending Moment reaching even 125 percent of the limit condition appears to be an extremely rare event, once in approximately 10^{23} flights.

Table 17. Points of the Exceedance Probability Distribution

Wing Bending Moment (% DLL)	Probability of Exceeding WBM during a Flight
60	1
65	1
70	0.71
75	0.30
80	0.077
85	0.021
90	0.0034
95	0.00028
100	9.60E-06
105	1.10E-07
110	2.89E-10
115	1.35E-13
120	7.16E-18
125	2.67E-23
130	3.96E-30
135	1.21E-38
140	3.58E-49
145	4.27E-62
150	7.59E-78

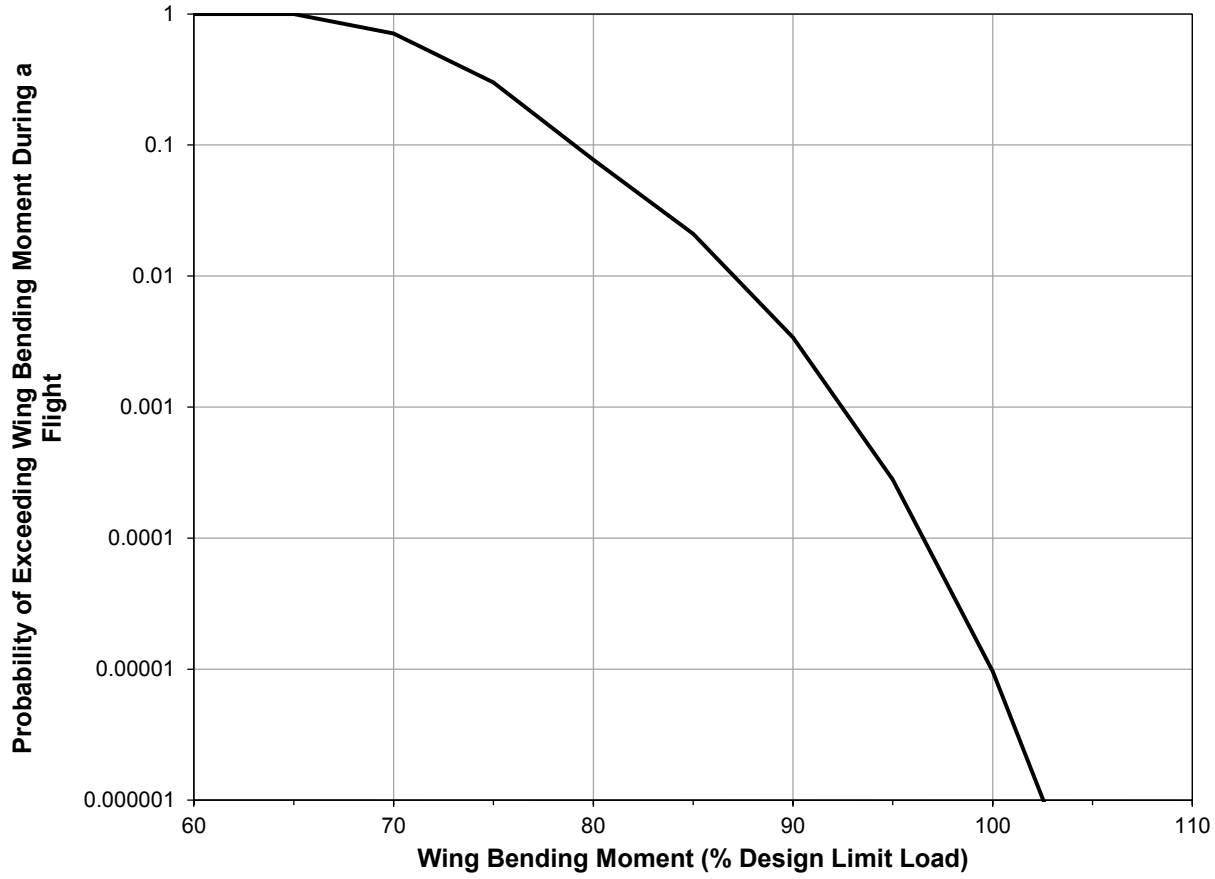

Figure 29. EDF for WBM in a Flight Extrapolated to 125 Percent Limit WBM

6.3.1.3 Numerical Integration of the Probability of Failure Integral

Figure 30 presents a comparison of the PDF of wing strength and the single flight EDF of wing bending moment. Note that the two curves are plotted on different scales. The structural reliability integral of Equation (56) integrates the product of these two curves over the domain of both functions. This integral must be evaluated numerically usually. This section steps through the numerical integration using an Excel spreadsheet.

There are many techniques for performing numerical integration. Any approach that is appropriate for these functions can be used. The trapezoidal rule will be used here to illustrate the concept. The calculation is performed using Table 18. The WBM range is divided into discrete intervals Δ of the same length, 5 percent DLL. The first column contains the Wing Bending Moment (WBM) at the endpoint of each interval in percent DLL. The strength PDF and load EDF are evaluated at the endpoint of each interval in the second and third columns, respectively. The product of the PDF and the EDF, denoted as *H(%DLL)*, is computed for each endpoint in the fourth column. Then, the trapezoidal rule computes the integral as

$$POF = \frac{\Delta}{2}(H(45) + 2H(50) + 2H(55) + \cdots + 2H(145) + H(150)). \qquad (61)$$

The resulting POF during a flight is shown at the bottom of Table 18. Remember the POF during a flight calculated in this example is the lifetime distribution evaluated for an increment of one flight. Since degradation of the structure is not considered, the increment of the lifetime distribution is the same for every flight. The total lifetime distribution is equal to the POF times the number of flights N_F,

$$F_L(N_F) = 3.76 \times 10^{-6} N_F. \tag{62}$$

The expected number of wing failures W_f in the fleet is equal to the lifetime distribution times the number of aircraft in the fleet N_A,

$$W_f(N_F, N_A) = 3.76 \times 10^{-6} N_F N_A, \tag{63}$$

since a unique feature of the left hand wing was of concern.

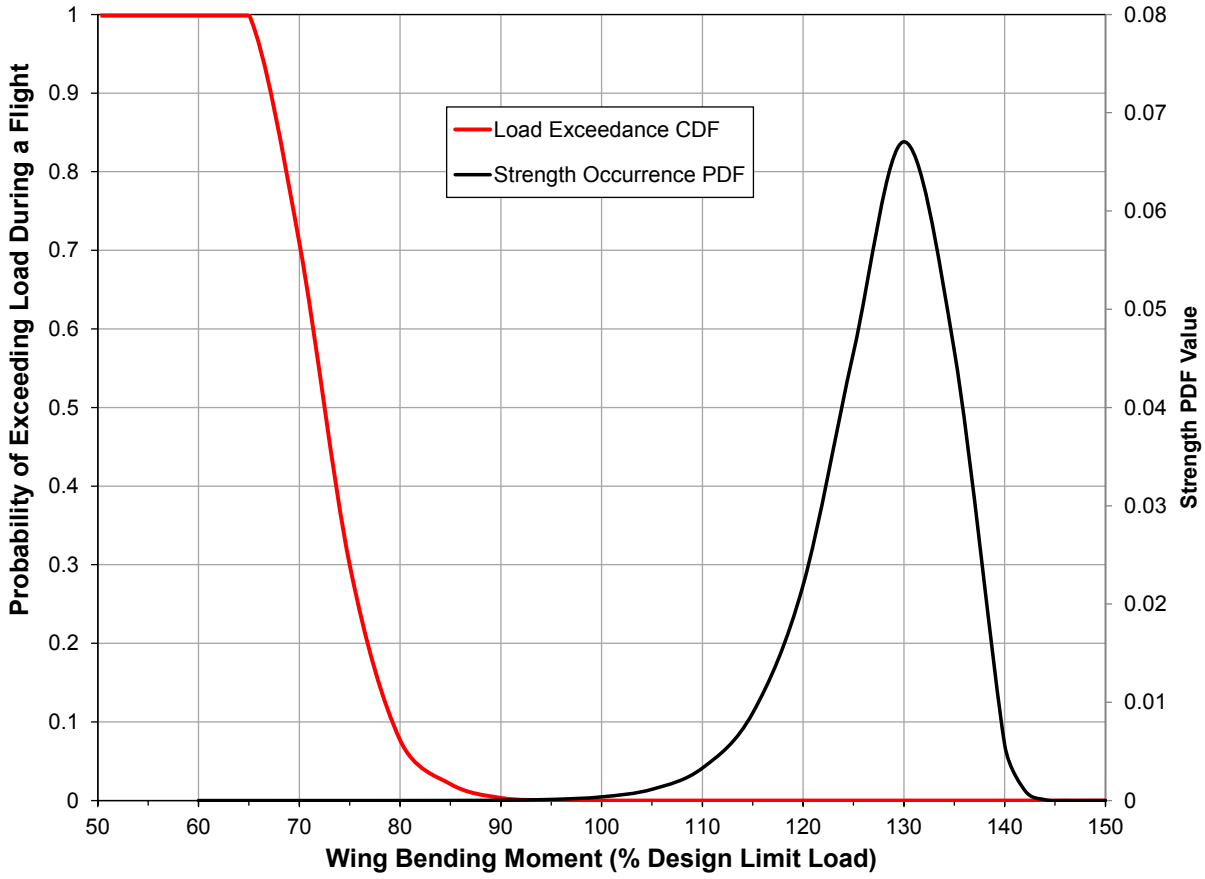

Figure 30. Plot of Load EDF and Wing Strength PDF

Table 18. Probability of Failure for Wing Buckling

WBM (% DLL)	Strength PDF, f_S	Load EDF, D_L	$H = f_S * D_L$
45	3.96E-12	1	3.96E-12
50	4.47E-11	1	4.47E-11
55	4.00E-10	1	4.00E-10
60	2.96E-09	1	2.96E-09
65	1.86E-08	1.0000	1.86E-08
70	1.03E-07	0.7148	7.33E-08
75	5.01E-07	0.3011	1.51E-07
80	2.21E-06	0.0766	1.69E-07
85	8.92E-06	0.0210	1.87E-07
90	3.32E-05	0.0034	1.13E-07
95	1.15E-04	2.80E-04	3.22E-08
100	3.74E-04	9.55E-06	3.57E-09
105	1.15E-03	1.06E-07	1.21E-10
110	3.30E-03	2.86E-10	9.46E-13
115	8.92E-03	1.33E-13	1.18E-15
120	2.19E-02	7.00E-18	1.54E-19
125	4.56E-02	2.58E-23	1.18E-24
130	6.70E-02	3.78E-30	2.53E-31
135	4.58E-02	1.14E-38	5.20E-40
140	5.69E-03	3.28E-49	1.86E-51
145	1.68E-05	3.79E-62	6.37E-67
150	1.622E-11	6.47E-78	1.05E-88
		POF =	3.76E-06

6.3.2 Sensitivity Study for the Probability of Failure

There are never sufficient data available to demonstrate that a particular probability model is correct for the application. There is seldom sufficient data available to provide precise estimates of the parameters of the model. Even when directly using an observed exceedance curve from operational data (i.e. without an assumed probability model), there is a question of fitting and extrapolating at the highest stress levels. Because of such unknowns, there is no available quantitative measure of the potential error in POF estimates. Therefore, the sensitivity of the calculated POF to the distribution models chosen and the parameters of the distribution should always be investigated. If the opportunity to gather additional data becomes available as in the example of Section 4.2.2, the sensitivity analysis indicates what additional data will increase confidence in the POF estimate.

This section assesses the sensitivity of the POF calculated in Section 6.3.1 to changes in the parameters of a distribution. Changes in the shape parameter of the load exceedance distribution

are in the range where the Weibull distribution becomes equivalent to an exponential, Rayleigh, and normal distributions. Thus, the sensitivity of the POF calculation to assumptions about the distribution type is also explored. If the calculated POF is found to change significantly with changes to either the distribution model or the parameters, this highlights where effort should be made to gather more information and data to increase confidence in the distribution models and ultimately the POF.

First, the sensitivity of the POF calculation to the size of the integration interval is investigated to be sure that the POF integration has converged. Then, parameter values for the strength distribution, and parameter values for the load exceedance distribution are investigated.

6.3.2.1 Sensitivity of the Probability of Failure to the Size of the Integration Increment

The integration increment, Δ in Table 18, is large which may introduce significant error into the calculation of the POF. At a minimum, two calculations of POF should be made using increments that are significantly different to be sure that the POF is not significantly underestimated or overestimated by the integration scheme. However, it is better if a number of POF calculations with different strength/load increment sizes are performed in the event that there are oscillations in the convergence of the reliability function. The POF can be considered converged if the change in POF with changes in the strength/load increment size is less than some value. What this value should be is problem dependent, but it should never be more than 10% of the POF.

The second calculation of POF uses an integration increment of 0.5 percent DLL. The integration is truncated at 105 percent DLL since the values in Table 18 indicated that there is very little probability of a failure at WBM values above 105 percent DLL. For WBM values less than 90 percent DLL, the load EDF was only defined at every 5 percent DLL. The load EDF was interpolated between the known points using the equation

$$F_L(x) = 10^{\left[log(F_L(x_i))+\left(\frac{log(F_L(x_i))-log(F_L(x_{i+1}))}{x_i-x_{i+1}}\right)(x-x_i)\right]}, \quad (64)$$

where x_i is a value in the first column of Table 17, x_{i+1} is the value in the row below, and x is a WBM value greater than x_i and less than x_{i+1}. For WBM values greater than 90 percent DLL, the load EDF is defined in terms of a Weibull distribution so EDF values at increments of 0.5 percent DLL can be easily calculated. The strength PDF is defined as a continuous distribution over the entire domain. The details of the calculation are presented in Table 19. For this smaller integration increment, the POF during a flight was calculated to be 3.73×10^{-6}. This is less than a 1 percent difference. Thus, the POF integration has converged at 5 percent DLL increments. An increment of 5 percent DLL will be used in the remainder of the sensitivity analysis.

Table 19. Calculation of POF during a Flight Using 0.5 Percent DLL Intervals

WBM (% DLL)	Strength PDF, f_S	Load EDF, D_L	$H = f_S * D_L$	WBM (% DLL)	Strength PDF, f_S	Load EDF, D_L	$H = f_S * D_L$	WBM (% DLL)	Strength PDF, f_S	Load EDF, D_L	$H = f_S * D_L$
50	4.47E-11	1	4.47E-11	68.5	6.23E-08	0.7868	4.90E-08	87	1.52E-05	0.0109	1.66E-07
50.5	5.62E-11	1.0000	5.62E-11	69	7.37E-08	0.7603	5.60E-08	87.5	1.74E-05	0.0091	1.58E-07
51	7.04E-11	1.0000	7.04E-11	69.5	8.70E-08	0.7347	6.39E-08	88	1.98E-05	0.0076	1.50E-07
51.5	8.82E-11	1.0000	8.82E-11	70	1.03E-07	0.7100	7.28E-08	88.5	2.26E-05	0.0063	1.41E-07
52	1.10E-10	1.0000	1.10E-10	70.5	1.21E-07	0.6514	7.87E-08	89	2.57E-05	0.0051	1.32E-07
52.5	1.37E-10	1.0000	1.37E-10	71	1.42E-07	0.5976	8.49E-08	89.5	2.92E-05	0.0042	1.23E-07
53	1.71E-10	1.0000	1.71E-10	71.5	1.67E-07	0.5483	9.16E-08	90	3.32E-05	0.0034	1.13E-07
53.5	2.12E-10	1.0000	2.12E-10	72	1.96E-07	0.5030	9.86E-08	90.5	3.77E-05	0.0027	1.03E-07
54	2.62E-10	1.0000	2.62E-10	72.5	2.30E-07	0.4615	1.06E-07	91	4.28E-05	0.0022	9.40E-08
54.5	3.24E-10	1.0000	3.24E-10	73	2.69E-07	0.4234	1.14E-07	91.5	4.86E-05	0.0017	8.47E-08
55	4.00E-10	1.0000	4.00E-10	73.5	3.15E-07	0.3885	1.22E-07	92	5.50E-05	0.0014	7.57E-08
55.5	4.92E-10	1.0000	4.92E-10	74	3.68E-07	0.3564	1.31E-07	92.5	6.23E-05	0.0011	6.71E-08
56	6.05E-10	1.0000	6.05E-10	74.5	4.30E-07	0.3270	1.41E-07	93	7.06E-05	0.0008	5.90E-08
56.5	7.43E-10	1.0000	7.43E-10	75	5.01E-07	0.3000	1.50E-07	93.5	7.98E-05	0.0006	5.14E-08
57	9.09E-10	1.0000	9.09E-10	75.5	5.84E-07	0.2617	1.53E-07	94	9.02E-05	0.0005	4.44E-08
57.5	1.11E-09	1.0000	1.11E-09	76	6.80E-07	0.2283	1.55E-07	94.5	1.02E-04	0.0004	3.80E-08
58	1.36E-09	1.0000	1.36E-09	76.5	7.90E-07	0.1992	1.57E-07	95	1.15E-04	0.0003	3.22E-08
58.5	1.65E-09	1.0000	1.65E-09	77	9.18E-07	0.1738	1.60E-07	95.5	1.30E-04	0.0002	2.71E-08
59	2.01E-09	1.0000	2.01E-09	77.5	1.07E-06	0.1516	1.62E-07	96	1.46E-04	0.0002	2.25E-08
59.5	2.44E-09	1.0000	2.44E-09	78	1.24E-06	0.1323	1.63E-07	96.5	1.65E-04	0.0001	1.86E-08
60	2.96E-09	1	2.96E-09	78.5	1.43E-06	0.1154	1.65E-07	97	1.86E-04	8.16E-05	1.52E-08
60.5	3.58E-09	1.0000	3.58E-09	79	1.66E-06	0.1007	1.67E-07	97.5	2.09E-04	5.86E-05	1.22E-08
61	4.33E-09	1.0000	4.33E-09	79.5	1.91E-06	0.0878	1.68E-07	98	2.35E-04	4.16E-05	9.78E-09
61.5	5.22E-09	1.0000	5.22E-09	80	2.21E-06	0.0766	1.69E-07	98.5	2.64E-04	2.93E-05	7.73E-09
62	6.29E-09	1.0000	6.29E-09	80.5	2.55E-06	0.0686	1.75E-07	99	2.97E-04	2.04E-05	6.05E-09
62.5	7.57E-09	1.0000	7.57E-09	81	2.94E-06	0.0612	1.80E-07	99.5	3.33E-04	1.40E-05	4.67E-09
63	9.09E-09	1.0000	9.09E-09	81.5	3.39E-06	0.0544	1.84E-07	100	3.74E-04	9.55E-06	3.57E-09
63.5	1.09E-08	1.0000	1.09E-08	82	3.90E-06	0.0481	1.88E-07	100.5	4.19E-04	6.43E-06	2.70E-09
64	1.31E-08	1.0000	1.31E-08	82.5	4.49E-06	0.0424	1.90E-07	101	4.70E-04	4.28E-06	2.01E-09
64.5	1.56E-08	1.0000	1.56E-08	83	5.16E-06	0.0372	1.92E-07	101.5	5.27E-04	2.82E-06	1.48E-09
65	1.86E-08	1.0000	1.86E-08	83.5	5.92E-06	0.0324	1.92E-07	102	5.89E-04	1.83E-06	1.08E-09
65.5	2.22E-08	0.9663	2.15E-08	84	6.79E-06	0.0282	1.91E-07	102.5	6.59E-04	1.18E-06	7.76E-10
66	2.65E-08	0.9338	2.47E-08	84.5	7.79E-06	0.0244	1.90E-07	103	7.37E-04	7.47E-07	5.51E-10
66.5	3.15E-08	0.9024	2.84E-08	85	8.92E-06	0.0210	1.87E-07	103.5	8.24E-04	4.68E-07	3.85E-10
67	3.74E-08	0.8720	3.27E-08	85.5	1.02E-05	0.0179	1.83E-07	104	9.20E-04	2.89E-07	2.66E-10
67.5	4.44E-08	0.8426	3.74E-08	86	1.17E-05	0.0153	1.78E-07	104.5	1.03E-03	1.76E-07	1.81E-10
68	5.26E-08	0.8142	4.29E-08	86.5	1.33E-05	0.0129	1.72E-07	105	1.15E-03	1.06E-07	1.21E-10
										POF =	3.73E-06

6.3.2.2 Assessing Sensitivity to Parameters of the Strength Distribution

The strength was assumed to follow a Weibull distribution whose mean was assumed to be equal to the one known failure at 128 percent DLL. The shape parameter was estimated to be 24. Freudenthal and Wang [15] found the shape parameter for the ultimate strength of critical elements of the airframe, and thus of airframes, to be 19. Data on the strength of C-141 wing component and full-scale wing tests in Campion, et al., [16] can be fit by a Weibull distribution with a shape parameter of 16. The shape parameter of the Weibull distribution determines the scatter about the mean; a large shape parameter means less scatter.

First, look at how the POF changes as the mean of the strength distribution changes, and thus the scale parameter changes. Remember from Section 6.3.1.1, Equation (30) that with a shape parameter of 24 the scale parameter β is equal to

$$\beta = \mu / 0.9776. \tag{65}$$

The POF as a function of the mean of the strength distribution is plotted in Figure 31. POF values at intervals of 5 percent DLL change in the mean strength were determined by re-calculating the scale parameter for each new mean strength and re-evaluating the strength PDF. Lower mean strength values result in higher POFs. It is unlikely that the mean strength of the wing is greater than 148 percent DLL, the value where the POF becomes acceptable. Therefore, more data on the mean strength of other wings in the fleet will not change the conclusion that the F-16 C/D wings need to be modified. In fact, the wings need to be strengthened to at least 148 percent DLL.

The POF as a function of the shape parameter for a fixed mean strength of 128 percent DLL is presented in Figure 32. Recall that the scale parameter also changes since,

$$\beta = \frac{128\%\ DLL}{\Gamma\left(1+\frac{1}{\alpha}\right)}. \tag{66}$$

As the shape parameter decreases, the scatter in the strength increases and the POF increases. So, even though the value of the shape parameter may be high compared to Freudenthal's estimate, reducing the value of the shape parameter will not change the conclusion that the F-16 C/D wings need to be modified. The shape parameter needs to be in the range of 33 to 34 before the POF is below 10^{-7}.

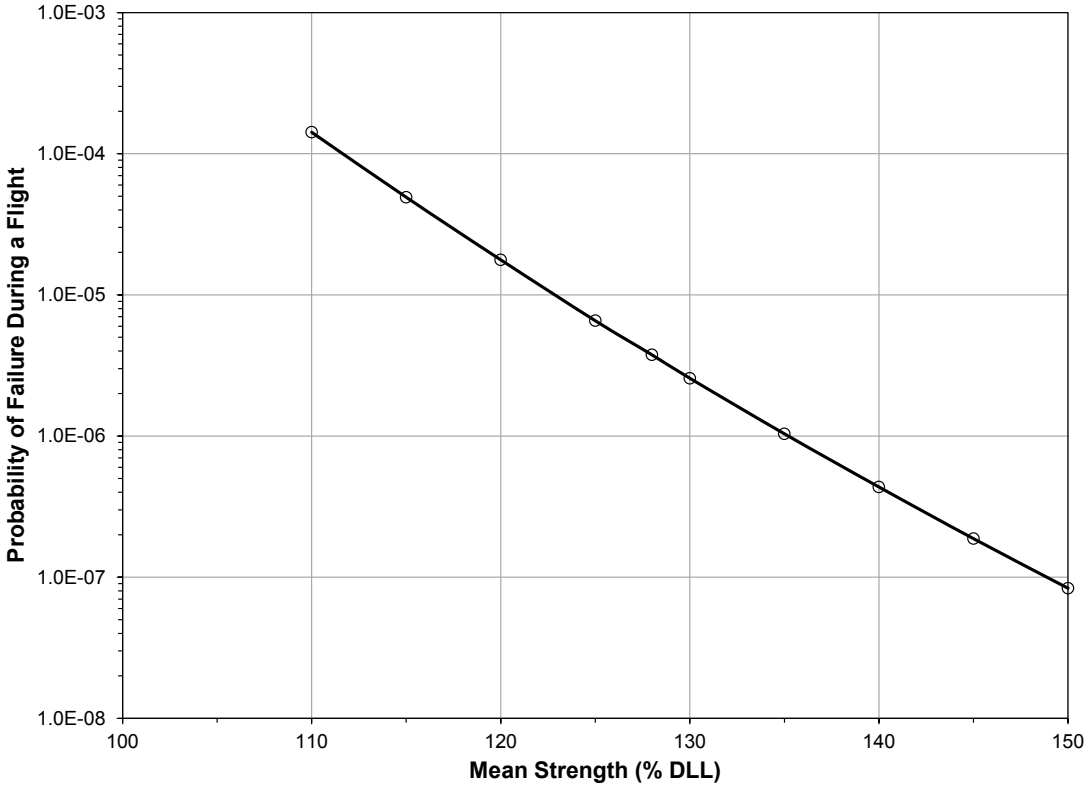

Figure 31. POF as a Function of Mean Strength with a Shape Parameter of 24

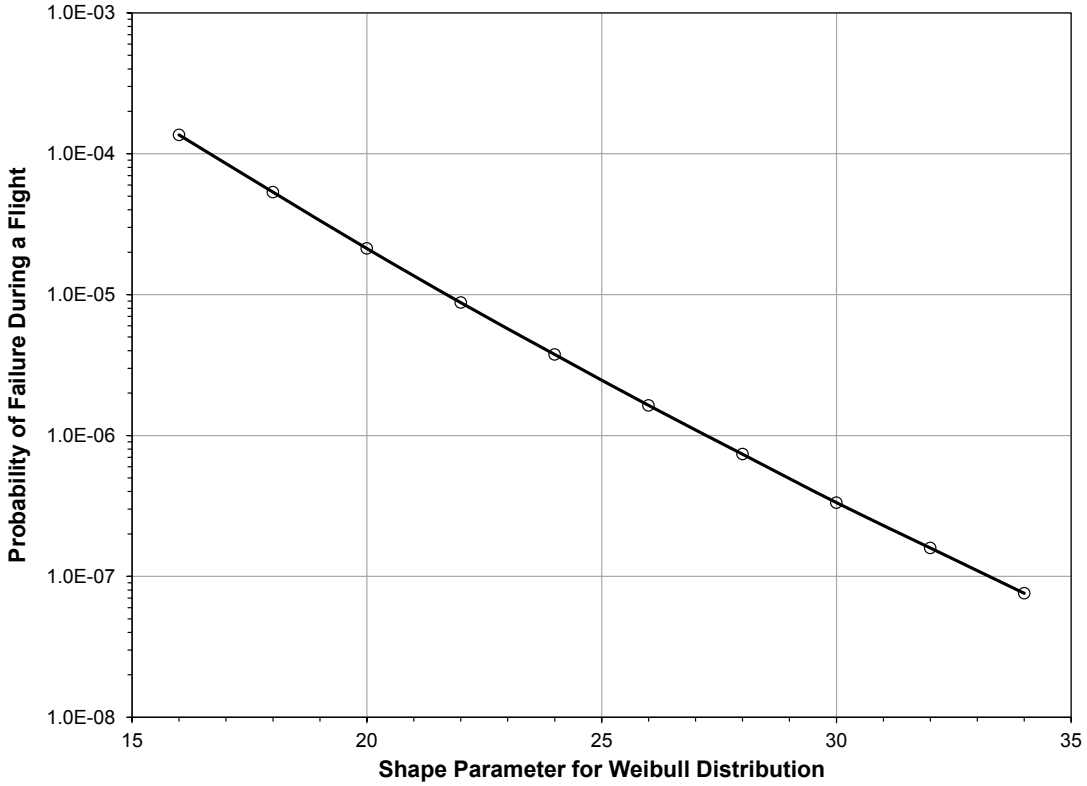

Figure 32. POF as a Function of the Shape Parameter with a Mean Strength of 128 Percent DLL

6.3.2.2.1 Assessing Sensitivity to Extrapolation of Exceedance Distribution

The load EDF in this example was extrapolated from 90 percent DLL to 150 percent DLL based upon a curve fit to the four data points between 80 percent DLL and 91 percent DLL. This is not much data upon which to base this extrapolation. In this section, the sensitivity of the POF to this extrapolation will be investigated by changing the shape parameter of the Weibull distribution used for extrapolation. The Weibull distribution will be forced to pass through the point (90 percent DLL, 0.0034) at the end of the known exceedance points. The scale parameter becomes

$$\beta = exp\left\{ ln(0.9) - \frac{1}{\alpha} ln\left[ln\left(\frac{1}{0.0034} \right) \right] \right\}. \quad (67)$$

Changing the shape parameter of a Weibull distribution can make it equal to other common distributions. When the shape parameter is 3.5, the Weibull distribution is symmetric like a normal distribution. A shape parameter of 2 gives a Rayleigh distribution. And a shape parameter of 1 is an exponential distribution. So, this section is also assessing the sensitivity of the POF to the distribution model chosen to extrapolate the exceedance curve.

The effect of changes to the shape parameter on the extrapolation of the EDF is shown in Figure 33. As the shape parameter decreases, the probability of a load equal to 150 percent DLL occurring increases. This will increase the POF.

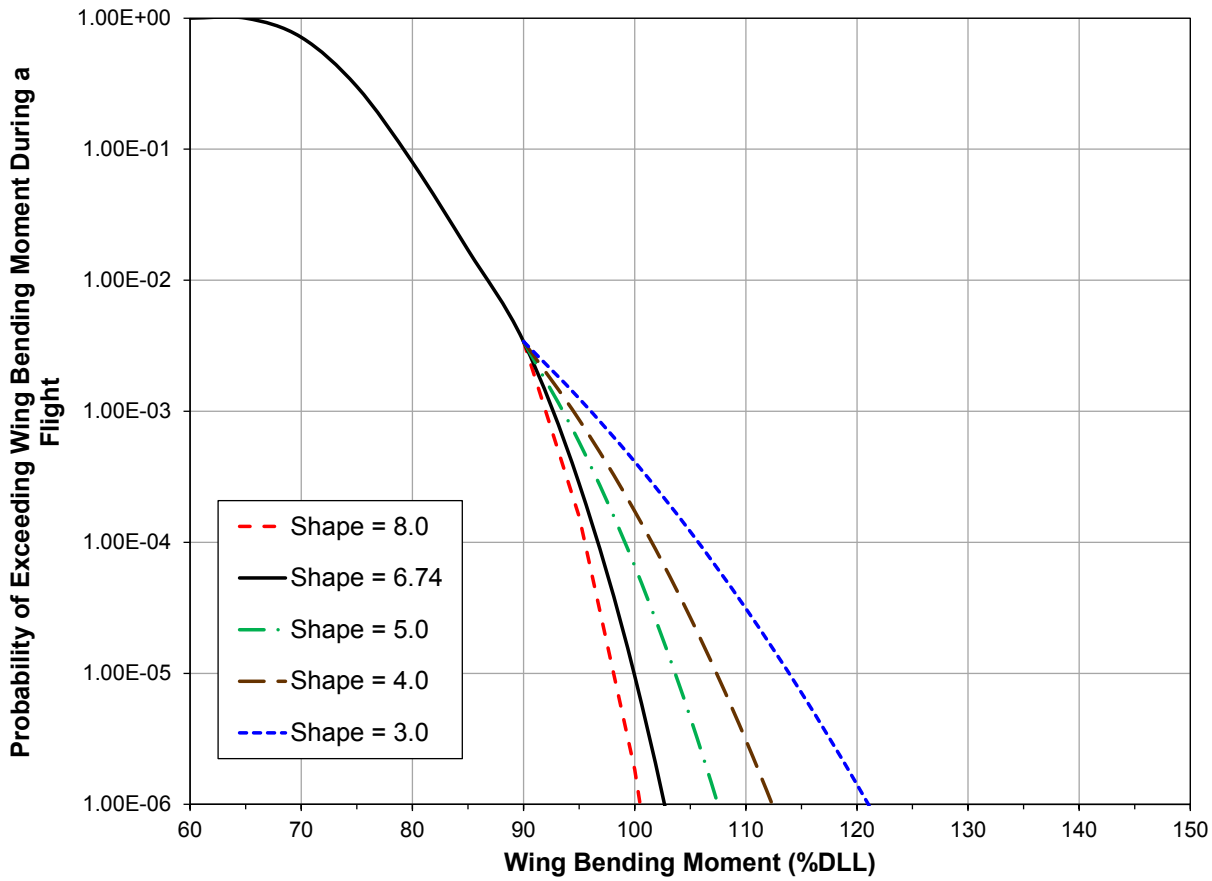

Figure 33. The Effect of Shape Parameter on Extrapolation of the EDF

The resulting POF for these different load EDFs are given in Table 20 for a strength PDF that is a Weibull distribution with shape parameter of 24 and a scale parameter of 130.9 percent D LL. Notice that the POF has a minimum for the extrapolation of the EDF at a shape parameter of approximately 5.0. The POF is still unacceptable for every extrapolation of the exceedance curve. A modification to the wings is still necessary.

Table 20. Variation of POF with Load EDFs

Exceedance Shape Parameter	Exceedance Scale Parameter	POF
1.00	15.84	3.44E-04
2.00	37.76	2.65E-05
3.00	50.44	5.61E-06
4.00	58.29	3.63E-06
5.00	63.58	3.37E-06
6.74	69.55	3.75E-06
8.00	72.43	4.31E-06

The sensitivity study showed that the POF for buckling of the wings was unacceptable for any reasonable changes in the strength PDF and the load EDF. There is no additional data that could be collected that would change the decision to strengthen the wings. So, while there might be some uncertainty about the value of the POF, it is certain that the wings need to be strengthened in order to meet structural integrity requirements.

6.3.3 Two Random Variables Example: Fracture Toughness and Maximum Load

Consider the case where a crack is found in an airframe component, but the aircraft needs to flown somewhere to be repaired. This might be the situation when an aircraft is deployed when a crack is found, and it needs to be flown back to the depot for the repair. The failure mode of concern here is fracture of the part. As long as the maximum applied stress intensity K_{app} in the flight remains less than the fracture toughness of material K_c, fracture will not occur. The POF equation is

$$P_f = Pr\left(K_c \le K_{app}\right) = \int_0^\infty D_{K_{app}}(x) f_{K_C}(x) dx. \tag{68}$$

The applied stress intensity is equal to

$$K_{app} = \sigma_{app} \beta \sqrt{\pi a}, \tag{69}$$

where a is the length of the crack, β is a factor that depends on the part geometry and the crack length, and σ_{app} is the maximum stress applied to the part. If the next flight is not too severe, as might be the case when flying from one base to another (noting that atmospheric turbulence can still be encountered), the crack is not going to grow much during the flight. The crack length can be assumed constant during the flight. Thus, $\beta\sqrt{(\pi a)}$ becomes a constant multiplier on σ_{app}. K_{app}

is a random variable because σ_{app} is a random variable. The fracture toughness K_c is the other random variable in the problem.

The calculation of the POF for this example is discussed in the following sections.

6.3.3.1 Calculation of the Stress Intensity Factor

A 1.25 inch crack was detected at a 0.25 inch diameter hole near a wing root in 7050-T7351 plate material. The idealized geometry is shown in Figure 34. The stress-intensity factor, *K*, for this geometry with a thru-thickness, radial-cracked hole is [17]

$$K = \sigma\beta\sqrt{\pi a} \tag{70}$$

where

$$\beta = \beta_{hole}\beta_{width}, \tag{71}$$

$$\beta_{hole} = 0.7071 + 0.7548z + 0.3415z^2 + 0.642z^3 + 0.9196z^4, \tag{72}$$

$$z = \frac{1}{1 + \frac{a}{r}}, \tag{73}$$

and

$$\beta_{width} = \sqrt{\sec\left(\frac{\pi}{2} \cdot \frac{2r+a}{W-a}\right)}\,. \tag{74}$$

For this geometry and crack size, the stress intensity becomes

$$K = 1.572 \cdot \sigma. \tag{75}$$

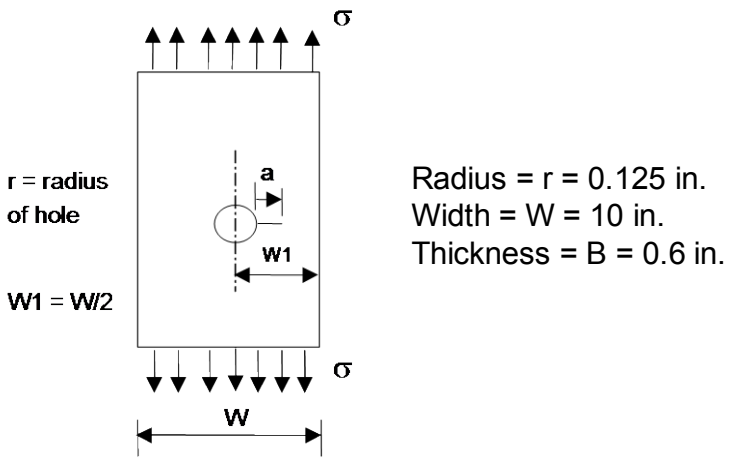

Figure 34. Geometry for Fracture Reliability Example
Plate loaded in uniform tension with a through-thickness, radial cracked hole

6.3.3.2 Determine the Probability Distribution for the Fracture Toughness

For 0.60 inch thick 7050-T7351 aluminum plate in the L-T orientation, the best engineering data available are K_{Ic} results for 31 samples excised from 7050-T7351 plate ranging in thickness from

1.0 inch to 6.0 inches and machined into specimens 1.0 inch to 2.0 inches thick [18]. The data are rank ordered in Table 21 using median rank, Equation (26).

Table 21. Al 7050-T7351 Fracture Toughness K_{Ic} Data [18]

K_{Ic} (ksi√in)	Median Rank
28.6	0.0223
28.9	0.0541
29.1	0.0860
29.3	0.1178
29.3	0.1497
29.7	0.1815
33.3	0.2134
33.4	0.2452
33.5	0.2771
33.6	0.3089
33.6	0.3408
34.0	0.3726
34.2	0.4045
34.3	0.4363
34.3	0.4682
34.3	0.5000
34.5	0.5318
34.8	0.5637
35.0	0.5955
35.1	0.6274
35.5	0.6592
35.9	0.6911
36.4	0.7229
36.5	0.7548
36.9	0.7866
39.3	0.8185
39.3	0.8503
39.5	0.8822
41.5	0.9140
43.0	0.9459
43.4	0.9777

Plotting the data on normal, lognormal, and Weibull probability plots gave correlations R^2 of 93.9 percent, 94.4 percent, and 89 percent, respectively. Since the data plots the most linear (highest R^2) on a lognormal plot, the lognormal distribution will be used to model the fracture toughness. The data is plotted on a lognormal probability plot in Figure 35. MLE was used to estimate the best fit line representing the best-fit distribution. A two-sided 95 percent confidence band is constructed using the method described in Section 0.

The mean of the natural logarithm of the fracture toughness is 3.545 corresponding to a fracture toughness of 34.6 ksi√in. The standard deviation is 0.11. Accordingly, the fracture toughness is modeled by the lognormal CDF

$$Pr(K_C < k) = \Phi\left(\frac{\ln(k) - \ln(34.6)}{0.11}\right) \tag{76}$$

where $\Phi(z)$ is the standard normal CDF that has mean = 0 and standard deviation = 1.

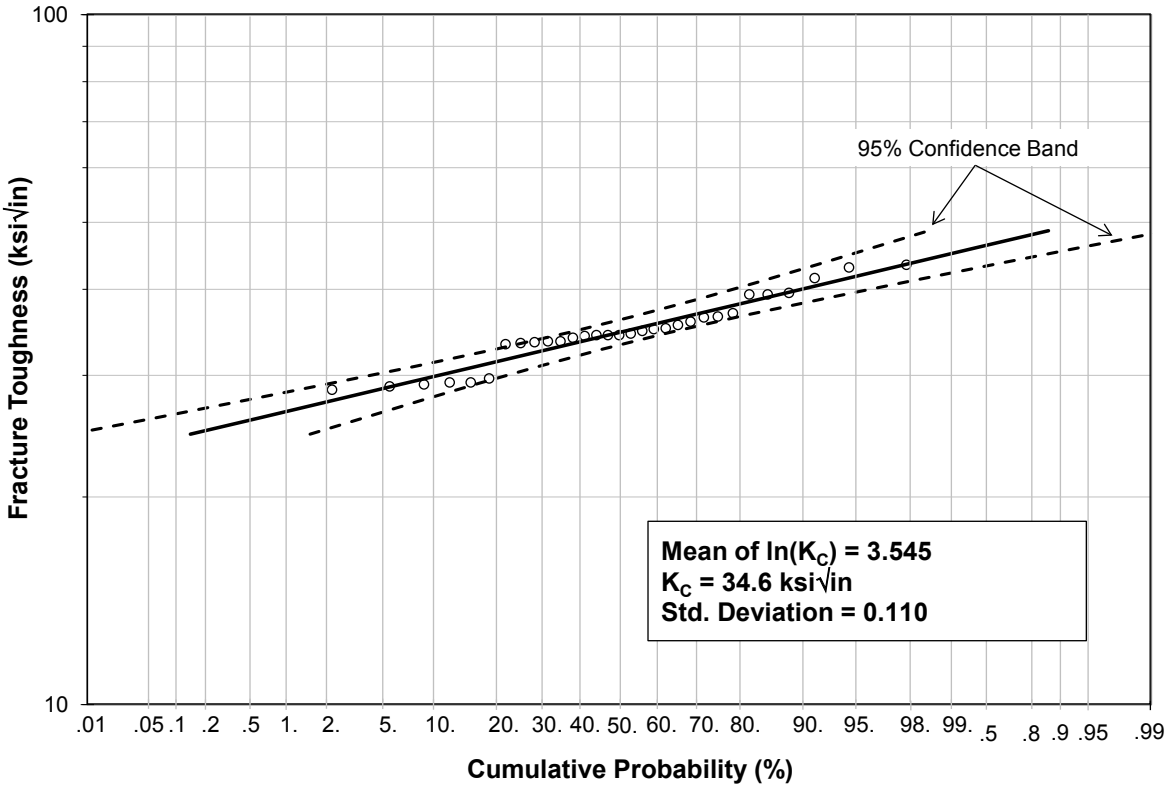

Figure 35. Lognormal Probability Plot of Fracture Toughness for Al 7050-T7351 Plate

6.3.3.3 The Stress Exceedance Distribution Function

Load exceedance data should be separated by mission type, or mission phase, if possible, as in Table 22. The peak N_z exceedances for a fighter aircraft broken out by mission type in Table 22 are the *Handbook of Military Aircraft Design Normal Load Factor Exceedance Data* [19]. The two most benign mission types are the Transition mission and the Instrument/Ferry mission. The exceedance plot in Figure 36 shows that while the Transition flight has more N_z peaks overall, the number of exceedances in the Transition flight decreases very rapidly above 8.0g's and has fewer exceedances above about 8.3g's. It is not clear how the differences between these two mission types will affect the POF. So, the POF using both exceedance curves will be calculated with the idea that these two missions will provide an idea of what could actually happen during a flight to a repair station.

Table 22. Maneuver N_z Exceedance per 1,000 FH by Mission for Fighter Aircraft [19]

N_z	Transition	Instrument/ Ferry	Air Combat Maneuvers	Air-to-Air	Air-to-Ground
2.0	23,466	6,391	36,894	27,847	38,373
2.5	22,347	5,917	34,913	25,620	36,642
3.0	17,439	4,645	28,220	19,927	29,666
3.5	12,945	3,254	22,129	15,146	22,878
4.0	10,092	2,456	17,697	11,277	17,602
4.5	7,362	1,805	13,173	8,431	12,753
5.0	5,015	1,154	9,732	6,642	8,571
5.5	3,635	888	7,523	4,964	5,537
6.0	2,454	562	5,489	3,613	3,233
6.5	1,641	444	3,628	2,299	1,814
7.0	966	355	2,396	1,423	1,178
7.5	521	207	1,620	876	417
8.0	245	89	669	438	125
8.5	30.7	59	187	292	63
9.0	-	29.6	26.8	109	20.9
9.5	-	-	-	73	10.4

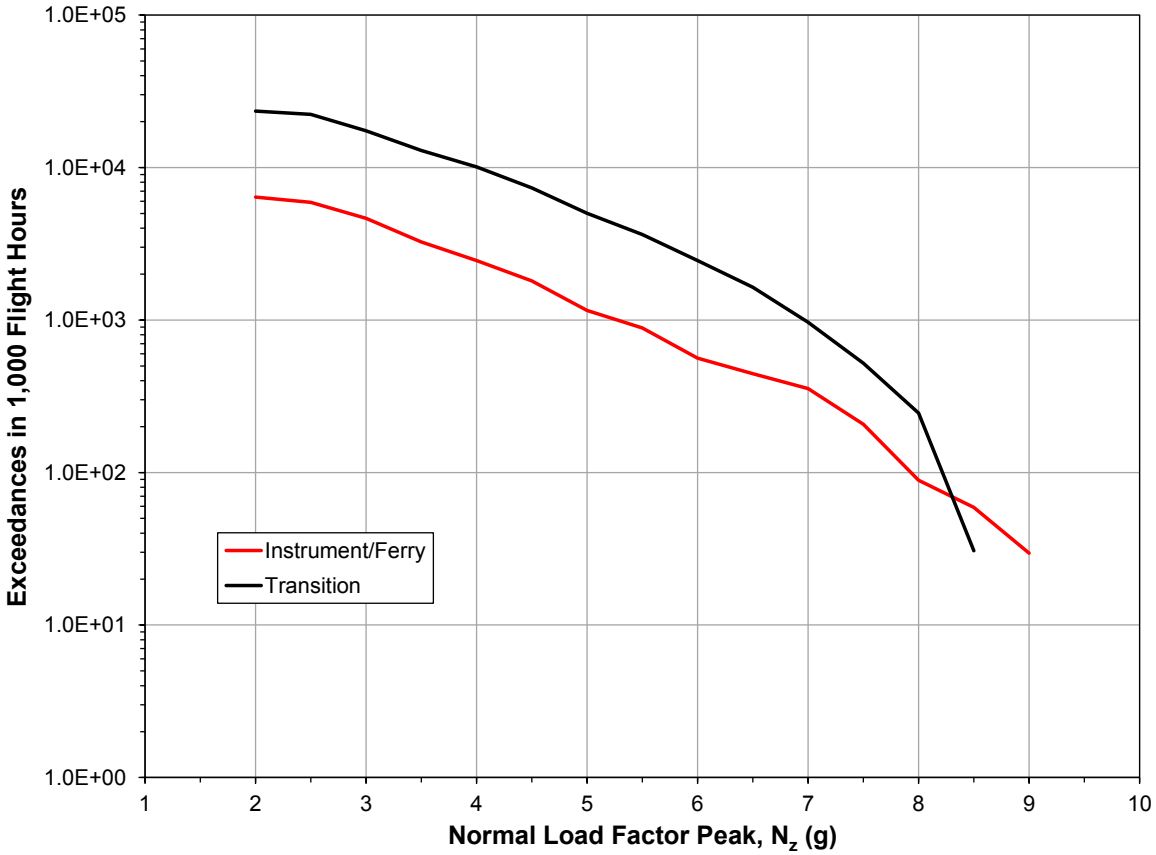

Figure 36. Peak N_z Exceedances for Transition and Instrument/Ferry Flights

The procedure used in Section 6.3.1.2 will be used to construct the EDF's for the two mission types. The average length of either a Transition or an Instrument/Ferry flight is 1.25 hours. There are 800 flights in 1000 FH. The expected number of peak N_z exceedances during a flight are found by dividing the exceedances in Table 22 by 800 flights. The results are shown in Table 23. Any peak that has more than one exceedance in a flight has an exceedance probability of 1.0. Assuming that only one peak occurs in the fractional exceedance in a flight (above 7.0g for the Transition mission, and 5.5g for the Instrument/Ferry mission), the fractional exceedance is the probability of exceeding an N_z value. And for the initial assessment, it will be assumed that N_z never exceeds 9.0g during a Transition flight and never exceeds 9.5g during an Instrument/Ferry flight. The resulting exceedance probabilities are given in Table 24.

The next step is to fit a distribution function to the exceedance probabilities. The Weibull distribution will be used because of its flexibility. The exceedance probabilities that are less than one and greater than zero were plotted on a Weibull plot in Figure 37. A LSE line was fit to the two datasets using Equation (23). The shape parameter for the Transition flight is 1.81, the scale parameter is 0.83g, and the minimum value is 7.0g. The shape parameter for the Instrument/Ferry flight is 1.19, the scale parameter is 1.42g, and the minimum value is 5.5g. The complete EDF for both types of flights are graphed in Figure 38.

Table 23. Peak N_z Exceedances in a Flight

N_z	Transition	Instrument/ Ferry
2.0	29.33	7.989
2.5	27.93	7.396
3.0	21.80	5.806
3.5	16.18	4.068
4.0	12.62	3.070
4.5	9.203	2.256
5.0	6.269	1.443
5.5	4.544	1.110
6.0	3.068	0.703
6.5	2.051	0.555
7.0	1.208	0.444
7.5	0.651	0.259
8.0	0.306	0.111
8.5	0.038	0.074
9.0	0	0.037
9.5	-	0

Table 24. Probability of Exceeding N_z Value During a Flight

N_z	Transition	Instrument/ Ferry
2.0	1.00	1.00
2.5	1.00	1.00
3.0	1.00	1.00
3.5	1.00	1.00
4.0	1.00	1.00
4.5	1.00	1.00
5.0	1.00	1.00
5.5	1.00	1.00
6.0	1.00	0.703
6.5	1.00	0.555
7.0	1.00	0.444
7.5	0.651	0.259
8.0	0.306	0.111
8.5	0.038	0.074
9.0	0	0.037
9.5	-	0

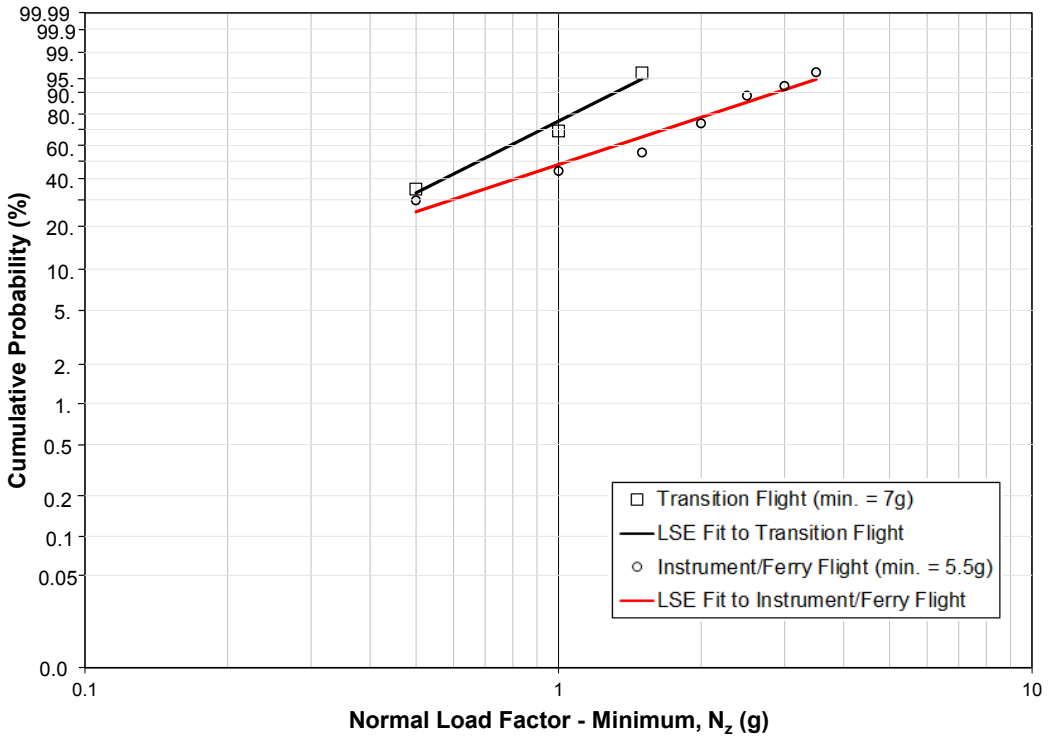

Figure 37. Weibull Extrapolation of N_z EDF for Transition and Instrument/Ferry Flights

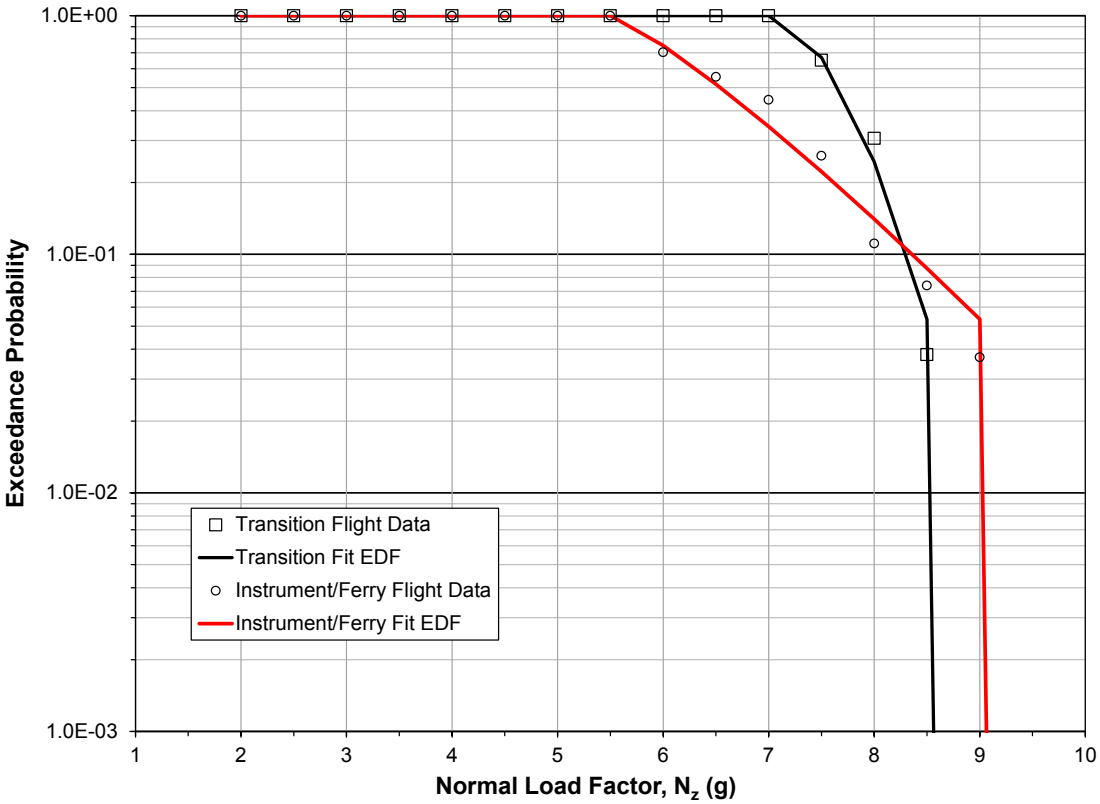

Figure 38. N_z EDFs for Transition and Instrument/Ferry Flights

The peak N_z must be converted to an internal load using a stress transfer function. The associated applied stress σ_{app} is determined from a stress analysis of the local detail using the derived internal load. Assume that this results in σ_{app} being equal to 1.741 times N_z.

The stress intensity EDF is derived by scaling the N_z EDF appropriately. Since

$$K_{app} = 1.572 \cdot \sigma_{app} = 1.572\ (1.741 \cdot N_z) \tag{77}$$

$$Pr(K_{app} > \mathrm{k}) = Pr(N_z > \mathrm{k}/2.737) \tag{78}$$

Substituting k/2.737 for N_z in the N_z EDF for the Transition flight yields

$$Pr\left(K_{app} > k\right) = \ 1, \ \text{if} \ \frac{k}{2.737} \leq 7, \tag{79a}$$

$$Pr\left(K_{app} > k\right) = exp\left[-\left(\frac{\frac{k}{2.737} - 7}{0.83}\right)^{1.81}\right], \qquad \text{if } 8.5 > \frac{k}{2.737} > 7, \tag{79b}$$

$$Pr\left(K_{app} > k\right) = 10^{232.05 - 27.45\left(\frac{k}{2.737}\right)}, \qquad \text{if } 9 > \frac{k}{2.737} \geq 8.5, \tag{79c}$$

and

$$Pr\left(K_{app} > k\right) = 0, \qquad \text{if } \frac{k}{2.737} \geq 9. \tag{79d}$$

The resulting EDF for the stress intensity factor during the Instrument/Ferry flight is

$$Pr\left(K_{app} > k\right) = \ 1, \ \text{if} \ \frac{k}{2.737} \leq 5.5, \tag{80a}$$

$$Pr\left(K_{app} > k\right) = exp\left[-\left(\frac{\frac{k}{2.737} - 5.5}{1.42}\right)^{1.19}\right], \qquad \text{if } 9 > \frac{k}{2.737} > 5.5, \tag{80b}$$

$$Pr\left(K_{app} > k\right) = 10^{245.83 - 27.46\left(\frac{k}{2.737}\right)}, \qquad \text{if } 9.5 > \frac{k}{2.737} \geq 9, \tag{80c}$$

and

$$Pr\left(K_{app} > k\right) = 0, \qquad \text{if } \frac{k}{2.737} \geq 9.5. \tag{80d}$$

6.3.3.4 Calculation of Probability of Failure (POF)

Now that the applied stress intensity EDFs and the fracture toughness PDF have been determined, the POF can be calculated. The relationship between the three distributions is shown graphically in Figure 39. From this graph, it is apparent that the limits of the numerical

integration should be from 15 ksi√in to 25 or 26 ksi√in depending upon which EDF is being used. There is very little contribution to the POF outside of this range.

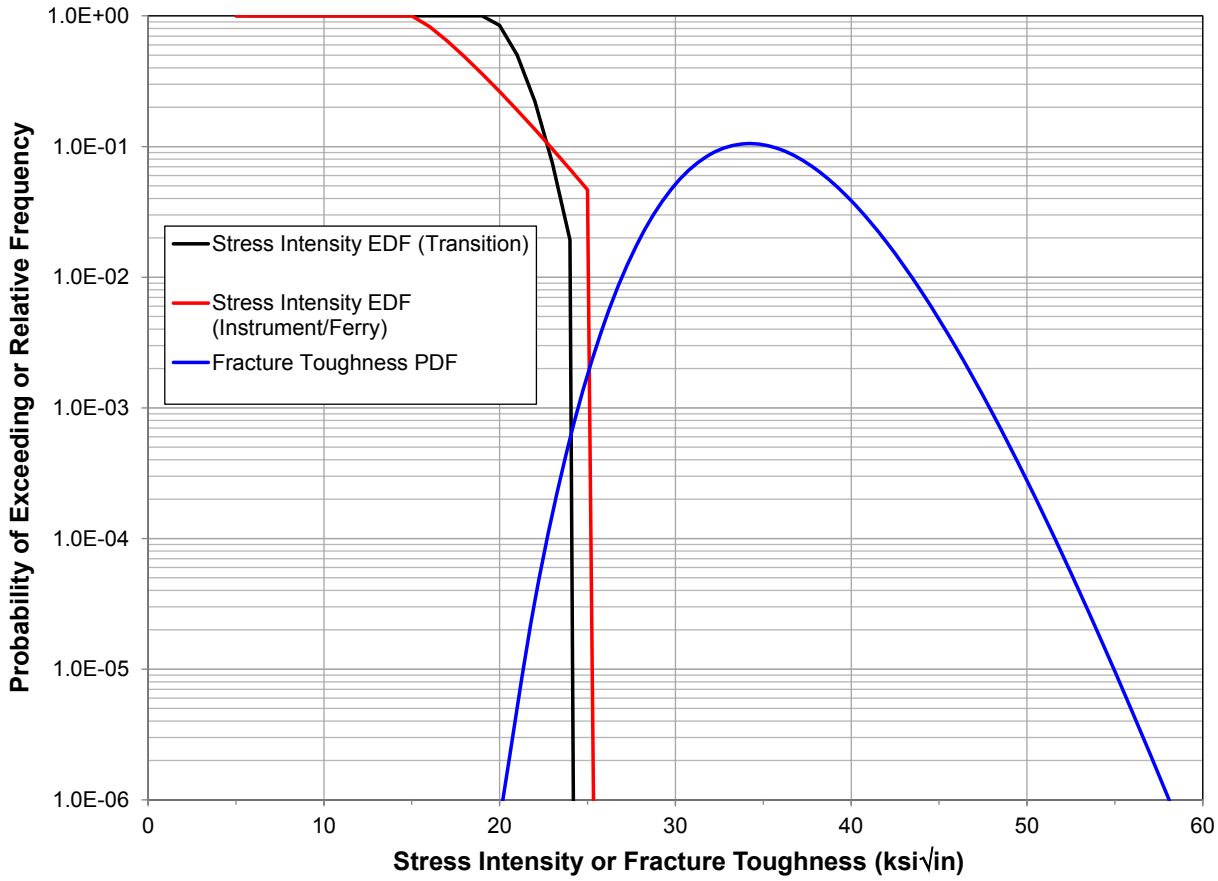

Figure 39. Plot of Applied Stress Intensity EDFs and Fracture Toughness PDF

The numerical integration of the POF equation using the Transition flight EDF is performed in Table 25. The upper limit of the integration is 25 ksi√in since the product of 2.737 and 9.0g (the upper limit of the N_z EDF) is 24.6 ksi√in. The trapezoidal rule was used to perform the integration with an interval Δ of 0.5 ksi√in. The POF for a Transition-type flight is 1.94×10^{-5}.

The numerical integration of the POF equation using the Instrument/Ferry flight EDF is performed using Table 26. The upper limit for this integration is 26 ksi√in, the product of 2.737 and 9.5g (the upper limit of the N_z EDF). The trapezoidal rule is used again to calculate the integral. The POF for an Instrument/Ferry-type flight is 7.71×10^{-5}.

Based upon these two results, a reasonable estimate of the POF for this component with a 1.25 in. long crack during a single flight to a repair station is around 5×10^{-5}. This is greater than 10^{-5} per flight probability of catastrophic failure specified in Mil-Std-1530C [3] as unacceptable. Opportunities to reduce the risk of failure should be further evaluated to ensure that the aircraft could be safely flown to the repair station. These risk reduction opportunities include further flight restrictions and temporary repairs. The POF is dominated by the chances of failure in stress intensity range of 20 to 25 ksi√in corresponding to N_z values of 7.3g to 9.1g. So, the

additional flight restrictions would need to ensure that an N_z of 7.25g is not exceeded during the flight.

Table 25. POF for Transition Flight EDF

Stress Intensity (ksi√in)	Stress Intensity EDF, D_{Kapp}	Fracture Toughness PDF, f_{KC}	$H = D_{Kapp} * f_{KC}$
15	1.00	6.49E-14	6.49E-14
15.5	1.00	5.81E-13	5.81E-13
16	1.00	4.45E-12	4.45E-12
16.5	1.00	2.96E-11	2.96E-11
17	1.00	1.73E-10	1.73E-10
17.5	1.00	8.91E-10	8.91E-10
18	1.00	4.11E-09	4.11E-09
18.5	1.00	1.71E-08	1.71E-08
19	1.00	6.43E-08	6.43E-08
19.5	0.97	2.21E-07	2.14E-07
20	0.85	6.99E-07	5.92E-07
20.5	0.68	2.04E-06	1.39E-06
21	0.50	5.52E-06	2.79E-06
21.5	0.35	1.40E-05	4.85E-06
22	0.22	3.30E-05	7.38E-06
22.5	0.13	7.35E-05	9.84E-06
23	0.075	1.54E-04	1.16E-05
23.5	0.0002	3.07E-04	7.08E-08
24	2.23E-09	5.79E-04	1.29E-12
24.5	2.16E-14	1.04E-03	2.25E-17
25	0.00	1.79E-03	0.00E+00
		POF =	1.94E-05

Table 26. POF for Instrument/Ferry Flight EDF

Stress Intensity (ksi√in)	Stress Intensity EDF, D_{Kapp}	Fracture Toughness PDF, f_{KC}	$H = D_{Kapp} * f_{KC}$
15	1.00	6.49E-14	6.49E-14
15.5	0.93	5.81E-13	5.38E-13
16	0.83	4.45E-12	3.69E-12
16.5	0.73	2.96E-11	2.17E-11
17	0.64	1.73E-10	1.11E-10
17.5	0.56	8.91E-10	5.00E-10
18	0.49	4.11E-09	2.00E-09
18.5	0.42	1.71E-08	7.17E-09
19	0.36	6.43E-08	2.32E-08
19.5	0.31	2.21E-07	6.84E-08
20	0.26	6.99E-07	1.84E-07
20.5	0.22	2.04E-06	4.58E-07
21	0.19	5.52E-06	1.05E-06
21.5	0.16	1.40E-05	2.25E-06
22	0.14	3.30E-05	4.49E-06
22.5	0.11	7.35E-05	8.41E-06
23	0.10	1.54E-04	1.48E-05
23.5	0.081	3.07E-04	2.47E-05
24	0.067	5.79E-04	3.90E-05
24.5	0.056	1.04E-03	5.86E-05
25	1.02E-05	1.79E-03	1.82E-08
25.5	9.81E-11	2.94E-03	2.89E-13
26	9.44E-16	4.65E-03	4.39E-18
		POF =	7.71E-05

6.3.3.5 Sensitivity of Probability of Failure to Distribution Models

A sensitivity study should be conducted to determine the impact of uncertainty about the fracture toughness distribution and the EDF distributions on the POF. The sensitivity study is discussed in the following sections.

6.3.3.5.1 Uncertainty in the Fracture Toughness Distribution

The significance of the 95 percent confidence band on the fracture toughness distribution in Figure 35 is that if a different sample of multiple pieces was selected from the entire population of 7050-T7351 aluminum plate, the fracture toughness distribution from that sample will fall

within the confidence band 95 percent of the time. Since this aircraft is a different sample than the test specimens, the fracture toughness distribution for the aircraft might be different than the sample from test data. A likely fracture toughness distribution for the aircraft sample that yields the lowest POF has the low toughness tail of the distribution tangent to the upper curve of the 95 percent confidence band as shown by the red line in Figure 40. The standard deviation of this distribution (slope of the line) is 0.089 and the mean remains the same. The POF for this new fracture toughness distribution with the Instrument/Ferry EDF is 4.88 x 10^{-6}. The calculation is shown in Table 27. This is an order of magnitude decrease in the POF.

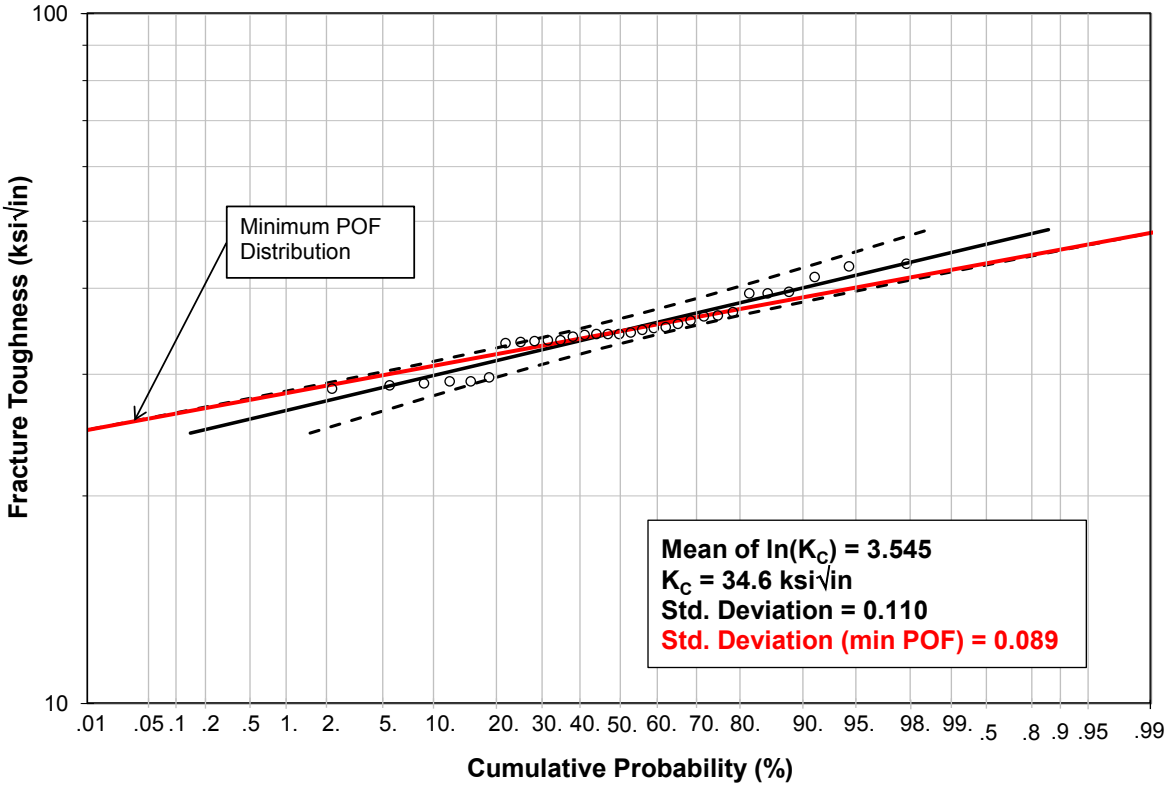

Figure 40. Minimum POF Fracture Toughness Distribution within 95 Percent Confidence Band

Table 27. POF for Fracture Toughness PDF with Standard Deviation of 0.089

Stress Intensity (ksi√in)	Stress Intensity EDF, D_{Kapp}	Fracture Toughness PDF, f_{KC}	$H = D_{Kapp} * f_{KC}$
15	1.00	1.87E-20	1.87E-20
15.5	0.93	5.41E-19	5.01E-19
16	0.83	1.23E-17	1.03E-17
16.5	0.73	2.27E-16	1.67E-16
17	0.64	3.40E-15	2.19E-15
17.5	0.56	4.24E-14	2.38E-14
18	0.49	4.45E-13	2.17E-13
18.5	0.42	3.97E-12	1.67E-12
19	0.36	3.06E-11	1.10E-11
19.5	0.31	2.05E-10	6.32E-11
20	0.26	1.20E-09	3.17E-10
20.5	0.22	6.25E-09	1.40E-09
21	0.19	2.90E-08	5.52E-09
21.5	0.16	1.21E-07	1.95E-08
22	0.14	4.57E-07	6.21E-08
22.5	0.11	1.57E-06	1.79E-07
23	0.10	4.93E-06	4.74E-07
23.5	0.081	1.42E-05	1.15E-06
24	0.067	3.80E-05	2.56E-06
24.5	0.056	9.42E-05	5.30E-06
25	1.02E-05	2.18E-04	2.22E-09
25.5	9.81E-11	4.71E-04	4.61E-14
26	9.44E-16	9.55E-04	9.02E-19
		POF =	4.88E-06

(using Instrument/Ferry Flight EDF)

A normal distribution described the fracture toughness data almost as well as the lognormal distribution. The normal distribution has higher probabilities in the tails than does the lognormal distribution. The MLE for a normal distribution to the fracture toughness data in Table 21 gives a mean value of 34.8 ksi√in and a standard deviation of 3.87. The curve for this normal distribution is compared to the lognormal distribution of Figure 35 on a lognormal probability plot in Figure 41. The normal distribution has higher cumulative probabilities in the 20 to 30 ksi√in range than does the lognormal distribution. The slope of the cumulative probability curve is also greater for the normal distribution which translates to higher PDF values. Thus, switching to a normal distribution will increase the POF. The POF with a normal distribution for the fracture toughness and the Instrument/Ferry EDF is 4.08×10^{-4}. The POF calculation is shown in Table 28.

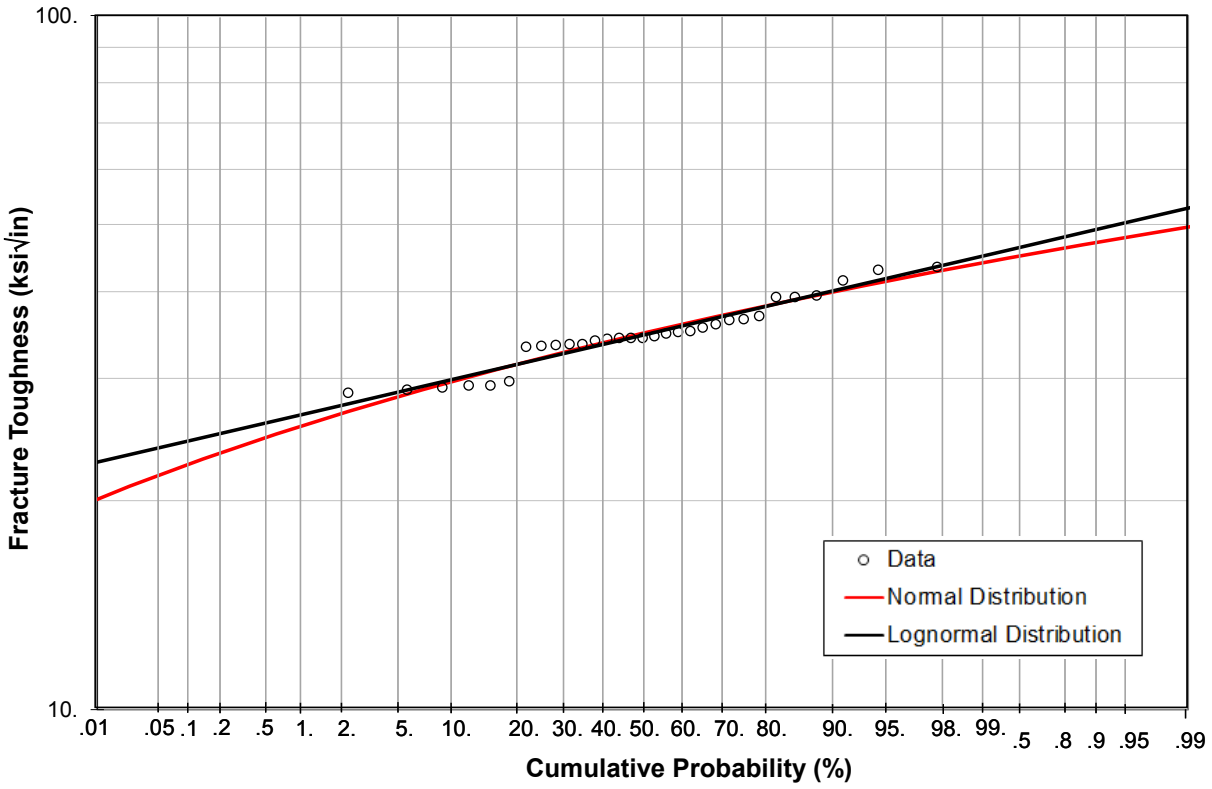

Figure 41. Normal and Lognormal Distributions Fit to Al 7050-T7351 Plate Fracture Toughness Data

Table 28. POF with Normal PDF for Fracture Toughness

Stress Intensity (ksi√in)	Stress Intensity EDF, D_{Kapp}	Fracture Toughness PDF, f_{KC}	$H = D_{Kapp} * f_{KC}$
15	1.00	2.13E-07	2.13E-07
15.5	0.93	4.10E-07	3.80E-07
16	0.83	7.74E-07	6.42E-07
16.5	0.73	1.44E-06	1.06E-06
17	0.64	2.63E-06	1.69E-06
17.5	0.56	4.72E-06	2.65E-06
18	0.49	8.34E-06	4.06E-06
18.5	0.42	1.45E-05	6.09E-06
19	0.36	2.48E-05	8.94E-06
19.5	0.31	4.16E-05	1.29E-05
20	0.26	6.88E-05	1.81E-05
20.5	0.22	1.12E-04	2.51E-05
21	0.19	1.79E-04	3.40E-05
21.5	0.16	2.81E-04	4.52E-05
22	0.14	4.34E-04	5.90E-05
22.5	0.11	6.60E-04	7.55E-05
23	0.10	9.87E-04	9.49E-05
23.5	0.081	1.45E-03	1.17E-04
24	0.067	2.10E-03	1.41E-04
24.5	0.056	2.99E-03	1.68E-04
25	1.02E-05	4.18E-03	4.25E-08
25.5	9.81E-11	5.74E-03	5.63E-13
26	9.44E-16	7.77E-03	7.34E-18
		POF =	4.08E-04

(using Instrument/Ferry Flight EDF)

6.3.3.5.2 Uncertainty in the N_z Exceedance Distributions

The N_z exceedances were extrapolated from records of 65 FH for the Transition mission and 34 FH for the Instrument/Ferry mission. So while the extrapolated data says that N_z during the Transition mission never exceeds 9.0g and never exceeds 9.5g during the Instrument/Ferry mission, all that can really be said is that an N_z of 9.0g was not exceeded during any Transition flights that were recorded. Given that an average flight is 1.25 hours, 65 FH is equivalent to 52 flights. So, it can only be said that the probability of exceeding an N_z of 9.0g during a Transition flight is less than 1/52 or 0.019. Similarly, the probability of N_z exceeding 9.5g during an Instrument/Ferry flight is less than 1/27, or 0.037. Thus, it was decided to extrapolate the Weibull distribution found in Section 6.3.3.3 to an N_z of 10g in Figure 42 to allow for tolerances in the flight control limits. The solid symbols in Figure 42 are the exceedance probability limits

calculated above for the two types of flights, 0.019 and 0.037. These extrapolated EDFs are compared to the EDFs previously derived in Section 6.3.3.3 in Figure 43.

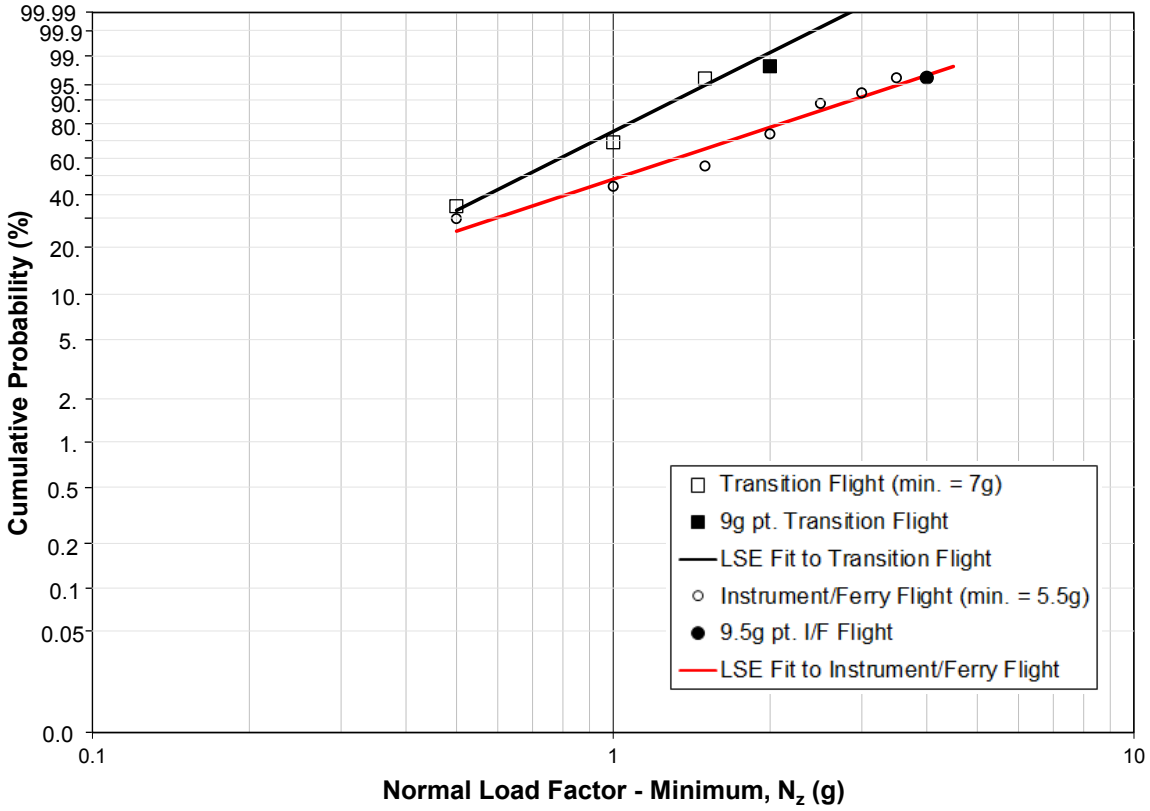

Figure 42. Weibull Plot of Extrapolation of N_z EDF to Higher N_z Values

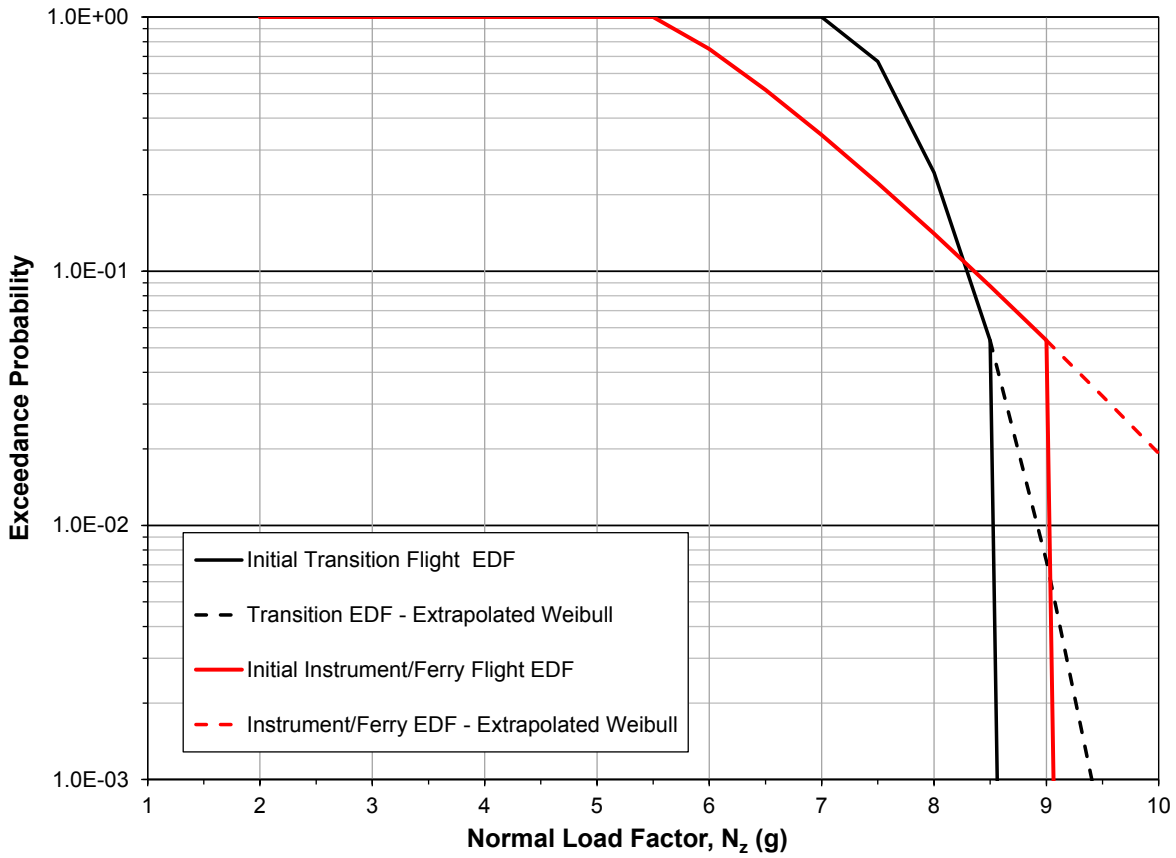

Figure 43. EDF Comparison for High N_z Tails

The stress intensity EDF for the Transition flight becomes

$$Pr\left(K_{app} > k\right) = 1, \qquad \text{if } \frac{k}{2.737} \leq 7, \tag{81a}$$

$$Pr\left(K_{app} > k\right) = exp\left[-\left(\frac{\frac{k}{2.737} - 7}{0.83}\right)^{1.81}\right], \qquad \text{if } 7 < \frac{k}{2.737} \leq 10, \tag{81b}$$

and

$$Pr\left(K_{app} > k\right) = 0, \qquad \text{if } \frac{k}{2.737} \geq 10. \tag{81c}$$

The stress intensity EDF for the Instrument/Ferry flight becomes

$$Pr\left(K_{app} > k\right) = 1, \qquad \text{if } \frac{k}{2.737} \leq 5.5, \tag{82a}$$

$$Pr\left(K_{app} > k\right) = exp\left[-\left(\frac{\frac{k}{2.737} - 5.5}{1.42}\right)^{1.19}\right], if\ 5.5 < \frac{k}{2.737} \leq 10, \qquad (82b)$$

and

$$Pr\left(K_{app} > k\right) = 0, \qquad \text{if } \frac{k}{2.737} \geq 10. \qquad (82c)$$

The POF is calculated for these alternate EDFs in Table 29 and Table 30. For the Transition flight, the POF increased by a factor of 2 over the initial POF estimate. For the Instrument/Ferry flight, the POF increased by a factor of 6 over the initial POF estimate.

Table 29. POF for Transition Flight EDF Extrapolated to 10g

Stress Intensity (ksi√in)	Stress Intensity EDF, D_{Kapp}	Fracture Toughness PDF, f_{KC}	$H = D_{Kapp} * f_{KC}$
18	1.00	4.11E-09	4.11E-09
18.5	1.00	1.71E-08	1.71E-08
19	1.00	6.43E-08	6.43E-08
19.5	0.97	2.21E-07	2.14E-07
20	0.85	6.99E-07	5.92E-07
20.5	0.68	2.04E-06	1.39E-06
21	0.50	5.52E-06	2.79E-06
21.5	0.35	1.40E-05	4.85E-06
22	0.22	3.30E-05	7.38E-06
22.5	0.13	7.35E-05	9.84E-06
23	0.075	1.54E-04	1.16E-05
23.5	0.040	3.07E-04	1.21E-05
24	0.020	5.79E-04	1.13E-05
24.5	0.009	1.04E-03	9.49E-06
25	0.0040	1.79E-03	7.13E-06
25.5	0.0016	2.94E-03	4.84E-06
26	0.0006	4.65E-03	2.97E-06
26.5	0.0002	7.06E-03	1.66E-06
27	0.0001	1.03E-02	8.42E-07
		POF =	4.44E-05

Table 30. POF for Instrument/Ferry Flight EDF Extrapolated to 10g

Stress Intensity (ksi√in)	Stress Intensity EDF, D_{Kapp}	Fracture Toughness PDF, f_{KC}	$H = D_{Kapp} * f_{KC}$
18	0.49	4.11E-09	2.00E-09
18.5	0.42	1.71E-08	7.17E-09
19	0.36	6.43E-08	2.32E-08
19.5	0.31	2.21E-07	6.84E-08
20	0.26	6.99E-07	1.84E-07
20.5	0.22	2.04E-06	4.58E-07
21	0.19	5.52E-06	1.05E-06
21.5	0.16	1.40E-05	2.25E-06
22	0.14	3.30E-05	4.49E-06
22.5	0.11	7.35E-05	8.41E-06
23	0.10	1.54E-04	1.48E-05
23.5	0.081	3.07E-04	2.47E-05
24	0.067	5.79E-04	3.90E-05
24.5	0.056	1.04E-03	5.86E-05
25	0.047	1.79E-03	8.40E-05
25.5	0.039	2.94E-03	1.15E-04
26	0.032	4.65E-03	1.51E-04
26.5	0.027	7.06E-03	1.90E-04
27	0.022	1.03E-02	2.30E-04
		POF =	4.04E-04

6.3.3.6 Conclusions Drawn from Two Random Variable Fracture POF Analysis

Based on the initial analyses and subsequent sensitivity study the POF for this component with a 1.25 in. crack is likely on the order of 5×10^{-5} during flight back to a repair station. This POF is too high to conclude that the flight can be made safely. Opportunities for reducing the POF should be explored before flying this aircraft.

6.4 Probability of Failure: Three Random Variables

This last example is a bit contrived, but it sets the stage for more realistic POF calculations where there is variability in the loading, uncertainty about the fracture toughness, and uncertainty about the crack size. This might be the case when nondestructive inspection indicates that a crack is present, but the location cannot be viewed so a physical measurement of the crack is not possible. This example in this will only determine the POF during the next flight.

6.4.1 Three Random Variables: Fracture Toughness, Applied Loads, and Crack Size

Consider the example in Section 6.3.3, but this time there is uncertainty about the true crack size. If the uncertainty is due to measurement error, it is usually modeled by a normal distribution. Since the point of the example is to show how to calculate POF when there are three random

variables, assume that the uncertainty about the crack size is described by a normal distribution with a mean of 1.25 inches and a standard deviation of 0.10 inches The same procedure would apply if other distribution functions are used. The information needed to work this example is summarized in Table 31 and Figure 44. Remember that σ_{app} is equal to 1.741 times N_z. The σ_{app} distribution used is the Weibull extrapolated N_z EDF for the Transition flight from Section 6.3.3.5.2 scaled appropriately.

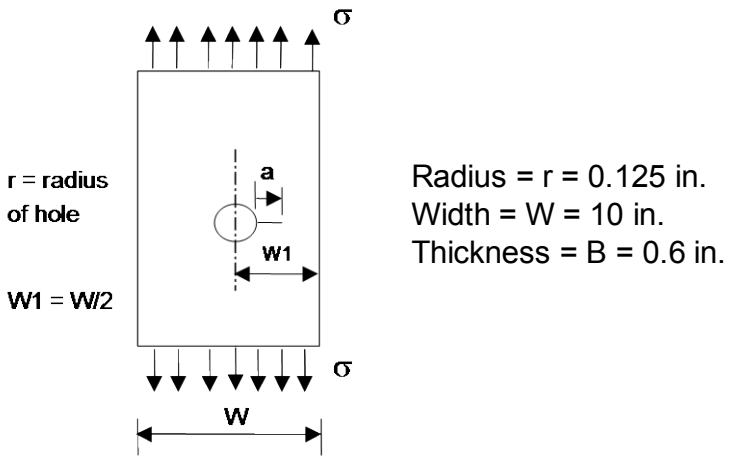

Figure 44. Geometry for Fracture Reliability Example (Repeated)
Plate loaded in uniform tension with a through-thickness, radial cracked hole

Table 31. Summary of Information for Three Random Variable Example

Variable	Description
Fracture Toughness CDF, K_C (ksi√in)	$Pr(K_C < k) = \Phi\left(\frac{ln(k) - ln(34.6)}{0.11}\right)$
Applied Stress EDF, σ_{app} (ksi) {Transition Flight EDF, Section 6.3.3.5.2}	$Pr(\sigma_{app} > s) = 1$, if $\frac{s}{1.741} \leq 7$; $Pr(\sigma_{app} > s) = exp\left[-\left(\frac{\frac{s}{1.741} - 7}{0.83}\right)^{1.81}\right]$, if $10 \geq \frac{s}{1.741} > 7$
Crack Size CDF, a (in)	$Pr(a < A) = \Phi\left(\frac{A - 1.25}{0.10}\right)$
Stress Intensity, K_{app} (ksi√in)	$K_{app} = \sigma_{app}\beta\sqrt{\pi a}$, $\beta = \beta_{hole}\beta_{width}$
β_{hole}	$\beta_{hole} = 0.7071 + 0.7548z + 0.3415z^2 + 0.642z^3 + 0.9196z^4$, $z = \frac{1}{1 + \frac{a}{r}}$
β_{width}	$\beta_{width} = \sqrt{\sec\left(\frac{\pi}{2} \cdot \frac{2r + a}{W - a}\right)}$

6.4.2 The Probability of Failure Equation

The equation for calculating the POF now becomes

$$P_F = Pr(K_c \leq K_{app}) = \int_0^{\infty}\int D_{K_{app}}(x,y) f_{K_C}(x)dx\, f_a(y)dy, \tag{83}$$

since the applied stress intensity is now a function of two random variables, σ_{app} and a,

$$K_{app} = \sigma_{app}\beta\sqrt{\pi a}. \tag{84}$$

The POF equation can also be written as

$$P_F = Pr\left(\sigma_c \le \sigma_{app}\right) = \int_0^{\infty}\int D_{\sigma_{app}}(x) f_{\sigma_C}(x,y)dx\, f_a(y)dy, \tag{85}$$

where the critical failure stress σ_C is a function of two random variables, K_C and a,

$$\sigma_C = \frac{K_C}{\beta\sqrt{\pi a}}\,. \tag{86}$$

However, calculating the POF for the product of two random variables is conceptually easier than for a quotient. So, the first formulation will be used in this example.

6.4.3 Calculating the Probability of Failure

The strategy for calculating the POF in this situation is to perform the inner integration over the stress intensity,

$$P_f(a_i) = \int_0^{\infty} D_{K_{app}}(x, a_i) f_{K_C}(x)dx, \tag{87}$$

at discrete, uniformly-spaced crack sizes a_i. Then use the values of $P_f(a_i)$ in performing the outer integration over the crack size. The crack size range for the integration and the desired discretization of the range must be decided upon at the start as this determines the $P_f(a_i)$'s that must be calculated.

The crack size range for the integration was chosen to be from -6 standard deviations to +6 standard deviations, i.e., from 0.65 inches to 1.85 inches. A crack size increment of 0.05 inches was selected to discretize the range. The determination of each $P_f(a_i)$ proceeds just like the integration in Section 6.3.3.4 for each crack size a_i.

From Section 6.3.3.5.2, the EDF for K_{app} is

$$Pr\left(K_{app} > k\right) = 1, \qquad \text{if } \frac{k}{1.741\beta\sqrt{\pi a_i}} \le 7\text{g}, \tag{88a}$$

$$Pr\left(K_{app} > k\right) = exp\left[-\left(\frac{\frac{k}{1.741\beta\sqrt{\pi a_i}} - 7}{0.83}\right)^{1.81}\right],$$

$$\text{if } 10\text{g} \ge \frac{k}{1.741\beta\sqrt{\pi a_i}} > 7\text{g}. \tag{88b}$$

The calculation of $\beta\sqrt{\pi a_i}$ is summarized in Table 32.

The fracture toughness distribution is unchanged from Section 6.3.3.2.

Table 32. Calculation of $\beta\sqrt{\pi a_i}$

Crack Size, a_i (in)	$z = 1/(1+a_i/r)$	β_{hole}	β_{width}	$\beta\sqrt{\pi a_i}$
0.65	0.1613	0.8410	1.0058	1.209
0.70	0.1515	0.8320	1.0065	1.242
0.75	0.1429	0.8242	1.0073	1.274
0.80	0.1351	0.8172	1.0081	1.306
0.85	0.1282	0.8111	1.0090	1.337
0.90	0.1220	0.8056	1.0100	1.368
0.95	0.1163	0.8007	1.0110	1.398
1.00	0.1111	0.7962	1.0121	1.428
1.05	0.1064	0.7922	1.0132	1.458
1.10	0.1020	0.7885	1.0144	1.487
1.15	0.0980	0.7851	1.0157	1.516
1.20	0.0943	0.7820	1.0171	1.544
1.25	0.0909	0.7791	1.0185	1.572
1.30	0.0877	0.7764	1.0200	1.601
1.35	0.0847	0.7740	1.0216	1.628
1.40	0.0820	0.7717	1.0233	1.656
1.45	0.0794	0.7695	1.0251	1.684
1.50	0.0769	0.7675	1.0270	1.711
1.55	0.0746	0.7656	1.0289	1.738
1.60	0.0725	0.7639	1.0310	1.766
1.65	0.0704	0.7622	1.0332	1.793
1.70	0.0685	0.7606	1.0355	1.820
1.75	0.0667	0.7591	1.0379	1.847
1.80	0.0649	0.7577	1.0404	1.875
1.85	0.0633	0.7564	1.0430	1.902

In Section 6.3.3.5.2, the $P_f(a_i)$ for a_i equal to 1.25 in. was calculated to be 4.44×10^{-5}. The calculations of $P_f(a_i)$ for other selected values of a_i are summarized in Table 33 through Table 36. In each of these tables, $P_f(a_i)$ is calculated using the trapezoidal rule applied to values in the last column. $P_f(a_i)$ is calculated over a reduced stress intensity range, 16 to 27 ksi$\sqrt{in}$, since there is little contribution to the probability below 16 ksi$\sqrt{in}$.

Table 33. Calculation of $P_f(a_i)$ for a_i equal to 1.00 inch

Stress Intensity (ksi√in)	Stress Intensity EDF, D_{Kapp}	Fracture Toughness PDF, f_{KC}	$H = D_{Kapp} * f_{KC}$
16	1	4.45E-12	4.45E-12
17	1	1.73E-10	1.73E-10
18	0.899	4.11E-09	3.70E-09
19	0.533	6.43E-08	3.43E-08
20	0.220	6.99E-07	1.53E-07
21	0.0650	5.52E-06	3.59E-07
22	0.0141	3.30E-05	4.65E-07
23	0.0023	1.54E-04	3.51E-07
24	0.0003	5.79E-04	1.60E-07
25	2.54E-05	1.79E-03	4.55E-08
26	1.79E-06	4.65E-03	8.31E-09
27	9.67E-08	1.03E-02	9.98E-10
		$P_f(a_i)$ =	1.58E-06

Table 34. Calculation of $P_f(a_i)$ for a_i equal to 1.30 inches

Stress Intensity (ksi√in)	Stress Intensity EDF, D_{Kapp}	Fracture Toughness PDF, f_{KC}	$H = D_{Kapp} * f_{KC}$
16	1	4.45E-12	4.45E-12
17	1	1.73E-10	1.73E-10
18	1	4.11E-09	4.11E-09
19	1	6.43E-08	6.43E-08
20	0.942	6.99E-07	6.58E-07
21	0.637	5.52E-06	3.52E-06
22	0.319	3.30E-05	1.05E-05
23	0.122	1.54E-04	1.88E-05
24	0.0362	5.79E-04	2.10E-05
25	0.0084	1.79E-03	1.51E-05
26	0.0016	4.65E-03	7.23E-06
27	0.0002	1.03E-02	2.36E-06
		$P_f(a_i)$ =	7.81E-05

Table 35. Calculation of $P_f(a_i)$ for a_i equal to 1.40 inches

Stress Intensity (ksi√in)	Stress Intensity EDF, D_{Kapp}	Fracture Toughness PDF, f_{KC}	$H = D_{Kapp} * f_{KC}$
16	1	4.45E-12	4.45E-12
17	1	1.73E-10	1.73E-10
18	1	4.11E-09	4.11E-09
19	1	6.43E-08	6.43E-08
20	1	6.99E-07	6.99E-07
21	0.866	5.52E-06	4.79E-06
22	0.544	3.30E-05	1.80E-05
23	0.261	1.54E-04	4.02E-05
24	0.097	5.79E-04	5.64E-05
25	0.029	1.79E-03	5.14E-05
26	0.0068	4.65E-03	3.15E-05
27	0.0013	1.03E-02	1.33E-05
		$P_f(a_i)$ =	2.10E-04

Table 36. Calculation of $P_f(a_i)$ for a_i equal to 1.50 inches

Stress Intensity (ksi√in)	Stress Intensity EDF, D_{Kapp}	Fracture Toughness PDF, f_{KC}	$H = D_{Kapp} * f_{KC}$
16	1	4.45E-12	4.45E-12
17	1	1.73E-10	1.73E-10
18	1	4.11E-09	4.11E-09
19	1	6.43E-08	6.43E-08
20	1	6.99E-07	6.99E-07
21	0.994	5.52E-06	5.49E-06
22	0.779	3.30E-05	2.57E-05
23	0.461	1.54E-04	7.11E-05
24	0.213	5.79E-04	1.23E-04
25	0.078	1.79E-03	1.40E-04
26	0.023	4.65E-03	1.07E-04
27	0.0055	1.03E-02	5.69E-05
		$P_f(a_i)$ =	5.01E-04

The total POF can then be calculated as

$$P_F = \int_0^{\infty} P_f(y) \cdot f_a(y) dy.$$

The integration is performed by applying the trapezoidal rule to the product of $P_f(a_i)$ and the $f_a(a_i)$ in Table 37. As would be expected, the uncertainty about the crack size increases the POF. Since the assumed uncertainty about the crack size is small, the increase in POF is not very large.

Table 37. Calculation of Total POF for Random Crack Size Example

Crack Size, a_i (in)	PDF, $f_a(a_i)$	$P_f(a_i)$	$f_a(a_i)*P_f(a_i)$
0.65	6.08E-08	1.38E-09	8.39E-17
0.70	1.08E-06	4.81E-09	5.18E-15
0.75	1.49E-05	1.50E-08	2.24E-13
0.80	0.0002	4.41E-08	7.05E-12
0.85	0.0013	1.18E-07	1.58E-10
0.90	0.0087	3.00E-07	2.61E-09
0.95	0.0443	7.04E-07	3.12E-08
1.00	0.1753	1.58E-06	2.77E-07
1.05	0.5399	3.40E-06	1.84E-06
1.10	1.2952	6.88E-06	8.91E-06
1.15	2.4197	1.34E-05	3.25E-05
1.20	3.5207	2.48E-05	8.71E-05
1.25	3.9894	4.42E-05	1.76E-04
1.30	3.5207	7.81E-05	2.75E-04
1.35	2.4197	1.29E-04	3.11E-04
1.40	1.2952	2.10E-04	2.72E-04
1.45	0.5399	3.32E-04	1.79E-04
1.50	0.1753	5.01E-04	8.79E-05
1.55	0.0443	7.37E-04	3.27E-05
1.60	0.0087	1.07E-03	9.32E-06
1.65	0.0013	1.48E-03	1.99E-06
1.70	0.0002	2.01E-03	3.21E-07
1.75	1.49E-05	2.65E-03	3.94E-08
1.80	1.08E-06	3.43E-03	3.70E-09
1.85	6.08E-08	4.30E-03	2.61E-10
		POF =	7.38E-05

A sensitivity study should be performed decreasing the crack size increment in order to be sure that the answer has converged. This is left for the reader to do if they wish. The sensitivity of the POF to the applied stress EDF and the fracture toughness PDF was investigated previously in Section 6.3.3.5. The sensitivity of the POF to the uncertainty about the appropriate crack size distribution and its parameters should also be investigated, but will not be done here.

7.0 CONCLUSION

This volume is intended to be the first in a series that provides guidance on how to perform structural reliability assessments of aircraft structure. In this volume, fundamental principles of structural reliability analysis were introduced and demonstrated in worked examples. A familiarity with probability theory and concepts was assumed. The complexity of the examples did not extend beyond assessing the reliability during the next increment of time, e.g., the next flight.

8.0 REFERENCES

1. "Dept. of Defense Standard Practice for System Safety," Mil-Std-882E, Dept. of Defense, 2012.

2. USAF Center of Excellence for Airworthiness, *United States Air Force (USAF) Airworthiness Bulletin (AWB)-013A,* "Risk Identification and Acceptance for Airworthiness Determination," Wright-Patterson Air Force Base, OH, Aeronautical Systems Center, 2011.

3. "Dept. of Defense Standard Practice - Aircraft Structural Integrity Program (ASIP)," Mil-Std-1530C, Dept. of Defense, Wright-Patterson AFB, OH 45433, 2005.

4. B. Lundberg, "Fatigue Life of Airplane Structures: the 18th Wright Brothers Lecture," *J. of Aeronautical Sciences,* vol. 22, no. 6, pp. 349-402, 1955.

5. J. W. Lincoln, "Method for Computation of Structural Failure Probability for an Aircraft," ASD-TR-80-5035, Aeronautical Systems Division, Wright-Patterson Air Force Base, 1980.

6. J. W. Lincoln, "Risk Assessment of an Aging Military Aircraft," *J. of Aircraft,* vol. 22, no. 8, pp. 687-691, 1985.

7. A. P. Berens, P. W. Hovey and D. A. Skinn, "Risk Analysis for Aging Aircraft Fleets," WL-TR-91-3066, Wright Laboratory, Wright-Patterson Air Force Base, 1991.

8. A. M. Freudenthal, J. M. Garrelts and M. Shinozuka, "The Analysis of Structural Safety," *Proc. of the American Society of Civil Engineers, Structural Division,* vol. 92, no. ST1, pp. 267-325, February 1966.

9. C. I. Babish, *Aircraft Structure Risk and Reliability Analysis Course,* Dayton, OH, 2004.

10. National Institute for Standards and Technology, "NIST/SEMATECH e-Handbook of Statistical Methods," 1 April 2012. [Online]. Available: http://www.itl.nist.gov/div898/handbook/. [Accessed 4 February 2013].

11. W. Nelson, *Applied Life Data Analysis*, New York: John Wiley & Sons, 1982.

12. A. M. Freudenthal, "Reliability Assessment of Aircraft Structures Based on Probabilistic Interpretation of the Scatter Factor," AFML-TR-74-198, Air Force Materials Laboratory, Wright-Patterson AFB, OH, 1975.

13. Structures Branch, Engineering Directorate, Aeronautical Systems Center, "Methodology for Determination of Equivalent Flight Hours and Approaches to Communicate Usage Severity," EN-SB-09-001, ASC/EN, Wright-Patterson Air Force Base, OH, 2009.

14. D. O. Cornog and J. W. Lincoln, "Risk Assessment of the F-16 Wing," in *Proceedings of the 1988 Structural Integrity Conference*, WRDC-TR-89-4071, San Antonio, TX, 1989.

15. A. M. Freudenthal and P. Y. Wang, "Ultimate Strength Analysis," AFML-TR-69-60, Air Force Materials Laboratory, Wright-Patterson Air Force Base, 1969.

16. M. C. Campion, L. C. Hanson and D. S. Morcock, "Implementation Studies for a Reliability-Based Static Strength Criteria System," AFFDL-TR-71-178, Air Force Flight Dynamics

Laboratory, Wright-Patterson Air Force Base, 1972.

17. P. C. Miedlar, A. P. Berens, A. Gunderson and J. P. Gallagher, "USAF Damage Tolerant Design Handbook: Guidelines for the Analysis and Design of Damage Tolerant Aircraft Structures," AFRL-VA-WP-TR-2003-3002, U.S. Air Force Research Laboratory, Wright-Patterson Air Force Base, OH, 2002.

18. D. A. Skinn, J. P. Gallagher, A. P. Berens, P. D. Huber and J. Smith, Damage Tolerant Design Handbook, Vols. Vol. 4, Chapter 8, Table 8.7.2.1, WL-TR-94-4055, Wright-Patterson AFB, OH 45433: Wright Laboratory, 1994.

19. R. J. Veldman and C. Peckham, "Handbook of Military Aircraft Design Normal Load Factor Exceedance Data," ASD-TR-82-5012, Aeronautical Systems Division; Air Force Systems Command, Wright-Patterson Air Force Base, 1982.

LIST OF ACRONYMS, ABBREVIATIONS AND SYMBOLS

Acronym	Description
A/C	Aircraft
CDF	Cumulative Distribution Function
DLL	Design Limit Load
EDF	Exceedance Distribution Function
EFH	Equivalent Flight Hours
FH	Flight Hour(s)
HRF	Hazard Rate Function
ksi	Kilopounds per Square Inch
LH	Left Hand
LSE	Least Squares Estimate
MLE	Maximum Likelihood Estimate
MLG	Main Landing Gear
PDF	Probability Density Function
RH	Right Hand
SFPOF	Single Flight Probability of Failure
UTS	Ultimate Tensile Strength
WBM	Wing Bending Moment
α	Shape parameter for Weibull Distribution
β	Scale parameter for Weibull Distribution
λ	Rate parameter for Exponential Distribution
μ	Mean of a Population
σ	Standard Deviation, or Stress

INDEX